치의과학박사 학위논문

The immunological effect of extracellular vesicles derived from macrophages and periodontal pathogens

대식세포와 치주병원균 유래 세포 밖 소포체의 면역 활성에 관한 연구

2023년 2월

서울대학교 대학원

치의과학과 면역 및 분자미생물학 전공

임 영 갑

The immunological effect of extracellular vesicles derived from macrophages and periodontal pathogens

by

Younggap Lim

Under the supervision of

Professor **Bong-Kyu Choi**, Ph. D.

A Thesis Submitted in Partial Fulfillment of

the Requirements for the Degree of

Doctor of Philosophy

February 2023

School of Dentistry

The Graduate School

Seoul National University

The immunological effect of extracellular vesicles derived from macrophages and periodontal pathogens

지도교수 최 봉 규

이 논문을 치의과학박사 학위논문으로 제출함
2022년 11월

서울대학교 대학원
치의과학과 면역 및 분자미생물학 전공
임 영 갑

임영갑의 치의과학박사 학위논문을 인준함
2023년 1월

위 원 장 _____ (인)

부위원장 _____ (인)

위 원 _____ (인)

위 원 _____ (인)

위 원 _____ (인)

Abstract

The immunological effect of extracellular vesicles derived from macrophages and periodontal pathogens

Younggap Lim
Program in Immunology and Molecular Microbiology
Department of Dental Science
The Graduate School
Seoul National University

Objectives

Extracellular vesicles (EVs) are nano-sized vesicles released from living cells that carry various biological molecules. EVs are attracting attention because of their physiological and pathological roles in intercellular communication. So far, there is limited information on the characteristics of EVs derived from host cells infected with periodontal pathogens and the differentiation of helper T cells through EVs of periodontal pathogens.

The aim of this study was to evaluate the proteome and inflammatory response of EVs released from host cells infected with a periodontal pathogen and the mode of helper T cell differentiation induced by periodontal pathogen-derived OMVs.

Methods

EVs derived from THP-1 macrophages infected with *Tannerella forsythia*

were isolated by size exclusion chromatography combined with iodixanol density gradient ultracentrifugation (DGUC). The size and concentration of EVs were measured by nanoparticle tracking analysis (NTA). The morphology of EVs was imaged by transmission electron microscopy (TEM). Protein profiles of EVs were analyzed by sodium dodecyl sulfate-polyacrylamide gel electrophoresis (SDS-PAGE), and EVs were stained with SYPRO Ruby protein gel solution. Eukaryotic EVs, non-vesicular aggregates, and *T. forsythia* proteins were analyzed by immunoblotting using host and bacteria-specific antibodies. The total proteome of EVs was analyzed by in-depth quantitative proteomics. To evaluate the immunostimulatory effects of EVs on THP-1 macrophages, cells were treated with EVs. The level of pro-inflammatory cytokines in the culture supernatants were measured by enzyme-linked immunosorbent assay (ELISA).

The OMVs of three periodontal pathogens, *Porphyromonas gingivalis*, *Treponema denticola*, and *T. forsythia*, were isolated by ultracentrifugation combined with DGUC. The size and concentration of OMVs were measured by NTA. The morphology of OMVs was imaged by TEM. To evaluate the immunostimulatory effects of dendritic cells (DCs) and mode of helper T cell differentiation by OMVs, murine bone marrow-derived DCs (BMDCs) were differentiated from bone marrow cells, and naïve $CD4^+$ T cells were isolated from splenocytes of eight-week-old C57BL/6N mice. BMDCs were treated with periodontal pathogen OMVs, and the expression level of surface MHC class II, CD80, CD86, and CD40 molecules was measured by flow cytometry. The expression level of pro-inflammatory cytokines, interleukin (IL)-12p70, IL-1β, IL-6, and IL-23, in the culture supernatant of BMDCs were measured by ELISA, and that of *Il12a*, *Il1b*, *Il6*, and *Il23a* in OMV-stimulated BMDCs was measured by quantitative real-time polymerase chain reaction (qRT-PCR). To analyze the proteolytic activity of periodontal pathogen OMVs against pro-inflammatory cytokines, recombinant murine IL-12p70, IL-1β, IL-6, and IL-23 were treated with periodontal pathogen OMVs, and the level

of remaining cytokines was measured by ELISA. To evaluate the mode of helper T cell differentiation, naïve $CD4^+$ T cells were cocultured with OMV-primed BMDCs for 4 days. Differentiation of naïve $CD4^+$ T cells into Th1 or Th17 cells was analyzed by measuring intracellular IFN-γ and IL-17A in $CD4^+$ T cells. To evaluate the effects of IL-6 and IL-12 secreted from BMDCs on the differentiation of Th1 or Th17 cells, naïve $CD4^+$ T cells were cocultured with OMV-primed BMDCs for 4 days in the presence or absence of neutralizing antibodies against IL-6 and IL-12.

Results

EVs derived from THP-1 macrophages infected with *T. forsythia* were divided into macrophage- and *T. forsythia*-derived EVs with different densities. Macrophage- and *T. forsythia*-derived EVs were in the low- and mid-density fraction, respectively. The size and morphology of the two distinct EVs were similar, but the protein profile was completely different. Eukaryotic EV markers, including CD9, CD63, and Alix, were detected only in macrophage-derived EVs, while *T. forsythia* proteins were highly enriched in *T. forsythia*-derived EVs. Compared with EVs from non-infected macrophages, levels of TNF-α, CXCL8, IL-1β, CPNE1, SPP1, PLSCR1, P2RX4, MMP9, SARS, VARS, STXBP2, HVCN1, CD82, RFTN1, LCP1, and ATP2B1 were increased in EVs from *T. forsythia*-infected macrophages. Meanwhile, macrophages-derived EVs induced TNF-α expression from THP-1 macrophages. *T. forsythia*-derived EVs were enriched with *T. forsythia* virulence factors, including nutrient-scavenging proteins, peptidases, glycosyl hydrolases, bacterial lipoproteins, GroEL, and BspA. Additionally, *T. forsythia*-derived EVs induced the expression of TNF-α, IL-1β, IL-6, and IL-8 from THP-1 macrophages through the TLR2 signaling pathway. Interestingly, soluble molecules secreted from THP-1 macrophages promoted *T. forsythia* to release EVs.

OMVs of *P. gingivalis*, *T. denticola*, and *T. forsythia*, also termed "red complex" bacteria, induced maturation of BMDCs as indicated by the expression of MHC class II, CD80, CD86, and CD40 molecules. OMVs of *P. gingivalis* and *T. forsythia* induced the expression of pro-inflammatory cytokines IL-1β, IL-6, IL-23, and IL-12p70 in BMDCs. However, in *T. denticola* OMV-primed BMDCs, pro-inflammatory cytokines were poorly detected in cell culture supernatants, which was attributed to posttranslational degradation due to the highly proteolytic nature of *T. denticola* OMVs. In cocultures of naïve $CD4^+$ T cells with OMV-primed BMDCs, OMVs of *P. gingivalis* and *T. denticola* induced Th17 cell differentiation, whereas those of *T. forsythia* preferentially induced Th1 cell differentiation. IL-6 and IL-12 released from OMV-primed BMDCs played pivotal roles in Th17 and Th1 polarization, respectively.

Conclusion

EVs derived from macrophages infected with *T. forsythia* carried pro-inflammatory cytokines and inflammatory mediators that may play a role in the inflammatory response in periodontitis. *T. forsythia*-derived EVs contained various virulence factors that induced pro-inflammatory responses through TLR2 activation. OMVs of *P. gingivalis* and *T. denticola* induced differentiation of Th17 cells, while those of *T. forsythia* favored Th1 cell polarization rather than Th17. These results demonstrate that in pathogen-infected cells, EVs derived from host cells and pathogens can have a synergistic effect on the inflammatory response, providing insight into the characterization of EVs derived from cells infected with a periodontal pathogen. OMVs derived from "red complex" bacteria induced maturation of BMDCs and differentiation of naïve $CD4^+$ T cells into Th1 or Th17 cells. Thus, EVs may be a useful tool for understanding pathogenic mechanisms of periodontal pathogens.

Keywords: Dendritic cells, Extracellular vesicles, Macrophages, Periodontal pathogens, Proteomics, T cells
Student Number: 2018-32257

Table of Contents

Abstract

Abbreviation

I. Introduction 1

1. Periodontitis 1

1.1. Microbiome and immune system 1

1.2. Periodontitis and periodontal pathogens 1

2. Immune cells and periodontitis 5

2.1. Helper T cell 6

2.2. Dendritic cell 6

2.3. B cell 7

2.4. Neutrophil 7

2.5. Macrophage 8

3. Extracellular vesicles 8

4. Aims of this study 9

II. Material and Methods 11

1. THP-1 cell culture 11

2. Bacteria culture 11

3. Isolation and characterization of EVs 12

3.1. Isolation of EVs derived from THP-1 macrophages infected with *T. forsythia* 12

3.2. Isolation of OMVs derived from periodontal pathogens 13

3.3. Nanoparticle tracking analysis (NTA) 14

3.4. Transmission electron microscopy (TEM) 14

3.5. Immunoblotting 14

3.6. SYPRO Ruby protein gel staining 15

4. Proteomics 16

4.1. EV sample preparation for proteome analysis 16

4.2. LC-MS/MS analysis 16

4.3. Data processing for label-free quantification.....17
4.4. Statistical analysis of the proteomic data.....17
4.5. Bioinformatics analysis.....18
5. *T. forsythia* culture in the EV-free conditioned medium of THP-1 macrophages.....19
6. CHO/CD14/TLR2 and CHO/CD14/TLR4 reporter cell assay 19
7. Mice.....20
8. Bone marrow-derived dendritic cells (BMDCs) 20
9. Coculture of naïve $CD4^+$ T cells with BMDCs.....20
10. Enzyme-linked immunosorbent assay (ELISA).....21
11. Degradation of pro-inflammatory cytokines by periodontal pathogen OMVs.....21
12. Quantitative real-time polymerase chain reaction (qRT-PCR).....22
13. Flow cytometry 23
14. Statistics 23
III. Results.....25
1. Identification of proteome profile and immune responses of EVs derived from macrophages infected with *T. forsythia*.....25
1.1. Two distinct types of EVs were identified from macrophages infected with *T. forsythia*. 25
1.2. Macrophage-derived EVs of non-infected and *T. forsythia*-infected macrophages were analyzed by in-depth quantitative proteomics. 32
1.3. *T. forsythia* proteins in *T. forsythia*-derived EVs were analyzed by in-depth quantitative proteomics. 42
1.4. *T. forsythia* cultured in EV-free conditioned medium of macrophages relased EVs. 50
1.5. Macrophage-derived EVs and *T. forsythia*-derived EVs induced pro-inflammatory responses. 53
2. Identification of the role in BMDCs maturation and helper T cell differentiation by periodontal pathogen OMVs. 57

2.1. Periodontal pathogen OMVs were isolated and characterized. 57
2.2. Periodontal pathogen OMVs induced maturation of BMDCs.....60
2.3. OMV-primed BMDCs secreted pro-inflammatory cytokines.....62
2.4. Naïve $CD4^+$ T cells were differentiated by OMV-primed BMDCs.66
2.5. IL-6 and IL-12 play a key role in the differentiation of naïve $CD4^+$ T cells by OMV-primed BMDCs into Th17 and Th1 cells, respectively. 70
IV. Discussion.....73
1. Identification of proteome and immune responses of EVs derived from macrophages infected with *T. forsythia*.....73
2. Identification of the role in BMDCs maturation and helper T cell differentiation by periodontal pathogen OMVs 79
V. Conclusion 84
VI. References.....85
List of Publications.....103
국문초록

Abbreviations

ANOVA	Analysis of variance
ATP2B1	Plasma membrane calcium-transporting ATPase 1
BHI	Brain heart infusion
BMDC	Bone marrow-derived dendritic cell
CD	Cluster of Differentiation
cDNA	Complementary DNA
CM	Conditioned medium
CPNE1	Copine-1
CXCL8	C-X-C Motif Chemokine Ligand 8
DC	Dendritic cells
DEPs	Differentially expressed proteins
DGUC	Density gradient ultracentrifugation
DNA	Deoxyribonucleic acid
ELISA	Enzyme-linked immunosorbent assay
EV	Extracellular vesicle
FBS	Fetal bovine serum
FDR	False discovery rate
GAPDH	Glyceraldehyde-3-phosphate dehydrogenase
GO	Gene Ontology
GOBP	Gene Ontology - Biological Process
GOCC	Gene Ontology - Cellular Component
GOMF	Gene Ontology - Molecular Function
HVCN1	Voltage-gated hydrogen channel 1
iBAQ	Intensity Based Absolute Quantification
IFN-γ	Interferon gamma

IL	Interleukin
LCP1	Plastin-2
LPS	lipopolysaccharide
MAMP	Microbe-associated molecular pattern
MMP9	Matrix metalloproteinase-9
MOI	Multiplicity of infection
MWCO	Molecular weight cut-off
NI	Non-infection
NOS	New oral spirochete broth
NT	Non-treatment
NTA	Nanoparticle tracking analysis
OMV	Outer membrane vesicle
PBS	Phosphate-buffered saline
PCA	Principal component analysis
PES	Polyethersulfone
PLSCR1	Phospholipid scramblase 1
PMA	Phorbol 12-Myristate 13-Acetate
PRR	Pattern recognition receptor
PVDF	Polyvinylidene difluoride
qRT-PCR	Quantitative real-time polymerase chain reaction
RFTN1	Raftlin
rmGM-CSF	Recombinant murine granulocyte-macrophage colony-stimulating factor
RNA	Ribonucleic Acid
RT	Room temperature
SARS	Serine tRNA ligases
SD	Standard deviation
SDS-PAGE	Sodium dodecyl sulfate-polyacrylamide gel electrophoresis

SPP1	Osteopontin
STXBP2	Syntaxin-binding protein 2
TBST	Tris-Buffered Saline with 0.1% Tween® 20 Detergent
TCA	Trichloroacetic acid
TEM	Transmission Electron Microscopy
TF	*T. forsythia* infection
TLR	Toll-like receptor
TNF	Tumor necrosis factor
VARS	Valine tRNA ligases

I. Introduction

1. Periodontitis

1.1. Microbiome and immune system

Microorganisms are living organisms that are too small to be seen with the naked eye. Microorganisms live in various habitats on Earth and significantly impact the surrounding environment [1]. The microbiome is the whole genome of microorganisms in a habitat and their byproducts, including nucleic acids, proteins, lipids, polysaccharides, and metabolites [2]. In addition to microbiota, which is the assemblage of living microorganisms in a habitat, phages, viruses, plasmids, prions, viroids, and free DNA are part of the microbiome [2]. A recent study reported that over 150,000 microbial genomes are identified from global body-wide human metagenomes [3]. The microbiome affects various physiological conditions in our body, including nutrient digestion, metabolism, immune system, and even mental health [4-6]. Therefore, the microbiome is called "the second genome," and its importance is being highlighted [7]. The structural and functional development of the human immune system in our body is closely related to the microbiome as the immune system cannot properly develop in germ-free conditions [8]. Immune systems are restored when non-pathogenic conventional microbes are recolonized [9]. Eubiosis is the status of a microbiome in a disease-free host [10]. In contrast, dysbiosis, which is the abnormal status of a microbiome, induces chronic unregulated immune responses that can cause inflammation and destroy nearby tissue [8]. One of the representative examples of microbial dysbiosis diseases is periodontitis.

1.2. Periodontitis and periodontal pathogens

The oral cavity is the second largest habitat for the human microbiome after the gut. Over 700 species of microbes reside in the human oral cavity [11]. Microbial dysbiosis in the subgingival biofilm induces uncontrolled chronic

inflammatory responses in the periodontium, which finally develops into periodontitis [11]. Periodontitis is characterized by gingival tissue destruction and bone resorption that leads to tooth loss [12]. Periodontitis is a significant concern for oral health and affects 20%–50% of the world's population [13]. The host responses against the periodontal pathogens in the subgingival biofilm play an essential role in connective tissue destruction and alveolar bone resorption due to increased pro-inflammatory cytokine production and osteoclastogenesis [14]. *Porphyromonas gingivalis*, *Tannerella forsythia*, and *Treponema denticola*, the so-called "red complex" bacteria, are major causative pathogens of periodontitis [15]. Red complex bacteria can survive within the host tissue due to their virulence factors that enable them to evade immune surveillance systems as well as proteolytic enzymes that provide amino acids for bacterial growth and disrupt the extracellular matrix of host tissues [16-18]. Additionally, periodontitis is related to the pathogenesis of various systemic diseases, including cardiovascular diseases, Alzheimer's disease, bone diseases, rheumatoid arthritis, oral and colorectal carcinoma, pregnancy complications, pneumonia, and diabetes [19]. Periodontal pathogens and their byproducts can enter the systemic circulation and affect the progression of these systemic diseases [20].

T. forsythia is a fusiform gram-negative anaerobic bacterium isolated from the human gingival pocket of patients with chronic periodontitis and is highly associated with the pathogenesis of periodontitis [21, 22]. Animal model experiments revealed that oral infection with *T. forsythia* induces activation of alveolar bone loss through the Toll-like receptor 2 (TLR2) signaling pathway [23, 24]. Moreover, periodontal pathogens can migrate to distant tissues and induce the development of systemic diseases [20]. For instance, *T. forsythia* was detected in atheromatous plaques of patients who underwent coronary artery bypass graft surgery and carotid endarterectomy [25], suggesting that *T. forsythia* might be associated with the pathogenesis of

cardiovascular diseases.

For the growth of *T. forsythia*, *N*-acetylmuramic acid (NAM), a component of the peptidoglycan cell wall of eubacteria, is required since *T. forsythia* lacks a metabolic pathway for NAM synthesis [26]. *T. forsythia* virulence factors, such as proteases, glycosidases, leucine-rich repeat family BspA, surface lipoproteins, and surface-layer associated glycoproteins, allow the bacterium to utilize available nutrients and survive within host tissue [18, 27]. Although *T. forsythia* is an asaccharolytic bacterium, it has various glycosidases. The nutrients that arise from the degradation of host oligosaccharides and proteoglycan through the action of *T. forsythia* glycosidases could be used by other oral bacteria for growth. Additionally, glycosidases of *T. forsythia* play a role in the progression of periodontitis since the integrity of host tissue is weakened by the degradation of oligosaccharides and proteoglycans [18]. BspA and bacterial lipoproteins induce the secretion of pro-inflammatory cytokines and chemokines from innate immune cells and gingival epithelial cells through the TLR2 signaling pathway [28-30]. Surface-layer (S-layer) is the distinct third layer outside the outer membrane of *T. forsythia* that plays a crucial role in evading phagocytosis by dendritic cells (DCs) and macrophages and suppressing Th17 responses [31].

P. gingivalis is a black-pigmented, asaccharolytic, anaerobic, non-motile gram-negative bacterium that is mostly associated with chronic periodontitis [32]. There is a correlation between the prevalence of *P. gingivalis* and periodontal pocket depth [33]. Animal model experiments revealed that oral inoculation of *P. gingivalis* to specific pathogen-free (SPF) mice induced inflammation in the periodontal region and resulted in alveolar bone loss, which were not observed in germ-free mice [34]. *P. gingivalis* is a “keystone pathogen;” it cannot induce inflammatory bone loss alone, but it impairs the host’s defense mechanisms, causing oral microbial dysbiosis that leads to

inflammatory bone loss [34, 35]. Hemin and vitamin K are essential for the growth of *P. gingivalis*. When grown under heme-limited condition, the virulence of *P. gingivalis* is reduced, and its morphology changes to that of short rods with few fimbriae; it subsequently produces large number of outer membrane vesicles (OMVs) [36].

Virulence factors of *P. gingivalis* include fimbriae, lipopolysaccharide (LPS), capsule, and cysteine proteinases (gingipains) [37]. *P. gingivalis* enters the gingival epithelial cells in a fimbriae-dependent manner [38]. Entering host cells is an evasive strategy against host immune surveillance systems [37]. Additionally, by secreting gingipains, *P. gingivalis* can degrade immunoglobulin, complements, chemokines, and cytokines, thereby impairing both innate and adaptive immunity [39]. Gingipains can also destroy host extracellular matrix components and affect vascular permeability, allowing *P. gingivalis* to enter the bloodstream, disseminate systemically, and colonize other organs [40]. *P. gingivalis* LPS elicits less inflammatory responses than other LPS due to its distinct structure compared to that of other gram-negative bacteria [37]. The weak inflammatory response to *P. gingivalis* LPS is considered a survival strategy against the host's innate immune surveillance system.

T. denticola is a spirochete present in the oral cavity of humans and is associated with chronic periodontitis [41]. Spirochetes have high motility due to periplasmic flagella, which twist into long spiral-shaped cells [42]. Generally, spirochetes are classified as gram-negative bacteria. However, phylogenetic studies have shown that the *Spirochaetes* phylum is distinct from both gram-negative and gram-positive bacteria [43]. *T. denticola* is frequently isolated along with *P. gingivalis* and *T. forsythia* in patient with periodontitis and is positively correlated with periodontal pocket depth and age [44]. Oral inoculation of *T. denticola* to mice resulted in alveolar bone resorption and the production of antibodies against 11 proteins. Among those

proteins, major outer sheath protein (Msp) and dentilisin were immunodominant [45]. Msp and dentilisin, which are in the outer sheath, are responsible for the virulence of *T. denticola* [41]. *T. denticola* can bind to human fibronectin, laminin, collagen, keratin, and fibrinogen via the Msp protein [46]. Dentilisin, which is a protease, contributes to the progression of periodontitis since it can degrade various host proteins, including extracellular matrix proteins, intercellular adhesion proteins, pro-inflammatory cytokines, and complement C3 [41]. The binding affinity of Msp and the proteolytic activity of dentilisin enable *T. denticola* to invade and colonize human gingival tissue. Furthermore, dentilisin activates the TLR2 signaling pathway, stimulating the production of matrix metalloproteinases (MMPs) in human periodontal ligament cells [47]. *T. denticola* has lipooligosaccharide (LOS) instead of LPS because treponemes lack the genes that encode LPS synthesis enzymes, but the function of LOS is similar to that of LPS [43]. *T. denticola* stimulates both the TLR2 and TLR4 signaling pathways; low numbers activate only TLR2, but high numbers can activate both TLR2 and TLR4. Msp and LOS are responsible for activation of the TLR2 and TLR4 pathways, respectively [48].

2. Immune cells and periodontitis

Immune cells that reside in the connective tissue of the gingiva regulate immune responses to various stimuli to maintain homeostasis. These immune cells, which include neutrophils, macrophages, DCs, T cells, and B cells, recognize bacteria and induce inflammatory responses to properly eliminate pathogens. However, periodontal pathogens can subvert the immune system and cause unregulated chronic inflammation, causing periodontitis. Therefore, identifying the response of immune cells to periodontal pathogens will help understand the pathogenesis of the periodontal diseases.

2.1. Helper T cell

Among the various immune cells, helper T cells play a central role in orchestrating the shapes of the immune system in the tissues. Helper T cells, including Th1, Th2, Th17, and Treg, are categorized by their functions. Among them, Th17 plays a central role in the inflammatory response in gingival tissue. In normal conditions, protective Th17 cells are induced by masticatory damage to the epithelium and promote immune surveillance of the gingival tissue environment [49]. However, pathogenic Th17 cells result from oral microbiome dysbiosis and induce destructive immune responses, including alveolar bone loss through IL-17A mediated mechanisms [50]. The expression level of IL-17 is increased in the sera and gingival tissues of patients with periodontitis [51, 52]. Additionally, the induction of pathogenic Th17 cells is related to the pathogenesis of periodontitis and other systemic diseases, including inflammatory bowel disease (IBD) [53]. Therefore, it is necessary to understand the mechanisms of oral pathogen-induced Th17 differentiation. Generally, differentiation of naïve $CD4^+$ T cells into effector helper T cells requires stimulation from antigen-presenting cells.

2.2. Dendritic cell

DCs are professional antigen-presenting cells (APCs) that take up and process antigens and present them to T cells to initiate adaptive immunity [54]. APCs express pattern-recognition receptors (PRRs), which recognize microbe-associated molecular patterns (MAMPs) that trigger innate immune responses. DCs mature through PRR signaling in tissues. They then migrate to the draining lymph nodes to present antigens to naïve T cells. Naïve $CD4^+$ T cells cannot recognize the antigen itself and only recognize the antigens presented by DCs through MHC class II molecules [55]. The clone of naïve $CD4^+$ T cells, which can recognize antigen-MHC class II complex of DCs, start to proliferate and differentiate into effector helper T cells. At that time, according to the cytokines secreted by DCs, naïve $CD4^+$ T cells differentiate

into a distinct lineage of helper T cell subsets to modulate immune responses in the appropriate direction [55]. Therefore, studies of DC activation by oral pathogens may provide insights into the mode of helper T cell differentiation.

2.3. B cell

B cells are adaptive immune cells that play a role in humoral immunity by secreting antibodies. B cells contribute to the protective immune response and maintain periodontal tissue homeostasis by producing antibodies against periodontal pathogens [56]. In a healthy state, memory B cells are the major B cell population in gingival tissue, but the ratio of memory B cells is decreased in periodontitis wherein antibody-secreting B cells are the dominant population [57]. Additionally, B cells substantially contribute to alveolar bone loss during inflammation since receptor activator of nuclear factor kappa-B ligand (RANKL), which induces differentiation and activation of osteoclasts, has greater expression in B cells in inflamed gingival tissues than in those in healthy gingival tissue [58, 59]. Therefore, B cells contribute to the immune response by not only secreting antibodies but also presenting antigens and secreting cytokines [56].

2.4. Neutrophil

Neutrophils are myeloid-derived innate immune cells that eliminate extracellular pathogens [60]. Neutrophils are the most abundant immune cells in the gingival crevice and periodontal pocket. During inflammation, the number of neutrophils in the gingival tissue and gingival crevice increases due to endogenous chemoattractants, including IL-8, IL-1β, and C5a, and exogenous bacteria chemotactic signals, including LPS and *N*-formyl-methionyl-leucyl-phenylalanine (fMLP) [60, 61]. Approximately 30,000 neutrophils per minute flow from the circulation into gingival tissue and migrate into the gingival crevice [62]. The extravasated neutrophils form a wall between the junctional epithelium and the dental plaque to kill the

microbes by phagocytosis, antimicrobial peptides, and reactive oxygen species (ROS) [63]. Genetic neutrophil defects show that fully functional neutrophils play a pivotal role in maintaining periodontal tissue health. For example, leukocyte adhesion deficiency causes a low neutrophil recruitment in periodontal tissue, resulting in aggressive periodontitis [60, 64]. Therefore, understanding the role of neutrophils in inflammatory responses in periodontal tissues is essential for treating periodontitis.

2.5. Macrophage

Macrophages are sentinels of various tissues and play a role in the maintenance of homeostasis by eliminating dead cells, clearing pathogens, and releasing danger-associated molecular patterns (DAMPs) [65]. Macrophages recognize invading pathogens through PRRs and release various chemokines and pro-inflammatory cytokines associated with the migration of immune cells and induction of inflammatory responses in nearby tissues. Periodontal tissue of patients with chronic periodontitis has a higher number of macrophages than that of healthy people [66]. *P. gingivalis* oral infection in mice resulted in macrophage recruitment to the gingival tissue and contributed to bone loss [67]. Additionally, in a mouse model of *P. gingivalis* oral inoculation and ligature, alveolar bone loss did not occur when macrophages were removed [67, 68]. Therefore, control of inflammation in the periodontium by macrophages is essential. In those processes, microorganisms may directly interact with immune cells to induce immune responses, but recent studies reported that extracellular vesicles released by microorganisms can play such a role.

3. Extracellular vesicles

Extracellular vesicles (EVs) are nano-sized vesicles released from living cells and carry various biological cargoes of donor cells such as proteins, lipids, nucleic acids, and metabolites [69]. EVs represent the physiological

status of donor cells and affect the physiology of recipient cells [70, 71]. Eukaryotic EVs are divided into exosomes, microvesicles, apoptotic bodies, and others according to their origin. Exosomes originate from the inner luminal vesicles (ILV) of the multivesicular body (MVB), microvesicles bud off from the plasma membrane, and apoptotic bodies are shed from apoptotic cells [70]. Since EVs have similar functions to their parent cells, studies on EVs have increased. It was confirmed that EVs of DCs primed with antigens of cancer cells could stimulate tumor antigen-specific T cells similar to DCs or transfer those antigens to other DCs for priming of naïve T cells [70, 72]. EVs derived from macrophages infected with pathogens carry immunostimulatory molecules that induce inflammatory responses in recipient cells [73]. Meanwhile microorganisms also release EVs. Gram-negative bacteria release outer membrane vesicles (OMVs), while gram-positive bacteria release membrane vesicles (MVs) [74]. Bacterial EVs can induce local and systemic inflammatory responses as they easily spread to the host tissues through the bloodstream and carry bacterial virulence factors [75, 76]. There is growing evidence that EVs derived from periodontal pathogens are associated with arteriosclerosis, Alzheimer's disease, rheumatoid arthritis, diabetes, and systemic bone loss [77-79].

4. Aims of the study

EVs may play a central role in the pathogenesis of periodontitis. This study aimed to evaluate the proteome and inflammatory response of EVs released from host cells infected with a periodontal pathogen and the mode of helper T cell differentiation induced by periodontal pathogen-derived OMVs.

First, it was hypothesized that EVs derived from *T. forsythia*-infected macrophages carry inflammatory mediators of macrophages and virulence factors of *T. forsythia,* which affect the pathogenesis of periodontitis and periodontitis-related systemic disease. To prove this hypothesis, the proteomic profiles and inflammatory responses of EVs derived from THP-1

macrophages infected with *T. forsythia* were analyzed.

Second, it was hypothesized that OMVs from "red complex" bacteria, *P. gingivalis*, *T. denticola*, and *T. forsythia*, could affect DC maturation and $CD4^+$ T cell differentiation. To prove this hypothesis, the maturation of DCs and mode of helper T cell differentiation induced by OMVs derived from red complex bacteria were analyzed using mouse bone marrow-derived DCs (BMDCs) and splenic naïve $CD4^+$ T cells.

II. Materials and Methods

1. THP-1 cell culture

THP-1 cells (ATCC TIB-202), a human monocytic cell line, were cultured in RPMI 1640 medium (Welgene, Daegu, South Korea) supplemented with 10% heat-inactivated fetal bovine serum (FBS; HyClone Laboratories, Inc., Logan, UT, USA), 100 U/ml penicillin and 100 μg/ml streptomycin (Gibco, Waltham, MA, USA) in a humidified 5% CO_2 atmosphere at 37°C. THP-1 macrophages were prepared as previously described [80]. THP-1 cells were differentiated into macrophages by treatment with 500 nM phorbol 12-Myristate 13-Acetate (PMA; Sigma-Aldrich, St. Louis, MO, USA) for 3 hours and washed with sterile phosphate-buffered saline (PBS; Welgene) followed by overnight incubation without PMA. To analyze TLR2-mediated cytokine secretion, THP1-Dual™ and THP1-Dual™ KO-TLR2 cells (InvivoGen, San Diego, CA, USA) were used. To maintain cells, 100 μg/ml Normocin™ (InvivoGen), 10 μg/ml blasticidin (InvivoGen), and 100 μg/ml Zeocin™ (InvivoGen) were added according to the manufacturer's instruction. THP-1 cells were routinely confirmed that free of mycoplasma contamination using e-Myco™ plus² Mycoplasma PCR Kit (iNtRON Biotechnology, Seongnam, South Korea).

2. Bacteria culture

P. gingivalis ATCC 33277 was cultured in brain heart infusion (BHI; BD Biosciences, San Jose, CA, USA) broth supplemented with 5 μg/ml hemin (Sigma-Aldrich) and 1 μg/ml vitamin K_3 (menadione; Sigma-Aldrich) under anaerobic conditions (10% CO_2, 10% H_2, and 80% N_2) at 37°C for 48 hours. *T. denticola* ATCC 33521 and *T. forsythia* ATCC 43037 were cultured in new oral spirochete broth (NOS; ATCC medium 1494) under anaerobic conditions at 37°C for 60 and 48 hours, respectively. For *T. forsythia*, 5 μg/ml hemin, 1 μg/ml vitamin K_3, and 10 μg/ml *N*-acetylmuramic acid (NAM; Sigma-

Aldrich) were added.

3. Isolation and characterization of EVs

3.1. Isolation of EVs derived from THP-1 macrophages infected with *T. forsythia*

THP-1 macrophages were washed three times with sterile PBS and then incubated in RPMI 1640 without FBS and antibiotics supplementation. The multiplicity of infection (MOI) 50 of *T. forsythia* infected to the THP-1 macrophages. The conditioned medium (CM) of *T. forsythia*-infected THP-1 macrophages was harvested at 48 hours post infection. Dead cells, cell debris, and large particles in the CM were removed by differential centrifugation at 300 × *g* for 10 minutes at 4°C, 2,000 × *g* for 10 minutes at 4°C, and 10,000 × *g* for 30 minutes at 4°C, respectively. Then, the centrifuged CM was filtered through a 0.22 μm pore polyethersulfone (PES) membrane filter system (Corning, New York, NY, USA). The clarified CM was concentrated by a 100 kDa molecular weight cut-off (MWCO) centrifugal filter (Centricon®; Merck Millipore, Burlington, MA, USA). The crude EVs were isolated from the concentrated CM by qEV® size exclusion chromatography (Izon Science, Christchurch, New Zealand) according to the manufacturer's instructions. Briefly, 0.5 ml of concentrated CM was loaded to the qEV® column, and then 0.5 ml of each fraction was harvested. The concentration of nanoparticles in each fraction was analyzed by nanoparticle tracking analysis (NTA). The nanoparticle enriched fractions (routinely fraction #7 to #11) were combined and named "crude EVs". For further experiments, the crude EVs were concentrated using a 10 kDa MWCO centrifugal filter (Amicon®; Merck Millipore). For density gradient ultracentrifugation (DGUC), the crude EVs were mixed with 60% iodixanol solution (OptiPrep™; Sigma-Aldrich) to make a 40% iodixanol solution (3.5 ml), then set at the bottom of an ultracentrifuge tube. Sterile PBS was mixed with 60% iodixanol solution to

make 35% (1.3 ml), 30% (2.4 ml), 25% (1.5 ml), 20% (2.8 ml) and 5% (1.5 ml) iodixanol solutions. The diluted iodixanol solution was carefully overlaid at the top of the 40% iodixanol-crude EVs to make a discontinuous density gradient. The gradient samples were centrifuged at 100,000 × *g* for 18 hours at 4°C using an Optima XE-100 (Beckman Coulter) with an SW 40 Ti (Beckman Coulter) swing bucket rotor. After ultracentrifugation, an equal volume (1.3 ml) of each fraction was harvested from the top of the gradient samples. NTA analyzed the nanoparticle concentration of each fraction. To remove iodixanol, nanoparticle enriched fractions were mixed with sterile PBS, ultracentrifuged at 120,000 × *g* for 2 hours at 4°C using Optima XE-100 with an SW 40 Ti swing bucket rotor, and discarded supernatant. The pellet was resuspended with sterile PBS and stored at −80°C until use.

3.2. Isolation of OMVs derived from periodontal pathogens

Each bacterial culture supernatant (400 ml) was collected and centrifuged at 10,000 × *g* for 10 minutes at 4°C. Then, cell-free culture supernatants were filtered using a 0.22 μm PES membrane filter system. The filtered culture supernatants were subjected to ultracentrifugation at 120,000 × *g* for 3 hours at 4°C using Optima XE-100 with a Type 45 Ti rotor (Beckman Coulter). The supernatants were discarded, and the pellets were resuspended in sterile PBS followed by ultracentrifugation at 120,000 × *g* for 2 hours at 4°C using an SW 40 Ti swing bucket rotor. The pellets were resuspended in PBS and mixed with 60% iodixanol solution to obtain a 40% solution (3.5 ml). The iodixanol-diluted pellets were laid on the bottom of an ultracentrifuge tube, and 35% (1.3 ml), 30% (2.4 ml), 25% (1.5 ml), 20% (2.8 ml) and 5% (1.5 ml) iodixanol solution diluted with PBS was overlaid. The discontinuous density gradient layers were ultracentrifuged at 100,000 × *g* for 18 hours at 4°C using an SW 40 Ti swing bucket rotor. The same volume (1.3 ml) of each fraction was harvested from top to bottom. The nanoparticle concentrations in each fraction were analyzed by NTA. The nanoparticle-enriched fractions were

mixed with PBS (10 ml) and ultracentrifuged at 120,000 × *g* for 2 hours at 4°C using an SW 40 Ti swing bucket rotor. After removal of the supernatant, the OMV pellets were resuspended with sterile PBS. The protein concentration of the OMVs were analyzed by Pierce™ BCA Protein Assay Kit (Thermo Fisher Scientific, Waltham, MA, USA) according to the manufacturer's instructions. The isolated OMVs were aliquoted and stored at −80°C until use.

3.3. Nanoparticle tracking analysis (NTA)

NanoSight LM10 (Malvern Instruments Ltd., Worcestershire, UK) was used to analyze the size and concentration of nanoparticles in samples. Each sample was diluted in nanoparticle-free PBS to adjust the proper concentration range. NTA software (Ver. 2.5, Malvern Instruments Ltd.) was used for data analysis, and the acquisition settings used in this experiment were as follows: screen gain, 12; camera level, 15; and detection threshold, 3.

3.4. Transmission Electron Microscopy (TEM)

Each EV sample (5 μl) was loaded to glow-discharged formvar/carbon-coated copper grid (Electron Microscopy Sciences, Hatfield, PA, USA) for 1 minute and was washed twice with distilled water, then was stained with 2% uranyl acetate for 1 minute. Negative stained EV samples were imaged by TEM (LIBRA 120; Carl Zeiss, Jena, Germany) at 120 kV.

3.5. Immunoblotting

EV samples were directly mixed with 5X sample buffer (1 M Tris-HCl, pH 6.8, 50% glycerol, 10% SDS, 5% 2-mercaptoethanol, and 0.1% bromophenol blue) and then were boiled at 95°C for 10 minutes. The samples were subjected to sodium dodecyl sulfate-polyacrylamide gel electrophoresis (SDS-PAGE) and transferred to polyvinylidene difluoride (PVDF)

membranes (Merck Millipore) followed by blocking with 5% non-fat dry milk (Cell Signaling Technology, Danvers, MA, USA) in Tris-Buffered Saline with 0.1% Tween® 20 Detergent (TBST) for 1 hour at room temperature (RT). The blocked membranes were incubated with primary antibodies overnight at 4°C. The membranes were washed with TBST three times each for 10 minutes followed by incubation with horseradish peroxidase-conjugated secondary antibodies (R&D Systems, Minneapolis, MN, USA) for 1 hour at RT. After washing with TBST three times each for 10 minutes, the membranes were soaked in ECL solution (Dyne Bio, Seongnam, South Korea) and were detected using ChemiDOC (Bio-Rad, Hercules, CA, USA). The primary antibodies used in this study were as follows: anti-CD63 (ab134045, Abcam, Cambridge, UK), anti-CD9 (ab92726, Abcam), anti-Alix (#2171, Cell Signaling Technology), anti-β-actin (#612656, BD Biosciences), anti-fibronectin (F3648, Sigma-Aldrich), anti-Histone H3 (#9715, Cell Signaling Technology), and anti-*T. forsythia* (D377-3, MBL, Nagoya, Japan).

3.6. SYPRO Ruby protein gel staining

The EV samples were directly mixed with 5X sample buffer and boiled at 95°C for 10 minutes. The samples were subjected to SDS-PAGE, and a gel was stained with SYPRO Ruby protein gel staining solution (Invitrogen, Waltham, MA, USA) according to the manufacturer's instructions. Briefly, a gel was fixed in 100 ml fixation solution (50% methanol, 7% acetic acid, and 43% deionized water) two times each for 30 minutes at RT. The fixed gel was stained overnight in 60 ml SYPRO Ruby protein gel staining solution at RT. The stained gel was washed once with 100 ml washing buffer (10% methanol, 7% acetic acid, and 83% deionized water) for 30 minutes and washed twice with 100 ml deionized water for 5 minutes. The gel was imaged by ChemiDOC.

4. Proteomics

4.1. EV sample preparation for proteome analysis

The EVs in each DGUC fraction were precipitated by 10% trichloroacetic acid (TCA). For EV protein digestion, a pellet of EV was reconstituted in 50 µl of SDT buffer [2% SDS, 0.1 M dithiothreitol (DTT) in 0.1 M Tris HCl, pH 8.0]. After being heated at 95°C, the denatured proteins were digested by a filter-aided sample preparation (FASP) method as previously described [81] with some modifications. Briefly, protein samples were loaded onto a 30 kDa MWCO centrifugal filter (Amicon®), and buffer was exchanged with UA solution (8 M UREA in 0.1 M Tris-HCl, pH 8.5) via centrifugation. After three buffer exchange with UA solution, the reduced cysteines were alkylated with 0.05 M iodoacetamide (IAA) in UA solution for 30 minutes at RT in the dark. Thereafter, UA buffer was twice exchanged for 40 mM ammonium bicarbonate (ABC). The protein samples were digested with trypsin/LysC (enzyme to substrate ratio of 1:100) at 37°C for 16 hours. The resulting peptides were collected in new tubes via centrifugation, and an additional elution step was performed using 40 mM ABC and 0.5 M NaCl. All resulting peptides were acidified with 10% trifluoroacetic acid and desalted using homemade C18-StageTips as described [81]. Desalted peptides were completely dried with a vacuum dryer and stored at −80°C.

4.2. LC-MS/MS analysis

LC-MS/MS analysis methods was performed using Quadrupole Orbitrap mass spectrometers, Q-exactive plus (Thermo Fisher Scientific) coupled to an Ultimate 3000 RSLC systems (Dionex, Sunnyvale, CA, USA) with a nano electrospray source as previously described with some modifications [81]. Peptide samples were separated on the 2-column setup with a trap column (75 µm I.D. × 2 cm, C18 3 µm, 100 Å) and analytical column (75 µm I.D. × 50 cm, C18 1.9 µm, 100 Å). Prior to sample injection, the dried peptide samples were redissolved in solvent A (2% acetonitrile and 0.1% formic acid). After

the samples were loaded onto the nano LC, a 180-min gradient from 8% to 30% solvent B (100% acetonitrile and 0.1% formic acid) was applied to all samples. The spray voltage was 2.0 kV in positive ion mode and the temperature of the heated capillary was set to 320°C. Mass spectra were acquired in data-dependent mode using a top 15 method on a Q Exactive. The Orbitrap analyzer scanned precursor ions with a mass range of 350–1800 m/z and resolution of 70,000 at m/z 200. Higher-energy collisional dissociation (HCD) scans were acquired on the Q Exactive at a resolution of 35,000. HCD peptide fragments were acquired at a normalized collision energy of 28. The maximum ion injection times for the survey and MS/MS scans were 20 and 80 ms, respectively.

4.3. Data processing for label-free quantification

Mass spectra were processed with MaxQuant (version 1.6.1.0) [82]. MS/MS spectra were searched against the Human Uniprot protein sequence database (December 2014, 88,657 entries) and NCBI XXXX protein sequence database (GCF_006385365.1_ASM638536v1_protein.fasta) using the Andromeda search engine [83]. Primary searches were performed using a 6-ppm precursor ion tolerance for total protein level analysis. The MS/MS ion tolerance was set to 20 ppm. Cysteine carbamido-methylation was set as a fixed modification. *N*-acetylation of proteins and oxidation of methionine were set as variable modifications. Enzyme specificity was set to full tryptic digestion. Peptides with a minimum length of six amino acids and up to two missed cleavages were considered. The required false discovery rate (FDR) was set to 1% at the peptide, protein, and modification levels. To maximize the number of quantification events across samples, matching between runs was performed.

4.4. Statistical analysis of the proteomic data

Statistical analyses for the proteomic data were performed using Perseus

software [84]. Initially, proteins identified as only identified by site, reverse, and contaminants were removed. The expression level of proteins in each fraction was estimated by determining their Intensity Based Absolute Quantification (iBAQ) values calculated using MaxQuant software. Because of the skewed distribution of the data, log2 transformation was conducted for these values. Valid values were filtered with proteins with a minimum of 70% quantified values in at least one diagnostic group. Missing values were imputed based on a normal distribution (width = 0.3, down-shift = 1.8) to simulate signals of low-abundance proteins. Two-sided t-tests were performed for pairwise comparison of proteomes to detect differentially expressed proteins (DEPs). The protein abundances were subjected to z-normalization followed by hierarchical clustering with Pearson's correlation distance.

4.5. Bioinformatics analysis

Gene ontology (GO) enrichment analysis in the Biological Process, Cellular Component, and Molecular Function category was performed using ShinyGO (V0.76.1) bioinformatics tool [85]. For visualization of the predicted associations for significantly expressed proteins, the STRING database (ver. 11.5) was used [86]. Subcellular localization of *T. forsythia* proteins was analyzed by CELLO v2.5 (http://cello.life.nctu.edu.tw/) from the Molecular Bioinformatics Center of National Chiao Tung University [87]. The lipid attachment site of each *T. forsythia* protein was predicted by the ExPASy-PROSITE protein domain database (https://prosite.expasy.org/). *T. forsythia* proteins were categorized into their functions and domains as described in the GenBank database of National Center for Biotechnology Information (NCBI).

5. *T. forsythia* culture in the EV-free conditioned medium of THP-1 macrophages

THP-1 macrophages infected with *T. forsythia* were cultured in RPMI 1640 without FBS and antibiotics supplementation for 24 hours in a humidified 5% CO_2 atmosphere at 37°C. The CM was harvested and clarified by differential centrifugation at 300 × *g* for 10 minutes at 4°C, 2,000 × *g* for 10 minutes at 4°C, and 10,000 × *g* for 30 minutes at 4°C. Biomolecules over 100 kDa, non-vesicular aggregates, and EVs in the clarified CM were eliminated by 100 kDa MWCO ultrafiltration. The filtrate was confirmed free of nanoparticles by NTA. The filtrate was treated with live *T. forsythia* in 150 mm cell culture dishes for 24 hours under humidified 5% CO_2 atmosphere at 37°C. The *T. forsythia* CM was harvested and centrifuged at 10,000 × *g* for 10 minutes at 4°C, then the pellet was discarded. As described above, the EVs in *T. forsythia* CM were isolated by size exclusion chromatography combined with DGUC.

6. CHO/CD14/TLR2 and CHO/CD14/TLR4 reporter cell assay

CHO/CD14/TLR2 and CHO/CD14/TLR4 reporter cells were obtained from Douglas Golenbock (Boston Medical Center, Boston, MA, USA). CHO/CD14/TLR2 or CHO/CD14/TLR4 cells (3×10^5 cells/well) were seeded to 48-well culture plates in the presence of G418 (1 mg/ml) and hygromycin B (0.4 mg/ml) for 20 hours. Then, the cells were stimulated with the indicated EVs for 16 hours. Pam3CSK4 (100 ng/ml, Invitrogen) and ultrapure LPS (100 ng/ml, Invitrogen) were used as a positive control for TLR2 and TLR4, respectively. Thereafter, the cells were stained with FITC anti-human CD25 antibody (BD Biosciences). The expression of CD25 was analyzed by measuring FITC fluorescence intensity of the cells using a FACS LSRFortessa X-20 (BD Biosciences). The FCS data files were analyzed using FlowJo software version 10.1 (BD Biosciences).

7. Mice

Eight-week-old C57BL/6N mice were purchased from Orient Bio (Seongnam, South Korea). All mouse experiments were approved by the Institutional Animal Care and Use Committee of Seoul National University (SNU-210602-1).

8. Bone marrow-derived dendritic cells (BMDCs)

Bone marrow cells were isolated from the femur and tibia of eight-week-old C57BL/6N mice. The isolated bone marrow cells were cultured in RPMI 1640 supplemented with 10% heat-inactivated FBS, 100 U/ml penicillin, 100 μg/ml streptomycin, 20 ng/ml recombinant murine granulocyte-macrophage colony-stimulating factor (rmGM-CSF; Peprotech, Rocky Hill, NJ, USA), and 55 μM β-mercaptoethanol (Gibco) for 7 days (37°C, 5% CO_2). On day 3, fresh medium was added. On day 7, floating cells were harvested and labeled with biotin anti-CD11c antibody (BioLegend, San Diego, CA, USA) and subsequently incubated with anti-biotin microbeads (Miltenyi Biotec, Bergisch Gladbach, Germany). The $CD11c^+$ cells were isolated using an MS column (Miltenyi Biotec) according to the manufacturer's instructions. The isolated $CD11c^+$ BMDCs were stimulated with 10 μg/ml periodontal pathogen OMVs in RPMI 1640 complete medium (10% heat-inactivated FBS, 100 U/ml penicillin, and 100 μg/ml streptomycin) for 24 hours. The expression of cell surface markers and cytokines was analyzed via flow cytometry and ELISA, respectively.

9. Coculture of naïve $CD4^+$ T cells with BMDCs

Naïve $CD4^+$ T cells were isolated from the spleen of eight-week-old C57BL/6N mice using a naïve $CD4^+$ T cell isolation kit (STEMCELL Technologies, Vancouver, BC, Canada). $CD11c^+$ BMDCs were stimulated with 10 μg/ml OMVs of periodontal pathogens in RPMI 1640 complete

medium for 5 hours and then washed with sterile PBS. OMV-primed BMDCs were cocultured with naïve $CD4^+$ T cells (DCs:T cells = 1:5) in the presence of 55 μM β-mercaptoethanol and 0.3 ng/ml anti-CD3ε antibody (clone 145-2C11; Bio X Cell, West Lebanon, NH, USA) in RPMI 1640 complete medium for 4 days (37°C, 5% CO_2). For neutralization of cytokines, 10 μg/ml anti-mouse-IL-6 antibody (clone MP5-20F3; Bio X Cell) and anti-mouse-IL-12p40 antibody (clone C17.8; Bio X Cell) were used.

10. Enzyme-linked immunosorbent assay (ELISA)

The expression levels of human TNF-α, IL-1β, IL-6, and IL-8 in the culture supernatant of THP-1 macrophages treated with EVs derived from THP-1 macrophages infected with *T. forsythia* were measured using an ELISA kit (R&D systems) according to the manufacturer's instructions. The expression levels of murine IL-1β, IL-4, IL-6, IL-23, and IL-12p70 in the culture supernatants of BMDCs stimulated with OMVs of periodontal pathogens were measured using an ELISA kit (BioLegend and R&D Systems). The optical density of each well was measured with an Epoch2 microplate reader (BioTek Instruments Inc., Winooski, VT, USA) at wavelengths of 450 nm and 540 nm.

11. Degradation of pro-inflammatory cytokines by periodontal pathogen OMVs

In 96-well cell culture plates, 1 ng/ml of recombinant murine IL-1β (R&D Systems), IL-6 (Peprotech), IL-23 (R&D Systems), and IL-12p70 (Peprotech) were incubated with OMVs (1 and 10 μg/ml) in 200 μl/well RPMI 1640 complete medium for 24 hours at 37°C in humidified aerobic conditions (5% CO_2). BMDCs were stimulated with 100 ng/ml Pam3CSK4 for 24 hours at 37°C. Culture supernatants of Pam3CSK4-treated BMDCs were incubated with *T. denticola* OMVs in the presence or absence of 2 mM phenylmethylsulfonyl fluoride (PMSF, Thermo Fisher Scientific), a serine

protease inhibitor, for 1 hour. Additionally, *T. denticola* OMVs were heated at 95°C for 10 minutes and incubated with culture supernatants of Pam3CSK4-treated BMDCs for 1 hour. The levels of the remaining cytokines in the medium or culture supernatants were measured by ELISA.

12. Quantitative real-time polymerase chain reaction (qRT-PCR)

RNA of $CD11c^+$ BMDCs was isolated using an easy-BLUE™ total RNA extraction kit (iNtRON Biotechnology) according to the manufacturer's instructions. The concentration of total RNA was quantified using a NanoDrop spectrophotometer (Thermo Fisher Scientific). To eliminate genomic DNA contamination, DNase I (Amplification Grade; Thermo Fisher Scientific) was treated to the total RNA samples according to the manufacturer's instructions. Complementary DNA (cDNA) was synthesized in a 30 μl reaction volume using 1 μg of DNase-treated RNA, oligo dT primer (Cosmo Genetech, Seoul, South Korea), and an M-MLV reverse transcriptase kit (Promega, Madison, WI, USA) according to the manufacturer's instructions. For qRT-PCR, cDNA (2 μl) was mixed with primer pairs (200 nM each) and 10 μl of Power SYBR® Green Master mix (Applied Biosystems, Waltham, MA, USA) in a 20 μl reaction volume. After an initial denaturation at 95°C for 5 minutes, cDNA was amplified for 40 cycles of denaturation (95°C, 15 second) and annealing (60°C, 1 minute) using a StepOne™ Plus real-time PCR system (Applied Biosystems). Gene expression levels as determined by qRT-PCR were normalized against glyceraldehyde-3-phosphate dehydrogenase (GAPDH) levels and calculated according to the $2^{-\Delta\Delta CT}$ method. The primers used in this experiment were as follows: *Gapdh*, forward 5′-AAT GGT GAA GGT CGG TGT GAA-3′ and reverse 5′-CAA TCT CCA CTT TGC CAC TGC-3′; *Il12a*, forward 5′-GAA GAC ATC ACA CGG GAC CAA-3′ and reverse 5′-CCA GGC AAC TCT CGT TCT TGT-3′; *Il23a*, forward 5′-CCA GCG GGA CAT ATG AAT CTA C-3′ and reverse 5′-

TGT CCT TGA GTC CTT GTG GG-3′. *Il1b* and *Il6* were used as previously described [88].

13. Flow cytometry

The Fc receptors on $CD11c^+$ BMDCs were blocked with TruStain FcX™ PLUS (anti-mouse CD16/32; BioLegend). The surface molecules of BMDCs were stained with FITC anti-mouse I-A/I-E antibody (MHC class II; clone M5/114.15.2; BioLegend), BB700 anti-mouse CD40 antibody (clone 3/23; BD Biosciences), APC anti-mouse CD80 antibody (clone 16-10A1; BioLegend), and PE anti-mouse CD86 antibody (clone GL-1; BioLegend).

For intracellular staining of $CD4^+$ T cells, the cells were incubated with 50 ng/ml PMA, 1 μM ionomycin (Sigma-Aldrich), and GolgiPlug™ (BD Biosciences) for 5 hours. The cells were stained with Ghost Dye™ Violet 510 (Tonbo Bioscience, San Diego, CA, USA) and fixed with Cyto-Fast™ Fix/Perm buffer (BioLegend) followed by washing with Cyto-Fast™ Perm/Wash buffer (BioLegend). The intracellular cytokines were stained with PE anti-mouse IFN-γ antibody (clone XMG1.2; BioLegend), Brilliant Violet 421™ anti-mouse IL-4 antibody (clone 11B11; BioLegend), and Alexa Fluor® 647 anti-mouse IL-17A antibody (clone TC11-18H10; BD Biosciences). Surface CD4 was stained with BB700 anti-mouse CD4 antibody (clone RM4-5; BD Biosciences). The fluorescence intensity of the cells was measured with a FACS LSRFortessa X-20. The FCS data files were analyzed using FlowJo software.

14. Statistics

The mean value ± standard deviation (*SD*) was determined for each group. Student's *t*-test was used to determine the significance of differences between two groups. One-way analysis of variance (ANOVA) with Dunnett's or Tukey's post-hoc test was used to determine the significance of differences between more than two groups. Two-way ANOVA with Sidak's post-hoc test

was used to examine the difference between two categorical independent variables. A *p*-value less than 0.05 was considered statistically significant. All statistical analyses were performed using GraphPad Prism software (GraphPad Software Inc., San Diego, CA, USA).

III. Results

1. Identification of proteome profile and immune responses of EVs derived from macrophages infected with *T. forsythia*

1.1 Two distinct types of EVs were identified from macrophages infected with *T. forsythia*.

EVs were isolated from the CM of *T. forsythia*-infected macrophages by size exclusion chromatography combined with DGUC. As a control, EVs from the CM of non-infected macrophages were isolated and analyzed simultaneously (Figure 1). The density gradient fractions were divided into 10 fractions (NI-F1 to NI-F10 for non-infected cells, and TF-F1 to TF-F10 for *T. forsythia*-infected cells).

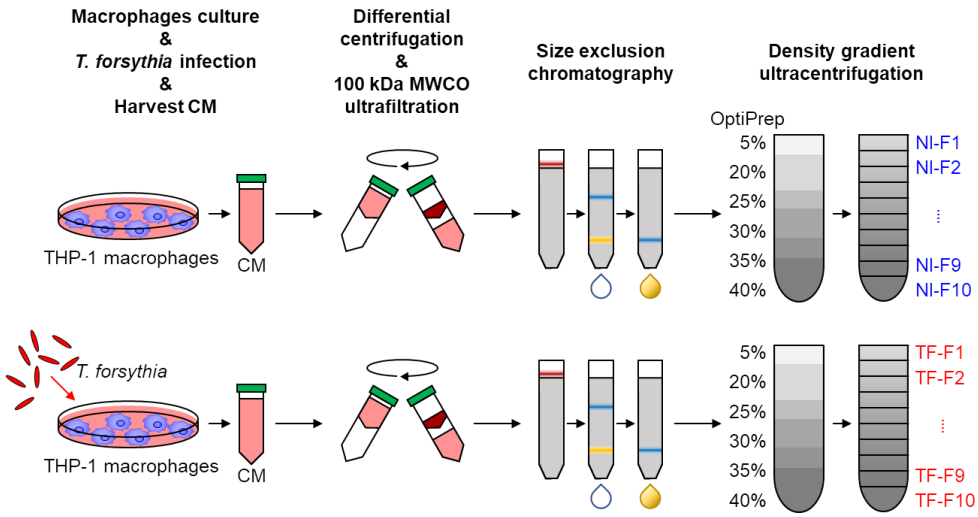

Figure 1. Schematic diagram of the isolation procedure of EVs derived from non-infected and *T. forsythia*-infected THP-1 macrophages. THP-1 macrophages were infected with MOI 50 of live *T. forsythia* for 48 hours. As a control, non-infected macrophages were simultaneously cultured for 48 hours simultaneously. CM of non-infected and *T. forsythia*-infected THP-1 macrophages were harvested. Dead cells and large debris in the CM were eliminated by differential centrifugation. The clarified CM was concentrated by 100 kDa MWCO ultrafiltration. The crude EVs were isolated from the concentrated CM by size exclusion chromatography and subjected to DGUC. Ten fractions were collected from top to bottom of a density gradient sample.

Regarding EVs from non-infected macrophages, the nanoparticles were enriched in NI-F2 and NI-F3, while few nanoparticles were observed in NI-F4 to NI-F10 (Figure 2a). The protein profiles of NI-F2 and NI-F3 were completely different from those of NI-F4 to NI-F10 (Figure 2b). TEM images showed that EVs were detected in NI-F2 (Figure 2c), whereas there were only small non-vesicular aggregates in NI-F5 and NI-F7. The markers of mammalian EVs, such as CD9 and CD63, were enriched in NI-F2 and NI-F3 (Figure 2d). However, host proteins, such as fibronectin and histone H3 that are known as non-vesicular aggregates proteins [89], were enriched in NI-F5 to NI-F8. β-Actin was detected in all the fractions except NI-F1. These results indicate that pure EVs were successfully separated from non-vesicular protein aggregates by DGUC.

Unlike EVs from non-infected macrophages, crude EVs derived from *T. forsythia*-infected macrophages were divided into three by DGUC (Figure 2a and 2b). TEM images showed that EVs were detected in not only TF-F2 but also in TF-F5, while non-vesicular aggregates, which are similar in size to EVs, were observed in TF-F7 (Figure 2c). The expression patterns of mammalian EV markers (CD9 and CD63) and non-vesicular proteins (fibronectin and histone H3) were similar to those of non-infected crude EVs (Figure 2d). Furthermore, *T. forsythia* proteins were highly enriched in TF-F4 to TF-F6 (Figure 2d).

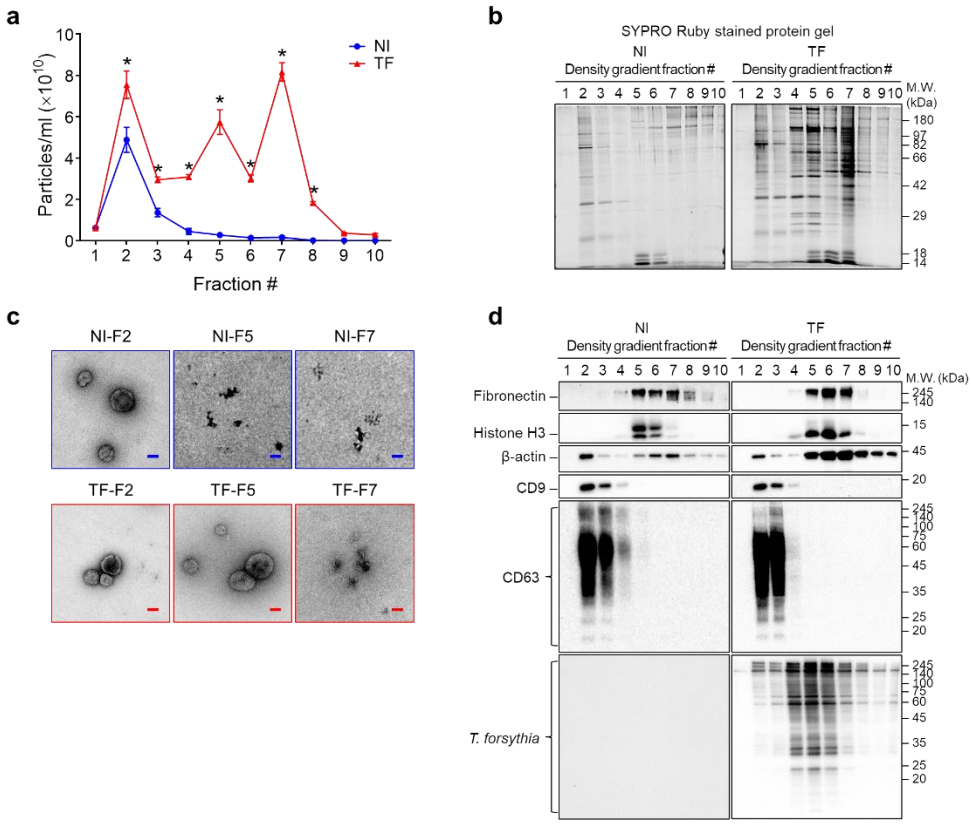

Figure 2. Characterization of EVs derived from THP-1 macrophages infected with *T. forsythia*. (a) Nanoparticle concentration of each density gradient fraction was analyzed by NTA. (b) Each density gradient fraction was subjected to SDS-PAGE and stained with SYPRO Ruby protein gel staining solution. The fluorescence of protein bands was imaged by ChemiDOC. (c) The indicated fractions were negatively stained and imaged by TEM. Scale bar: 50 nm. (d) Density gradient fractions were analyzed by immunoblotting using indicated antibodies. The experiments were performed at least three times independently. The data are presented as the mean ± *SD* of triplicate assays and were analyzed by two-way ANOVA. NI, non-infection; TF, *T. forsythia*-infection. * $p < 0.05$.

Next, to analyze whether mammalian EV markers and *T. forsythia* proteins are real vesicular proteins, crude EVs derived from *T. forsythia*-infected macrophages were treated with trypsin and subjected to DGUC (Figure 3). In F8–F10, the distinct bands around 16 and 20 kDa were soybean trypsin inhibitor, and 25–30 kDa bands were trypsin (Figure 4b). Trypsinization barely affected the particle concentration, protein profile, and morphology of EVs in TF-F2 and TF-F5 when analyzed by NTA, SDS-PAGE, and TEM (Figure 4a to 4c). Mammalian EV markers (Alix and CD63) in TF-F2 were not affected by trypsin treatment (Figure 4d). However, the particle concentration and protein profile in TF-F7 were remarkably reduced by trypsin treatment (Figure 4a and 4b). Interestingly, human proteins (fibronectin, histone H3, and β-actin) in TF-F5 and TF-F7 were eliminated, but *T. forsythia* proteins in F5 were negligibly eliminated by trypsin treatment (Figure 4d), suggesting that these human proteins were located to the outside of bacterial EVs. These results demonstrate that macrophage- and *T. forsythia*-derived EVs coexist at different densities in *T. forsythia* infections.

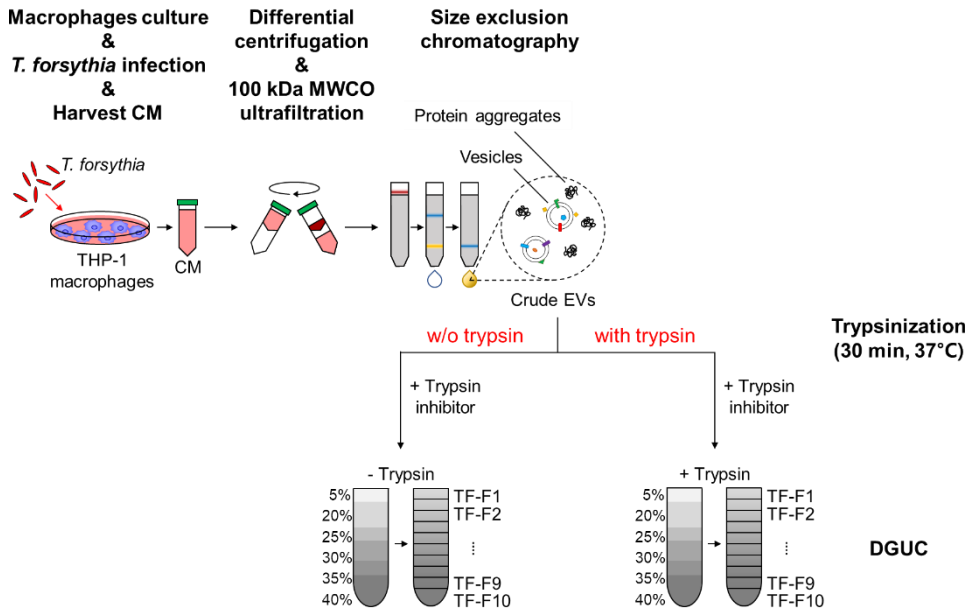

Figure 3. Schematic diagram of EV trypsinization. The crude EVs were isolated by size exclusion chromatography from CM of THP-1 macrophages infected with MOI 50 of live *T. forsythia*. Trypsin was applied to the crude EVs for 30 minutes at 37°C, and soybean trypsin inhibitor was added to terminate trypsinization. Trypsinized crude EVs were subjected to DGUC. Ten fractions were collected from top to bottom of a density gradient sample.

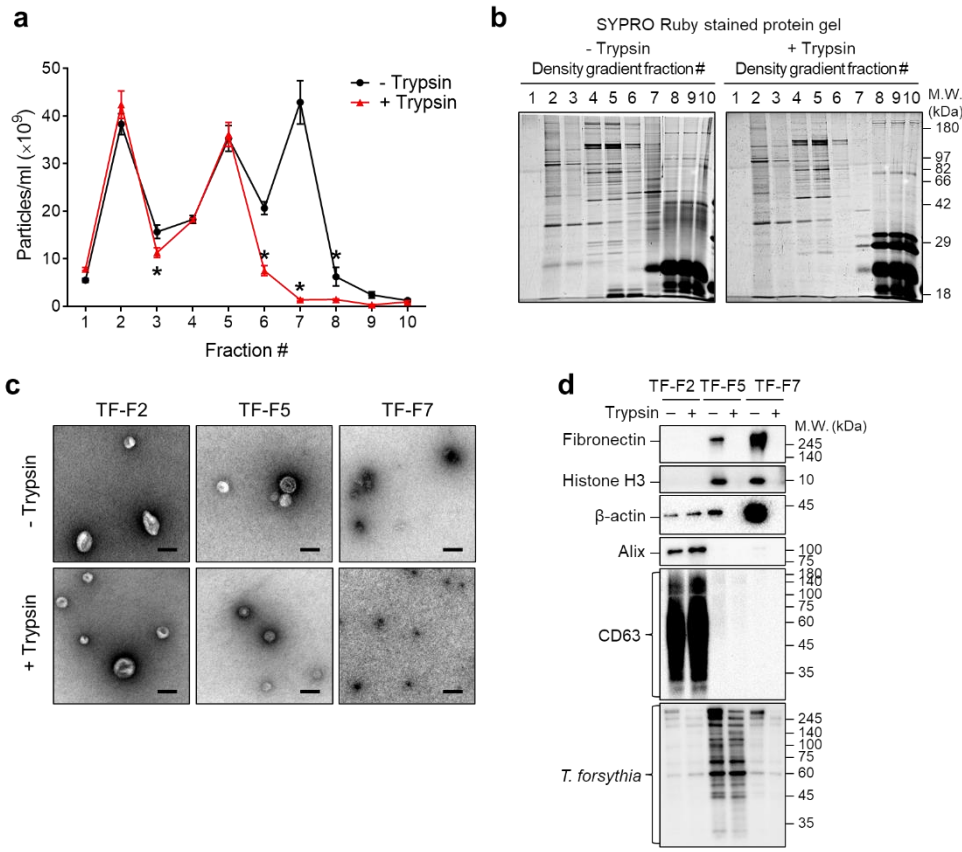

Figure 4. Elimination of non-vesicular proteins by trypsinization. (a) The nanoparticle concentration of each density gradient fraction of EVs after trypsinization was analyzed by NTA. (b) Each density gradient fraction was subjected to SDS-PAGE and was stained with SYPRO Ruby protein gel staining solution. The fluorescence of protein bands was imaged by ChemiDOC. (c) The indicated fractions were negatively stained and were imaged by TEM. Scale bar: 100 nm. (d) Indicated density gradient fractions were analyzed by immunoblotting using indicated antibodies. The experiments were performed at least three times independently. The data are presented as the mean ± *SD* of triplicate assays and were analyzed by two-way ANOVA. TF, *T. forsythia*-infection. * $p < 0.05$.

1.2 Macrophage-derived EVs of non-infected and *T. forsythia*-infected macrophages were analyzed by in-depth quantitative proteomics.

The proteomes of the two distinct EVs were analyzed by in-depth quantitative proteomics (Figure 5). The EVs of TF-F2 and TF-F5 from *T. forsythia*-infected macrophages were used for proteomic analysis, while those of NI-F2 from non-infected macrophages were used as controls.

Overall, 1,596 proteins were identified. There were 1,247 human proteins and 349 *T. forsythia* proteins. Principal component analysis (PCA) showed that the proteome compositions were completely different from each other (Figure 6).

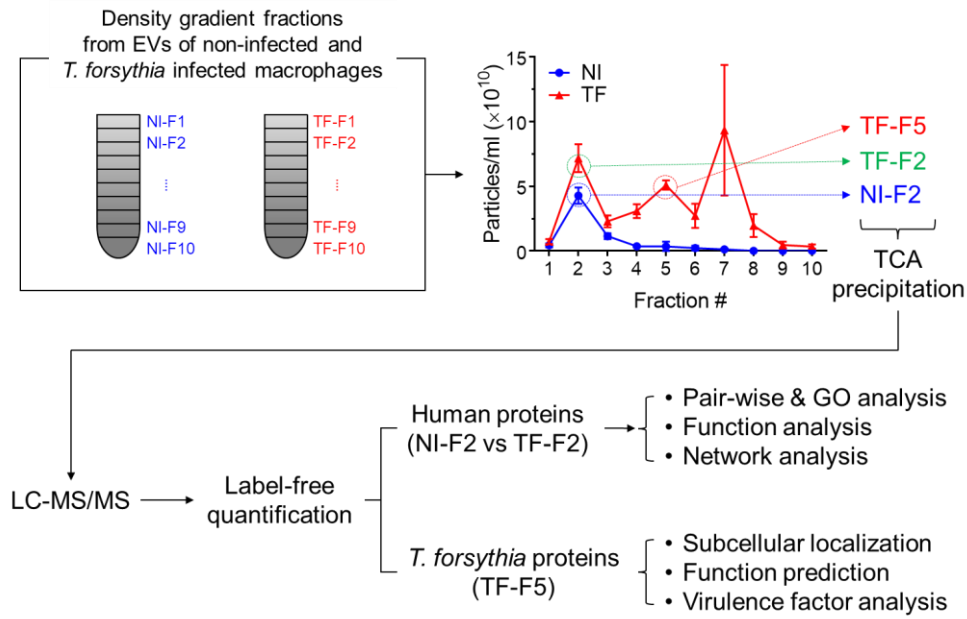

Figure 5. Schematic diagram of the procedure for proteomic analysis of EVs. Nanoparticle concentration of six independently performed DGUC samples were analyzed by NTA. NI-F2, TF-F2, and TF-F5 were pelleted by TCA precipitation methods and analyzed by LC-MS/MS. Human proteins in NI-F2 and TF-F2 were compared. *T. forsythia* proteins in TF-F5 were predicted for their subcellular localization, functions, and virulence factors. NI, non-infection; TF, *T. forsythia*-infection.

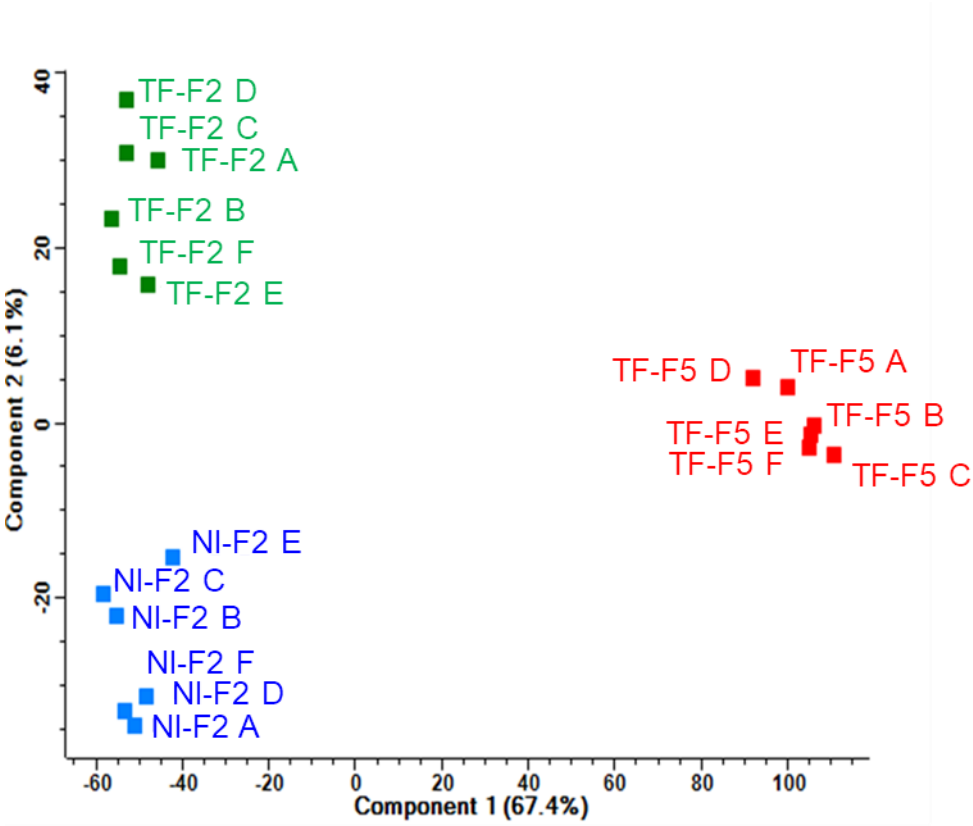

Figure 6. Principal components analysis of proteomes identified in NI-F2, TF-F2, and TF-F5. Principal component analysis (PCA) results of the proteomes of identified in the three different EVs. In-depth quantitative proteomic analysis was performed using EV samples from six independent experiments. NI, non-infection; TF, *T. forsythia*-infection.

The differentially expressed proteins of NI-F2 and TF-F2 were represented by a volcano plot (Figure 7a and Table 1). Among them, higher expression of proteins in TF-F2 than in NI-F2 was detected for pro-inflammatory cytokines (TNF, CXCL8, and IL-1β), copine-1 (CPNE1), osteopontin (SPP1), phospholipid scramblase 1 (PLSCR1), P2X purinoceptor 4 (P2RX4), matrix metalloproteinase-9 (MMP9), serine and valine tRNA ligases (SARS and VARS), syntaxin-binding protein 2 (STXBP2), voltage-gated hydrogen channel 1 (HVCN1), CD82, raftlin (RFTN1), plastin-2 (LCP1), and plasma membrane calcium-transporting ATPase 1 (ATP2B1), which are related with pathogenesis of periodontitis and other inflammatory diseases (Table 1). In contrast, complements (C3 and C4B), 14-3-3 proteins (SFN, YWHAQ, YWHAG, YWHAE, and YWHAB), and integrins (ITGAM, ITGAX, ITGA6, ITGA5, ITGAL, and ITGB1) were highly expressed in NI-F2 compared to TF-F2 (Table 1). Gene ontology (GO) was also analyzed (Figure 7b). GO Biological Process (GOBP) showed that proteins related to neutrophil activation (GO:0042119), granulocyte activation (GO:0036230), regulated exocytosis (GO:0045055), and leukocyte mediated immunity (GO:0002443) related proteins were enriched in TF-F2, whereas proteins associated with integrin-mediated signaling pathway (GO:0007229) and regulation of protein localization to membrane (GO:1905475) associated proteins were enriched in NI-F2 (Figure 7b). GO Cellular Component (GOCC) showed that chaperonin-containing T-complex (GO:0005832) was highly enriched in TF-F2, whereas integrin complex (GO:0008305) and protein complex involved in cell adhesion (GO:0098636) were enriched in NI-F2 (Figure 7b). GO Molecular Function (GOMF) showed that cadherin binding (GO:0045296) and cell adhesion molecule binding (GO:0050839) were enriched in TF-F2, whereas Rho GDP-dissociation inhibitor activity (GO:0005094) and protein kinase C inhibitor activity (GO:0008426) were highly enriched in NI-F2 (Figure 7b). The protein–protein interaction network of differentially expressed human proteins in NI-F2 and TF-F2 were plotted using the

STRING database (Figure 8). The proteins were clustered into immune system process, regulation of localization, RNA binding, integral component of membrane, acetylation, actin binding, and multivesicular body assembly. The results indicate that in *T. forsythia*-infection, macrophage-derived EVs carried various proteins that were associated with pro-inflammatory responses and immune cell activation.

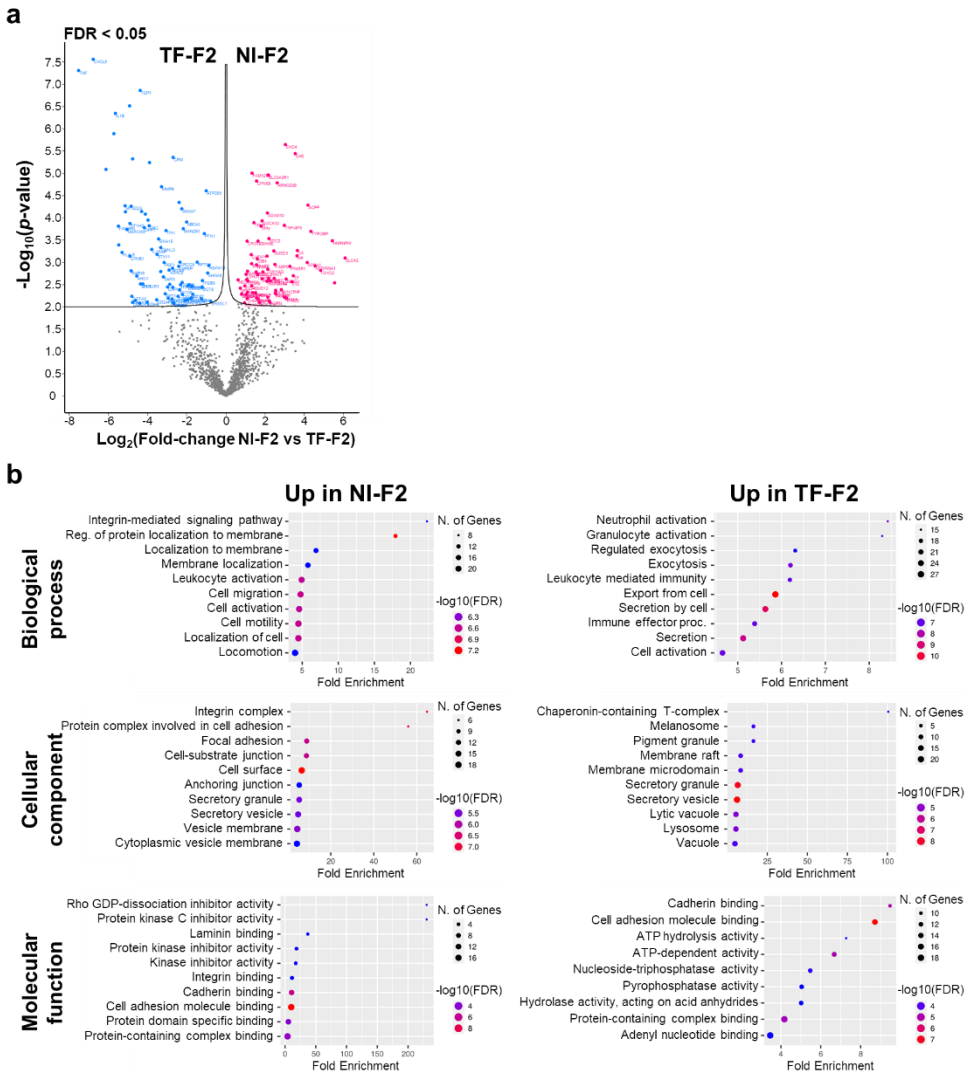

Figure 7. Analysis of differentially expressed human proteins in NI-F2 vs. TF-F2. (a) Volcano plot depicts differentially expressed proteins between NI-F2 and TF-F2. FDR is less than 0.05. (b) GO was analyzed for Biological Process, Cellular Component, and Molecular Function by ShinyGO V0.76. The dot plot showing the top 10 GO terms ranked by fold enrichment. In-depth quantitative proteomic analysis was performed using EV samples from six independent experiments. NI, non-infection; TF, *T. forsythia*-infection; FDR, false discovery rate.

Table 1. List of differentially expressed human proteins in TF-F2 vs NI-F2.

Uniprot Accession	Protein name	Gene name	$-\text{Log}_{10}$(*p*-value)	Difference[a]
I. Differentially expressed human proteins in TF-F2				
P01375	Tumor necrosis factor	TNF	7.3	-7.5
P10145	Interleukin-8	CXCL8	7.6	-6.8
P01584	Interleukin-1 beta	IL1B	6.3	-5.6
Q9NUQ9	Protein FAM49B	FAM49B	3.8	-5.5
P01889	HLA class I histocompatibility antigen, B-7 alpha chain	HLA-B	3.2	-5.3
Q8NA29	Sodium-dependent lysophosphatidylcholine symporter 1	MFSD2A	4.3	-5.2
P29966	Myristoylated alanine-rich C-kinase substrate	MARCKS	3.7	-5.1
Q99829	Copine-1	CPNE1	3.1	-4.9
Q9BSA4	Protein tweety homolog 2	TTYH2	3.9	-4.9
Q9NP72	Ras-related protein Rab-18	RAB18	2.8	-4.8
Q16772	Glutathione S-transferase A3	GSTA3	2.2	-4.8
Q9H3Z4	DnaJ homolog subfamily C member 5	DNAJC5	2.1	-4.8
Q9Y3L5	Ras-related protein Rap-2c	RAP2C	2.1	-4.6
P23526	Adenosylhomocysteinase	AHCY	2.7	-4.5
P17987	T-complex protein 1 subunit alpha	TCP1	6.9	-4.4
P10451	Osteopontin	SPP1	2.5	-4.4
O15162	Phospholipid scramblase 1	PLSCR1	2.5	-4.2
Q9UHL4	Dipeptidyl peptidase 2	DPP7	3.8	-4.2
P11766	Alcohol dehydrogenase class-3	ADH5	2.1	-4.0
P12931	Proto-oncogene tyrosine-protein kinase Src	SRC	3.8	-3.9
Q9NPH3	Interleukin-1 receptor accessory protein	IL1RAP	3.3	-3.8
Q99571	P2X purinoceptor 4	P2RX4	2.0	-3.7
Q9Y5K6	CD2-associated protein	CD2AP	2.2	-3.5
O75558	Syntaxin-11	STX11	3.2	-3.5
P40227	T-complex protein 1 subunit zeta	CCT6A	2.0	-3.5
P30679	Guanine nucleotide-binding protein subunit alpha-15	GNA15	3.5	-3.4
Q8IVF7	Formin-like protein 3	FMNL3	3.3	-3.3
P14780	Matrix metalloproteinase-9	MMP9	4.7	-3.3
P49591	Serine--tRNA ligase, cytoplasmic	SARS	2.7	-3.2
Q9UBV8	Peflin	PEF1	3.0	-3.2
P50897	Palmitoyl-protein thioesterase 1	PPT1	2.3	-3.1
P60174	Triosephosphate isomerase	TPI1	3.7	-3.1
Q9Y6W3	Calpain-7	CAPN7	2.4	-3.0
P09972	Fructose-bisphosphate aldolase C	ALDOC	2.2	-2.9
P45880	Voltage-dependent anion-selective channel protein 2	VDAC2	2.8	-2.9
Q15833	Syntaxin-binding protein 2	STXBP2	2.0	-2.8
P18077	60S ribosomal protein L35a	RPL35A	2.2	-2.7
O95197	Reticulon-3	RTN3	2.9	-2.7
Q02543	60S ribosomal protein L18a	RPL18A	2.1	-2.7
P14384	Carboxypeptidase M	CPM	5.4	-2.7
P26640	Valine--tRNA ligase	VARS	2.1	-2.7
Q9UBQ0	Vacuolar protein sorting-associated protein 29	VPS29	2.1	-2.6
P49327	Fatty acid synthase	FASN	2.2	-2.4
Q9UIQ6	Leucyl-cystinyl aminopeptidase	LNPEP	2.9	-2.4
Q9NZM1	Myoferlin	MYOF	2.4	-2.4
P13010	X-ray repair cross-complementing protein 5	XRCC5	3.0	-2.3
Q96D96	Voltage-gated hydrogen channel 1	HVCN1	2.5	-2.3
P20073	Annexin A7	ANXA7	4.2	-2.2
Q969P0	Immunoglobulin superfamily member 8	IGSF8	2.5	-2.2
O00571	ATP-dependent RNA helicase DDX3X	DDX3X	2.3	-2.2
O00754	Lysosomal alpha-mannosidase	MAN2B1	3.8	-2.2
B0I1T2	Unconventional myosin-Ig	MYO1G	2.1	-2.1
O95477	ATP-binding cassette sub-family A member 1	ABCA1	3.9	-2.0
P11586	C-1-tetrahydrofolate synthase, cytoplasmic	MTHFD1	2.2	-2.0
P26196	Probable ATP-dependent RNA helicase DDX6	DDX6	2.5	-1.9
P08133	Annexin A6	ANXA6	2.5	-1.9
O60884	DnaJ homolog subfamily A member 2	DNAJA2	2.2	-1.8
P54709	Sodium/potassium-transporting ATPase subunit beta-3	ATP1B3	2.2	-1.8
Q9UN37	Vacuolar protein sorting-associated protein 4A	VPS4A	2.5	-1.7
P27701	CD82 antigen	CD82	2.3	-1.7

Uniprot Accession	Protein name	Gene name	$-Log_{10}$(*p*-value)	Difference[a]
Q14699	Raftlin	RFTN1	3.0	-1.5
P13796	Plastin-2	LCP1	2.2	-1.3
P50990	T-complex protein 1 subunit theta	CCT8	2.4	-1.2
P05106	Integrin beta-3	ITGB3	2.6	-1.2
P07737	Profilin-1	PFN1	3.6	-1.1
P20020	Plasma membrane calcium-transporting ATPase 1	ATP2B1	4.6	-1.0
Q09666	Neuroblast differentiation-associated protein AHNAK	AHNAK	2.8	-0.9
P0DMV9	Heat shock 70 kDa protein 1B	HSPA1B	2.9	-0.9
Q99961	Endophilin-A2	SH3GL1	2.1	-0.8
II. Differentially expressed human proteins in NI-F2				
Q8NBI5	Solute carrier family 43 member 3	SLC43A3	3.1	6.1
P52272	Heterogeneous nuclear ribonucleoprotein M	HNRNPM	3.5	5.4
P01859	Ig gamma-2 chain C region	IGHG2	2.8	4.8
P01009	Alpha-1-antitrypsin	SERPINA1	2.9	4.5
O43914	TYRO protein tyrosine kinase-binding protein	TYROBP	3.7	4.3
P15309	Prostatic acid phosphatase	ACPP	4.3	4.2
P02647	Apolipoprotein A-I	APOA1	3.0	4.2
P01024	Complement C3	C3	3.3	3.7
P00738	Haptoglobin	HP	3.1	3.6
P0C0L5	Complement C4-B	C4B	5.4	3.5
Q9P0V8	SLAM family member 8	SLAMF8	2.0	3.5
P02787	Serotransferrin	TF	2.7	3.4
Q9UI08	Ena/VASP-like protein	EVL	2.6	3.4
P15260	Interferon gamma receptor 1	IFNGR1	2.9	3.3
Q9Y287	Integral membrane protein 2B	ITM2B	2.2	3.1
P0DOX5	Ig gamma-1 chain C region	IGHG1	2.6	3.1
Q9H223	EH domain-containing protein 4	EHD4	5.6	3.0
P01876	Ig alpha-1 chain C region	IGHA1	2.2	3.0
P21580	Tumor necrosis factor alpha-induced protein 3	TNFAIP3	3.8	3.0
O60506	Heterogeneous nuclear ribonucleoprotein Q	SYNCRIP	2.4	2.8
P52566	Rho GDP-dissociation inhibitor 2	ARHGDIB	4.8	2.6
P55899	IgG receptor FcRn large subunit p51	FCGRT	2.3	2.5
P31947	14-3-3 protein sigma	SFN	2.4	2.5
P01860	Ig gamma-3 chain C region	IGHG3	2.3	2.5
Q01469	Fatty acid-binding protein, epidermal	FABP5	3.0	2.5
P81605	Dermcidin;Survival-promoting peptide	DCD	2.6	2.5
Q96L08	Sushi domain-containing protein 3	SUSD3	3.3	2.4
P40121	Macrophage-capping protein	CAPG	2.1	2.3
O43760	Synaptogyrin-2	SYNGR2	2.6	2.3
P00450	Ceruloplasmin	CP	2.1	2.2
O00468	Agrin	AGRN	2.1	2.2
P34741	Syndecan-2	SDC2	3.5	2.2
Q8IV08	Phospholipase D3	PLD3	2.6	2.2
O14745	Na(+)/H(+) exchange regulatory cofactor NHE-RF1	SLC9A3R1	5.0	2.2
P27348	14-3-3 protein theta	YWHAQ	2.8	2.1
O14672	Disintegrin and metalloproteinase domain-containing protein 10	ADAM10	4.1	2.1
Q71DI3	Histone H3.2	HIST2H3A	2.6	2.1
P61981	14-3-3 protein gamma	YWHAG	2.1	2.0
Q7Z2W4	Zinc finger CCCH-type antiviral protein 1	ZC3HAV1	2.8	1.9
Q9P2B2	Prostaglandin F2 receptor negative regulator	PTGFRN	2.6	1.9
Q96BY6	Dedicator of cytokinesis protein 10	DOCK10	3.9	1.8
O43399	Tumor protein D54	TPD52L2	2.1	1.8
P16150	Leukosialin	SPN	3.8	1.8
P02671	Fibrinogen alpha chain	FGA	2.1	1.7
Q13571	Lysosomal-associated transmembrane protein 5	LAPTM5	2.1	1.7
P62258	14-3-3 protein epsilon	YWHAE	3.5	1.6
Q96C86	m7GpppX diphosphatase	DCPS	2.2	1.6
P11215	Integrin alpha-M	ITGAM	2.7	1.6
Q99828	Calcium and integrin-binding protein 1	CIB1	3.1	1.6
P20702	Integrin alpha-X	ITGAX	2.9	1.6
P23229	Integrin alpha-6	ITGA6	2.2	1.6
Q86YQ8	Copine-8	CPNE8	4.8	1.6
P05556	Integrin beta-1	ITGB1	2.8	1.5
P19623	Spermidine synthase	SRM	2.3	1.5

Uniprot Accession	Protein name	Gene name	$-Log_{10}$(*p*-value)	Difference[a]
P31946	14-3-3 protein beta/alpha	YWHAB	2.3	1.5
P06753	Tropomyosin alpha-3 chain	TPM3	3.9	1.4
P50281	Matrix metalloproteinase-14	MMP14	2.3	1.4
Q96TA1	Niban-like protein 1	FAM129B	5.0	1.3
O00232	26S proteasome non-ATPase regulatory subunit 12	PSMD12	2.5	1.3
O75044	SLIT-ROBO Rho GTPase-activating protein 2	SRGAP2	3.0	1.3
Q7L576	Cytoplasmic FMR1-interacting protein 1	CYFIP1	3.2	1.3
P08648	Integrin alpha-5	ITGA5	2.6	1.1
O95819	Mitogen-activated protein kinase kinase kinase kinase 4	MAP4K4	2.8	1.1
P53990	IST1 homolog	IST1	2.3	1.1
Q5TZA2	Rootletin	CROCC	3.5	1.1
O43633	Charged multivesicular body protein 2a	CHMP2A	2.2	1.1
P42356	Phosphatidylinositol 4-kinase alpha	PI4KA	2.6	1.1
P00338	L-lactate dehydrogenase A chain	LDHA	2.7	1.0
P62834	Ras-related protein Rap-1A	RAP1A	2.3	1.0
P20701	Integrin alpha-L	ITGAL	2.5	1.0
P52565	Rho GDP-dissociation inhibitor 1	ARHGDIA	2.1	0.9
P22732	Solute carrier family 2, facilitated glucose transporter member 5	SLC2A5	2.3	0.8
P62993	Growth factor receptor-bound protein 2	GRB2	2.3	0.8
P08582	Melanotransferrin	MFI2	2.4	0.7
Q9ULI3	Protein HEG homolog 1	HEG1	2.6	0.6

a Difference: Log_2(Fold-change NI-F2 vs. TF-F2)

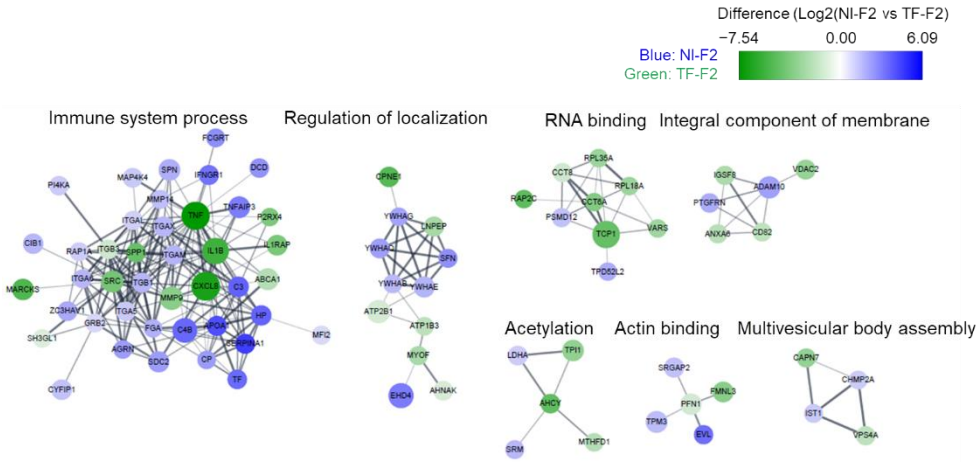

Figure 8. Analysis of differentially expressed human proteins in NI-F2 vs. TF-F2. Differentially expressed human proteins in NI-F2 and TF-F2 were combined, and their interactions were analyzed by Cytoscape based on the STRING database. The size of node represents the significance [$-\mathrm{Log}_{10}(p\text{-value})$]. Green nodes represent upregulated proteins in TF-F2, and blue nodes represent upregulated proteins in NI-F2. The thickness of the gray line represents confidence scores of protein–protein interactions derived from the STRING database. NI, non-infection; TF, *T. forsythia*-infection.

1.3 *T. forsythia* proteins in *T. forsythia*-derived EVs were analyzed by in-depth quantitative proteomics.

Proteomic analysis identified 349 *T. forsythia* proteins in TF-F5; 170 have been identified in previous reports on *T. forsythia* OMVs [90, 91], and 179 were identified in this study (Table 2). According to Yoo et al., 12 proteins were upregulated by *in vivo*-induced antigen technology (IVIAT) using serum from patients with periodontitis [92]. Among these proteins, seven were in TF-F5, including TonB-dependent receptor plug domain-containing protein (WP_046825933.1), RagB/SusD family nutrient uptake outer membrane protein (WP_046825921.1), two S9 family peptidases (WP_046825437.1 and WP_046824629.1), leucine-rich-repeat family virulence factor BspA (WP_052449061.1), OmpA family protein (WP_046824554.1), and beta-glucosidase BglX (WP_080948511.1). Subcellular localization of *T. forsythia* proteins was analyzed by CELLO database: outer membrane proteins account for the majority (138 proteins, 39.5%), followed by cytoplasmic (88 proteins, 25.2%), periplasmic (86 proteins, 24.6%), extracellular (32 proteins, 9.2%), and inner membrane (5 proteins, 1.4%) proteins (Table 2). This composition was similar to a previously reported proteome of *T. forsythia* OMVs [90]. Overall, 95 bacterial lipoproteins (27.2%) were predicted by the ExPASy-PROSITE protein domain database (Table 2). All *T. forsythia* proteins were categorized into their functions according to the domains described in the GenBank database. TonB-dependent receptors and its associated proteins occupied the largest portion of them (96 proteins, 27.5%). Twenty-one proteins (6.0%) were components of type IX secretion system (T9SS) and its substrates. Thirty-two proteins (9.2%) were peptidases, and twelve proteins (3.4%) were glycosyl hydrolases. Ten proteins (2.9%) were proteins with tetratricopeptide repeat domains. Four proteins (1.1%) were TolC family proteins. Three proteins (0.9%) were chaperonin, and two proteins (0.6%) were peroxidases. Twenty-two proteins (6.3%) had domains of unknown

function. Fifty-one proteins (14.6%) did not have any reported domains. Detailed information of TF-F5 *T. forsythia* proteins is listed on Table 2.

Table 2. List of *T. forsythia* proteins identified in TF-F5.

Accession	Definition	Amino acid	M.W. (kDa)	iBAQ	Previously reported proteins of Tf OMVs	Predicted Subsellular Location[c]	Lipoprotein[d]
I. TonB-dependent receptors and its associated proteins (96/349)							
i. TonB-dependent receptors (55/349)							
WP_046824810.1	TonB-dependent receptor	670	76.2	94140000		Outer Membrane	
WP_046825933.1	TonB-dependent receptor plug domain-containing protein	709	81.3	71073167		Outer Membrane	
WP_046824469.1	TonB-dependent receptor	770	87.2	54803500	a, b	Outer Membrane	
WP_087879765.1	TonB-dependent receptor	780	88.3	40526550		Outer Membrane	
WP_161794935.1	TonB-dependent receptor	767	87.4	35777250		Outer Membrane	
WP_046825715.1	TonB-dependent receptor	748	84.9	32609000		Outer Membrane	
WP_070098097.1	TonB-dependent receptor	852	95.2	27993667		Outer Membrane	
WP_046825711.1	TonB-dependent receptor	744	83.5	14834817		Outer Membrane	
WP_046826211.1	TonB-dependent receptor	928	104.2	13375917	a	Outer Membrane	
WP_046826221.1	TonB-dependent receptor	786	89.2	9320383		Outer Membrane	
WP_052449006.1	DUF5686 and carboxypeptidase regulatory-like domain-containing protein	897	102.3	9148317		Outer Membrane	
WP_046824884.1	TonB-dependent receptor	952	106.7	8590233		Outer Membrane	
WP_046824887.1	TonB-dependent receptor	780	87.5	8294233		Outer Membrane	
WP_052449124.1	TonB-dependent receptor	983	110.2	7792183		Outer Membrane	
WP_014226387.1	TonB-dependent receptor	818	92.2	6380600	a	Outer Membrane	
WP_046824590.1	carboxypeptidase regulatory-like domain-containing protein	1085	121.0	6245667	a, b	Outer Membrane	
WP_004585028.1	MULTISPECIES: carboxypeptidase regulatory-like domain-containing protein	891	100.4	5730183		Outer Membrane	
WP_052449117.1	TonB-dependent receptor	1154	129.0	5536433	a, b	Outer Membrane	
WP_046824978.1	TonB-dependent receptor	1179	132.7	4487350	a	Outer Membrane	
WP_052449113.1	TonB-dependent receptor	1148	128.3	4306783		Outer Membrane	
WP_161794958.1	SusC/RagA family TonB-linked outer membrane protein	1121	125.2	4070500		Outer Membrane	
WP_052449077.1	TonB-dependent receptor	1134	128.3	2995100		Outer Membrane	
WP_052449042.1	SusC/RagA family TonB-linked outer membrane protein	1072	119.4	2654435		Outer Membrane	
WP_080948581.1	TonB-dependent receptor	1154	128.8	2237838		Outer Membrane	
WP_046825765.1	TonB-dependent receptor	1156	130.3	2234495	a	Outer Membrane	
WP_080948590.1	TonB-dependent receptor	1131	125.4	1920207		Outer Membrane	
WP_046825251.1	TonB-dependent receptor	1100	122.4	1670988		Outer Membrane	
WP_080948655.1	TonB-dependent receptor	1127	124.6	1556477		Outer Membrane	
WP_046825525.1	SusC/RagA family TonB-linked outer membrane protein	1032	113.6	1479112	a, b	Outer Membrane	
WP_046825920.1	TonB-dependent receptor	1091	121.3	1451193	a, b	Outer Membrane	
WP_046824947.1	TonB-dependent receptor	1194	133.0	1236392	a, b	Outer Membrane	
WP_046825759.1	SusC/RagA family TonB-linked outer membrane protein	1055	116.2	1091712	a, b	Outer Membrane	
WP_052448943.1	SusC/RagA family TonB-linked outer membrane protein	984	111.4	1028220		Outer Membrane	
WP_046825522.1	SusC/RagA family TonB-linked outer membrane protein	1064	117.3	961290	a, b	Outer Membrane	
WP_041590774.1	TonB-dependent receptor	1096	123.0	934603	a	Outer Membrane	
WP_140230659.1	TonB-dependent receptor	1021	113.1	726948		Outer Membrane	
WP_080948647.1	TonB-dependent receptor	1049	117.8	681305		Outer Membrane	
WP_052449079.1	TonB-dependent receptor	1062	118.4	569730	a, b	Outer Membrane	
WP_046826204.1	TonB-dependent receptor	1014	112.2	396201	a, b	Outer Membrane	
WP_052449046.1	TonB-dependent receptor	1013	114.0	284142		Outer Membrane	
WP_046824487.1	TonB-dependent receptor	1009	112.3	283865		Outer Membrane	
WP_201774571.1	SusC/RagA family TonB-linked outer membrane protein	1022	111.8	209296		Outer Membrane	
WP_046825289.1	SusC/RagA family TonB-linked outer membrane protein	1006	110.8	185714	a, b	Outer Membrane	
WP_046825240.1	TonB-dependent receptor	1139	126.1	156004		Outer Membrane	
WP_046825949.1	TonB-dependent receptor	1036	115.3	115218		Outer Membrane	
WP_080948648.1	TonB-dependent receptor	1038	117.4	64500	a	Outer Membrane	
WP_052448976.1	TonB-dependent receptor	1067	117.5	44569	a, b	Outer Membrane	
WP_046825332.1	TonB-dependent receptor	1002	111.5	30100	a	Outer Membrane	
WP_052449101.1	TonB-dependent receptor	1062	119.5	24943		Outer Membrane	
WP_052449125.1	TonB-dependent receptor	1041	115.0	22715	a	Outer Membrane	
WP_052449008.1	TonB-dependent receptor	1144	128.3	19954		Outer Membrane	
WP_052449020.1	TonB-dependent receptor	1103	121.7	19052		Outer Membrane	
WP_046824757.1	SusC/RagA family TonB-linked outer membrane protein	1111	124.7	14148		Outer Membrane	
WP_046825693.1	TonB-dependent receptor	1005	111.8	12991		Outer Membrane	
WP_052449072.1	TonB-dependent receptor	1045	117.8	2405		Outer Membrane	
ii. SusD/RagB homologous proteins (36/349)							
WP_046826242.1	RagB/SusD family nutrient uptake outer membrane protein	522	59.4	186027333	a, b	Outer Membrane	O
WP_046825760.1	SusD/RagB family nutrient-binding outer membrane lipoprotein	517	58.0	123207333	a, b	Periplasmic	O
WP_046824472.1	RagB/SusD family nutrient uptake outer membrane protein	562	64.4	59171167	a, b	Periplasmic	O
WP_080948543.1	RagB/SusD family nutrient uptake outer membrane protein	495	56.7	54833617		Cytoplasmic	O
WP_014223517.1	SusD/RagB family nutrient-binding outer membrane lipoprotein	600	67.3	54486167	a, b	Extracellular	
WP_046825524.1	SusD/RagB family nutrient-binding outer membrane lipoprotein	626	71.1	48233833		Periplasmic	O

Accession	Definition	Amino acid	M.W. (kDa)	iBAQ	Previously reported proteins of Tf OMVs	Predicted Subsellular Location[c]	Lipoprotein[d]
WP_046825921.1	RagB/SusD family nutrient uptake outer membrane protein	586	65.2	35447500	a, b	Periplasmic	O
WP_046824539.1	RagB/SusD family nutrient uptake outer membrane protein	396	45.2	31821167	a, b	Cytoplasmic	O
WP_046824486.1	RagB/SusD family nutrient uptake outer membrane protein	544	61.5	23265450	a, b	Periplasmic	O
WP_041590723.1	RagB/SusD family nutrient uptake outer membrane protein	508	58.2	21876000	a	Cytoplasmic	
WP_052299298.1	RagB/SusD family nutrient uptake outer membrane protein	486	55.4	21096333		Cytoplasmic	O
WP_046825094.1	RagB/SusD family nutrient uptake outer membrane protein	574	65.2	20940067	a, b	Outer Membrane	O
WP_014225566.1	RagB/SusD family nutrient uptake outer membrane protein	527	58.5	18339733	a, b	Outer Membrane	O
WP_014224710.1	SusD/RagB family nutrient-binding outer membrane lipoprotein	550	61.5	10070000	a, b	Periplasmic	O
WP_046825454.1	RagB/SusD family nutrient uptake outer membrane protein	483	54.1	7308650	a, b	Periplasmic	O
WP_052449116.1	RagB/SusD family nutrient uptake outer membrane protein	511	58.1	6149600		Periplasmic	O
WP_014224393.1	RagB/SusD family nutrient uptake outer membrane protein	629	71.2	5875962		Periplasmic	O
WP_014225706.1	RagB/SusD family nutrient uptake outer membrane protein	669	75.7	4128398	a	Outer Membrane	O
WP_014225583.1	RagB/SusD family nutrient uptake outer membrane protein	568	65.1	3349985	a	Periplasmic	O
WP_046825367.1	RagB/SusD family nutrient uptake outer membrane protein	548	62.2	3324750	a	Periplasmic	O
WP_046824979.1	RagB/SusD family nutrient uptake outer membrane protein	631	73.0	3166467	a	Periplasmic	O
WP_014223948.1	RagB/SusD family nutrient uptake outer membrane protein	537	60.4	2572162	a, b	Outer Membrane	O
WP_014226385.1	RagB/SusD family nutrient uptake outer membrane protein	546	63.4	1883928	a, b	Cytoplasmic	O
WP_041590902.1	RagB/SusD family nutrient uptake outer membrane protein	581	67.1	1768398	b	Outer Membrane	O
WP_046825333.1	RagB/SusD family nutrient uptake outer membrane protein	519	58.4	1731037	a	Extracellular	O
WP_046825867.1	RagB/SusD family nutrient uptake outer membrane protein	503	57.6	1542047	a	Cytoplasmic	O
WP_161794928.1	SusD/RagB family nutrient-binding outer membrane lipoprotein	523	59.3	1528415		Outer Membrane	
WP_161794959.1	SusD/RagB family nutrient-binding outer membrane lipoprotein	510	58.6	1128786		Periplasmic	O
WP_014226096.1	RagB/SusD family nutrient uptake outer membrane protein	627	71.3	876353	a	Periplasmic	
WP_046824781.1	RagB/SusD family nutrient uptake outer membrane protein	449	51.0	647263		Cytoplasmic	O
WP_201774589.1	RagB/SusD family nutrient uptake outer membrane protein	496	55.0	519212		Periplasmic	
WP_014224757.1	RagB/SusD family nutrient uptake outer membrane protein	521	58.7	483617	a	Outer Membrane	
WP_046825741.1	RagB/SusD family nutrient uptake outer membrane protein	513	58.5	317818		Extracellular	O
WP_046825068.1	RagB/SusD family nutrient uptake outer membrane protein	590	67.7	316638		Cytoplasmic	
WP_046825184.1	RagB/SusD family nutrient uptake outer membrane protein	496	56.3	130706		Outer Membrane	
WP_046825687.1	RagB/SusD family nutrient uptake outer membrane protein	672	76.0	7809	a, b	Outer Membrane	O
iii. SusF/SusE homologous proteins (2/349)							
WP_080948653.1	SusF/SusE family outer membrane protein	461	49.8	7272283		Periplasmic	O
WP_161794973.1	SusF/SusE family outer membrane protein	379	41.8	6725433		Extracellular	O
iv. TonB and ExbB/ExbD (3/349)							
WP_014224380.1	MotA/TolQ/ExbB proton channel family protein	247	26.2	2854920	a	Inner Membrane	
WP_014224377.1	energy transducer TonB	232	25.5	1014317	a	Cytoplasmic	
WP_046826075.1	biopolymer transporter ExbD	197	22.4	125343		Periplasmic	
II. T9SS and its substrates (21/349)							
WP_087879716.1	PorT family protein	200	21.9	31880167		Periplasmic	
WP_161794962.1	PorT family protein	225	23.9	10765883		Outer Membrane	
WP_052449061.1	leucine-rich-repeat family virulence factor BspA	1081	113.7	9094583		Extracellular	
WP_041590792.1	type IX secretion system outer membrane channel protein PorV	392	43.5	3015000	a, b	Outer Membrane	
WP_046825062.1	leucine-rich repeat protein	1156	123.1	2980878	a, b	Periplasmic	
WP_161794970.1	T9SS type A sorting domain-containing protein	303	34.3	2665795		Periplasmic	
WP_046825257.1	hypothetical protein	1252	131.0	2418532	a, b	Extracellular	
WP_080948566.1	T9SS type A sorting domain-containing protein	556	60.1	1851483		Extracellular	
WP_046825727.1	membrane protein	412	46.8	1237307	a, b	Outer Membrane	
WP_046825848.1	T9SS type A sorting domain-containing protein	366	41.7	745872	a, b	Periplasmic	
WP_041590664.1	type IX secretion system protein PorQ	337	37.1	640450	a, b	Outer Membrane	
WP_046824827.1	type IX secretion system sortase PorU	1143	127.5	541728	a, b	Outer Membrane	O
WP_087879720.1	PorT family protein	220	25.0	411849		Outer Membrane	

Accession	Definition	Amino acid	M.W. (kDa)	iBAQ	Previously reported proteins of Tf OMVs	Predicted Subsellular Location[c]	Lipoprotein[d]
WP_046824969.1	PorT family protein	258	29.0	389717		Cytoplasmic	
WP_080948534.1	T9SS type A sorting domain-containing protein	948	105.1	279466		Outer Membrane	
WP_080948639.1	PorT family protein	241	27.0	255083		Outer Membrane	
WP_211346868.1	hypothetical protein	485	54.1	238797		Outer Membrane	
WP_080948584.1	Ig-like domain-containing protein	1102	119.6	148972		Extracellular	
WP_046826144.1	T9SS type A sorting domain-containing protein	439	51.1	56241	a	Outer Membrane	
WP_046825620.1	InlB B-repeat-containing protein, partial	764	44.4	51042	a	Outer Membrane	
WP_052449111.1	hypothetical protein	769	84.6	41195	a, b	Extracellular	
III. Peptidases (32/349)							
WP_046824802.1	S41 family peptidase	1080	121.7	15396883	a, b	Periplasmic	
WP_046825904.1	S46 family peptidase	716	81.3	9029117	a, b	Cytoplasmic	
WP_041590581.1	Do family serine endopeptidase	502	54.1	8160883	a, b	Outer Membrane	
WP_046824956.1	insulinase family protein	942	107.4	8140800	a, b	Cytoplasmic	
WP_046825514.1	M13 family metallopeptidase	677	77.2	3343550	a, b	Periplasmic	O
WP_201774585.1	S9 family peptidase	717	81.5	2372042		Outer Membrane	O
WP_046826209.1	aminopeptidase	398	44.9	2118135	a, b	Extracellular	
WP_014225756.1	C69 family dipeptidase	546	61.7	1735003	a, b	Periplasmic	
WP_080948606.1	S41 family peptidase	424	48.7	1342086	a, b	Outer Membrane	
WP_046824727.1	M48 family metallopeptidase	264	28.9	1190647	a	Periplasmic	O
WP_052449065.1	M56 family metallopeptidase	480	53.9	1106950		Inner Membrane	
WP_046825797.1	dihydrofolate reductase	686	78.3	908190	a, b	Cytoplasmic	O
WP_046826048.1	prolyl oligopeptidase family serine peptidase	923	105.6	869057	a	Periplasmic	
WP_046825072.1	S41 family peptidase	477	54.1	598978		Outer Membrane	O
WP_140230634.1	prolyl oligopeptidase family serine peptidase	689	78.1	517940		Periplasmic	
WP_046826150.1	S41 family peptidase	567	63.6	512090	a	Cytoplasmic	
WP_046824846.1	S41 family peptidase	432	49.3	456233	a	Outer Membrane	
WP_014224179.1	S41 family peptidase	338	39.0	414159	a, b	Cytoplasmic	O
WP_046826215.1	carboxypeptidase-like regulatory domain-containing protein	764	88.2	305915	a	Outer Membrane	
WP_014224429.1	C40 family peptidase	360	39.9	225154		Periplasmic	
WP_052449090.1	S9 family peptidase	846	95.7	209929		Outer Membrane	
WP_087879727.1	M28 family peptidase	333	37.1	159647		Cytoplasmic	O
WP_046825437.1	S9 family peptidase	696	78.1	151529	a	Periplasmic	O
WP_046824550.1	carboxypeptidase-like regulatory domain-containing protein	875	97.7	139590		Outer Membrane	
WP_046824629.1	S9 family peptidase	725	81.7	123663		Periplasmic	
WP_052449094.1	M56 family metallopeptidase	621	70.7	123307		Outer Membrane	
WP_046824595.1	S41 family peptidase	532	60.2	74304		Cytoplasmic	
WP_052448955.1	transglutaminase	919	104.0	63324		Cytoplasmic	O
WP_046825299.1	outer membrane beta-barrel protein	773	86.9	58430		Outer Membrane	
WP_046824921.1	S9 family peptidase	722	81.7	55747	a	Outer Membrane	
WP_046825792.1	tail fiber domain-containing protein	362	39.5	39841	a	Outer Membrane	
WP_046825809.1	peptidoglycan DD-metalloendopeptidase family protein	408	47.0	8483		Outer Membrane	
IV. Glycosyl hydrolases (12/349)							
WP_046825029.1	family 20 glycosylhydrolase	777	86.5	5176950	a, b	Cytoplasmic	
WP_046826229.1	exo-alpha-sialidase	539	59.6	4718150	a, b	Outer Membrane	
WP_014224118.1	glycoside hydrolase family 125 protein	489	55.9	1129365	a, b	Cytoplasmic	
WP_080948511.1	beta-glucosidase BglX	757	82.5	931922		Cytoplasmic	
WP_046826129.1	DUF4982 domain-containing protein	836	94.8	206253		Cytoplasmic	
WP_046826203.1	glycoside hydrolase family 97 protein	708	81.0	175357		Periplasmic	
WP_046825875.1	GH92 family glycosyl hydrolase	753	83.1	116603		Periplasmic	O
WP_046824466.1	family 10 glycosylhydrolase	514	60.2	97406		Cytoplasmic	
WP_087879742.1	glycoside hydrolase family 95 protein	837	93.7	81971		Cytoplasmic	
WP_014226077.1	glucosylceramidase	486	54.8	49757		Outer Membrane	O
WP_087879739.1	family 10 glycosylhydrolase	471	53.0	34877		Periplasmic	
WP_046826115.1	GH92 family glycosyl hydrolase	766	87.7	30214	a	Extracellular	
V. Tetratricopeptide repeat proteins (10/349)							
WP_041590917.1	tetratricopeptide repeat protein	405	46.4	66361333	a, b	Periplasmic	
WP_046826085.1	tetratricopeptide repeat protein	563	61.9	53037333	a, b	Periplasmic	O
WP_046825261.1	tetratricopeptide repeat protein	999	114.4	3755017	a, b	Outer Membrane	
WP_014226146.1	hypothetical protein	455	51.1	1664478	a, b	Periplasmic	
WP_046824990.1	tetratricopeptide repeat protein	573	63.5	1209542	a	Periplasmic	
WP_087879751.1	CDC27 family protein	490	56.0	652993		Cytoplasmic	
WP_080948616.1	tetratricopeptide repeat protein	594	68.2	160673		Cytoplasmic	
WP_046824917.1	tetratricopeptide repeat protein	353	39.7	49909		Cytoplasmic	O
WP_046825730.1	tetratricopeptide repeat protein	695	80.5	30143	a	Cytoplasmic	
WP_046824455.1	tetratricopeptide repeat protein	1160	134.7	7256		Cytoplasmic	O
VI. TolC family proteins (4/349)							
WP_052448970.1	TolC family protein	452	51.4	6720788		Outer Membrane	
WP_052449039.1	TolC family protein	493	55.5	323811		Outer Membrane	
WP_046825448.1	TolC family protein	463	52.0	195726	a, b	Cytoplasmic	
WP_046825612.1	TolC family protein	504	58.3	72056		Outer Membrane	
VII. Chaperonin (3/349)							
WP_070098079.1	outer membrane protein assembly factor BamA	892	101.4	5748350		Outer Membrane	
WP_041590894.1	outer membrane protein assembly factor BamD	268	31.7	2664600	a, b	Outer Membrane	
WP_046825748.1	chaperonin GroEL	544	57.8	12160		Cytoplasmic	
VIII. Peroxidases (2/349)							
WP_014224706.1	glutathione peroxidase	199	22.5	10287100	a, b	Periplasmic	
WP_014225258.1	superoxide dismutase	194	22.0	1589670	a, b	Cytoplasmic	
IX. Proteins with domain of unknown function (22/349)							
WP_046824980.1	DUF1080 domain-containing protein	292	32.5	9225133	a, b	Periplasmic	O

Accession	Definition	Amino acid	M.W. (kDa)	iBAQ	Previously reported proteins of Tf OMVs	Predicted Subsellular Location[c]	Lipoprotein[d]
WP_046825761.1	DUF5012 domain-containing protein	229	25.2	23340833	a, b	Outer Membrane	O
WP_014225104.1	DUF4139 domain-containing protein	537	60.4	19909833	a	Cytoplasmic	
WP_046825355.1	DUF4831 family protein	356	39.7	10058367	a, b	Cytoplasmic	
WP_157755325.1	DUF4827 domain-containing protein	190	22.2	6351583		Cytoplasmic	
WP_014223783.1	DUF4270 domain-containing protein	472	54.4	5723692	a, b	Outer Membrane	O
WP_080561855.1	DUF1080 domain-containing protein	421	48.3	4449033		Cytoplasmic	O
WP_161794927.1	DUF1573 domain-containing protein	482	52.8	2455607		Cytoplasmic	
WP_046826222.1	hypothetical protein	424	47.5	1967215	a, b	Periplasmic	O
WP_046825969.1	DUF3078 domain-containing protein	293	32.8	1751598	a	Outer Membrane	
WP_046825940.1	DUF3858 domain-containing protein	544	61.4	1271043	a	Cytoplasmic	
WP_041590593.1	DUF4625 domain-containing protein	162	18.1	1233500	a, b	Periplasmic	O
WP_161794945.1	DUF5018 domain-containing protein	543	58.6	1229953		Outer Membrane	O
WP_014224865.1	DUF4292 domain-containing protein	276	31.5	707153	a	Cytoplasmic	
WP_046825529.1	DUF1343 domain-containing protein	412	46.6	528335		Cytoplasmic	
WP_014225879.1	DUF3078 domain-containing protein	514	61.0	475055		Outer Membrane	
WP_046825192.1	DUF1460 domain-containing protein	283	32.2	97464	a, b	Cytoplasmic	
WP_014225897.1	DUF5020 family protein	230	26.2	71250	a	Outer Membrane	
WP_041591118.1	DUF1573 domain-containing protein	133	14.0	67737	a	Extracellular	
WP_046824883.1	DUF4876 domain-containing protein	411	45.9	60406		Periplasmic	O
WP_080948614.1	DUF4832 domain-containing protein	472	53.4	56351		Cytoplasmic	
WP_087879763.1	DUF5103 domain-containing protein	417	48.9	30676		Outer Membrane	
X. Proteins without any reported domain (51/349)							
WP_140230695.1	hypothetical protein	227	25.0	95171833		Periplasmic	O
WP_046825523.1	hypothetical protein	284	32.5	76273333	a, b	Periplasmic	O
WP_152652238.1	hypothetical protein, partial	1533	22.2	31717500		Extracellular	
WP_041590592.1	hypothetical protein	126	13.3	24590500	b	Periplasmic	O
WP_046825842.1	hypothetical protein, partial	307	54.7	23300383	b	Cytoplasmic	
WP_140230593.1	hypothetical protein	1931	210.8	15707733		Extracellular	
WP_041590934.1	hypothetical protein	263	29.4	8019633	a, b	Periplasmic	O
WP_211346869.1	IgGFc-binding protein, partial	550	111.8	5419650		Extracellular	
WP_046826079.1	DUF4959 domain-containing protein	304	34.3	4912207		Periplasmic	
WP_046824517.1	hypothetical protein	1933	212.5	4634700	a, b	Extracellular	
WP_014225605.1	hypothetical protein	192	21.6	3883600	a, b	Cytoplasmic	
WP_140230685.1	hypothetical protein	259	29.2	3855750		Cytoplasmic	O
WP_046472582.1	DUF6242 domain-containing protein	452	50.5	3419483		Outer Membrane	O
WP_140230599.1	hypothetical protein	373	42.5	3022180		Outer Membrane	
WP_140230595.1	hypothetical protein	409	44.1	2817545		Cytoplasmic	
WP_075589073.1	hypothetical protein	287	33.6	2414268		Cytoplasmic	
WP_046825310.1	hypothetical protein	118	13.1	2231025	a, b	Cytoplasmic	O
WP_140230631.1	hypothetical protein	174	20.0	2197548		Periplasmic	
WP_046825699.1	hypothetical protein	141	15.8	1876625	a, b	Periplasmic	O
WP_046824888.1	hypothetical protein	404	44.5	1708545		Periplasmic	O
WP_140230681.1	hypothetical protein	1887	206.4	1694548		Extracellular	
WP_046826055.1	hypothetical protein	227	25.0	1196263	a, b	Inner Membrane	
WP_046826124.1	hypothetical protein	494	54.7	1027338	a, b	Outer Membrane	
WP_046824882.1	hypothetical protein	518	58.9	808682	a, b	Outer Membrane	
WP_080948579.1	hypothetical protein	148	16.1	764434		Extracellular	
WP_046825277.1	hypothetical protein	601	68.3	713168		Outer Membrane	
WP_046825307.1	hypothetical protein	202	22.9	698692	a, b	Extracellular	O
WP_140230660.1	hypothetical protein	366	42.1	687475		Outer Membrane	
WP_046825081.1	hypothetical protein	288	33.0	672997		Cytoplasmic	O
WP_140230643.1	hypothetical protein	192	22.0	672995		Cytoplasmic	
WP_052448988.1	hypothetical protein	244	27.7	616285		Cytoplasmic	
WP_046825937.1	hypothetical protein	450	49.4	415118		Outer Membrane	
WP_052449086.1	hypothetical protein	105	11.7	364795		Periplasmic	O
WP_014225797.1	hypothetical protein	125	14.3	277245		Cytoplasmic	O
WP_080948556.1	hypothetical protein	414	47.8	274272		Outer Membrane	
WP_046824861.1	hypothetical protein	156	17.6	228668	a, b	Cytoplasmic	O
WP_046826127.1	hypothetical protein	245	27.3	195270	a, b	Periplasmic	O
WP_140230692.1	hypothetical protein	365	41.5	176510		Cytoplasmic	
WP_014224149.1	hypothetical protein	794	92.8	169842		Outer Membrane	
WP_014225414.1	hypothetical protein	181	20.5	146538	a	Cytoplasmic	O
WP_046825935.1	hypothetical protein	210	23.4	87275	a, b	Outer Membrane	
WP_046825562.1	hypothetical protein	336	39.2	84082		Cytoplasmic	
WP_052449091.1	hypothetical protein	290	33.1	70875	a	Cytoplasmic	
WP_140230609.1	hypothetical protein	215	25.5	58469		Outer Membrane	
WP_014223749.1	hypothetical protein	197	22.5	54328		Cytoplasmic	
WP_046825757.1	DUF6345 domain-containing protein	536	60.4	43685		Outer Membrane	
WP_014225170.1	hypothetical protein	228	25.8	38368		Cytoplasmic	
WP_004584866.1	MULTISPECIES: hypothetical protein	220	25.3	34967		Outer Membrane	O
WP_046825649.1	spondin domain-containing protein	411	44.4	31659		Periplasmic	O
WP_087879764.1	hypothetical protein	308	35.5	24845		Outer Membrane	
WP_046826164.1	hypothetical protein	540	61.2	20040		Outer Membrane	O
XI. Others (96/349)							
WP_046825762.1	hypothetical protein	230	26.0	227381667	a, b	Periplasmic	O
WP_046825712.1	HmuY family protein	216	24.4	196977500	a, b	Periplasmic	O
WP_041590550.1	OmpA family protein	389	44.3	183211500	a, b	Periplasmic	
WP_014225890.1	TRL-like family protein	99	9.9	160931000	a	Extracellular	
WP_140230713.1	TlpA family protein disulfide reductase	363	42.0	70692333		Cytoplasmic	
WP_046824579.1	right-handed parallel beta-helix repeat-containing protein, partial	574	121.0	33376767	b	Extracellular	
WP_046825066.1	BT1926 family outer membrane beta-barrel protein	216	22.4	32672633	a, b	Outer Membrane	
WP_046825745.1	OmpH family outer membrane protein	172	19.7	29373550	a	Periplasmic	
WP_041590627.1	SPOR domain-containing protein	156	17.6	28663500	a, b	Periplasmic	
WP_014224806.1	OmpH family outer membrane protein	164	18.9	26762333	a, b	Periplasmic	
WP_080948622.1	InlB B-repeat-containing protein	370	40.7	21761450		Periplasmic	O

Accession	Definition	Amino acid	M.W. (kDa)	iBAQ	Previously reported proteins of Tf OMVs	Predicted Subsellular Location[c]	Lipoprotein[d]
WP_046825961.1	sugar phosphate isomerase/epimerase	297	33.7	17385633	a, b	Cytoplasmic	
WP_014226123.1	DUF4876 domain-containing protein	443	48.7	16323617	a, b	Extracellular	
WP_201774565.1	FKBP-type peptidyl-prolyl cis-trans isomerase	213	23.2	13956783		Periplasmic	
WP_046825546.1	carboxypeptidase-like regulatory domain-containing protein	418	48.5	13791583	a	Outer Membrane	
WP_014224982.1	Ig-like domain-containing protein	540	58.4	13197050		Outer Membrane	
WP_052449115.1	sugar phosphate isomerase/epimerase	328	36.7	12245267		Periplasmic	
WP_014223879.1	outer membrane protein transport protein	536	60.2	11065600	a, b	Outer Membrane	
WP_046825843.1	PDZ domain-containing protein	473	54.7	9209083	a, b	Outer Membrane	
WP_046826169.1	peptidylprolyl isomerase	453	52.4	8070333		Cytoplasmic	
WP_014223614.1	copper resistance protein NlpE	144	15.7	7889900	a, b	Cytoplasmic	O
WP_046824745.1	FKBP-type peptidyl-prolyl cis-trans isomerase	196	21.4	7822617	a, b	Periplasmic	O
WP_014224852.1	peptidylprolyl isomerase	532	61.5	7764483	a, b	Cytoplasmic	
WP_014225065.1	thioredoxin	151	16.9	6322092	a	Periplasmic	
WP_014225134.1	Gfo/Idh/MocA family oxidoreductase	493	54.6	5504667	a, b	Periplasmic	
WP_046825424.1	DUF1080 domain-containing protein	1158	126.5	4902217	a, b	Periplasmic	
WP_046824717.1	endonuclease/exonuclease/phosphatase family protein	278	31.4	4778542	a, b	Cytoplasmic	
WP_014225136.1	NigD-like protein	249	28.4	4543683		Periplasmic	
WP_046824488.1	alkaline phosphatase	562	62.5	4349833	a, b	Periplasmic	
WP_046824809.1	hypothetical protein	366	40.3	4050568	a, b	Extracellular	O
WP_046824516.1	AhpC/TSA family protein	371	40.9	3964183		Cytoplasmic	O
WP_046824554.1	OmpA family protein	228	23.8	3590417	a, b	Periplasmic	O
WP_046825948.1	SGNH/GDSL hydrolase family protein	256	28.6	3299150	a, b	Periplasmic	
WP_046825312.1	discoidin domain-containing protein	1209	136.7	3146430	a	Extracellular	O
WP_014225524.1	metallophosphoesterase family protein	335	37.5	3112372	a, b	Cytoplasmic	
WP_046825011.1	peptidylprolyl isomerase	224	25.2	2741710		Cytoplasmic	
WP_046824476.1	TIM barrel protein	296	32.9	2718233	a, b	Cytoplasmic	
WP_014223776.1	hypothetical protein	116	13.4	2367673		Cytoplasmic	O
WP_014224736.1	glucosaminidase domain-containing protein	323	37.5	2316012	a	Outer Membrane	
WP_140230687.1	hypothetical protein	370	40.1	2134147		Periplasmic	
WP_046825560.1	Gfo/Idh/MocA family oxidoreductase	468	51.8	1821627	a	Periplasmic	
WP_046825320.1	Omp28-related outer membrane protein	519	57.4	1774808	a	Extracellular	O
WP_046825205.1	polysaccharide biosynthesis/export family protein	269	30.2	1643552		Inner Membrane	O
WP_046826099.1	alpha/beta hydrolase	294	32.5	1601658		Cytoplasmic	
WP_014225403.1	GLPGLI family protein	284	32.3	1590168		Periplasmic	
WP_046825728.1	alkaline phosphatase family protein	528	59.9	1567102	a	Cytoplasmic	
WP_014225175.1	hypothetical protein	289	32.8	1414502	a	Outer Membrane	O
WP_046825563.1	VIT domain-containing protein	974	111.3	1365832	a	Cytoplasmic	
WP_014225844.1	alginate export family protein	429	49.5	1325832	a	Outer Membrane	
WP_046825513.1	SGNH/GDSL hydrolase family protein	571	64.7	1305759	a	Cytoplasmic	
WP_014225762.1	FKBP-type peptidyl-prolyl cis-trans isomerase	238	25.3	1298790	a	Periplasmic	O
WP_046826220.1	flavodoxin	188	21.0	1296548	a, b	Periplasmic	
WP_046825170.1	MG2 domain-containing protein	1864	207.5	1096802		Outer Membrane	O
WP_014223958.1	AhpC/TSA family protein	203	22.4	1090317	a, b	Periplasmic	
WP_014224160.1	Gfo/Idh/MocA family oxidoreductase	418	47.1	996650	a, b	Periplasmic	
WP_046826137.1	hypothetical protein	717	78.8	987103	a, b	Outer Membrane	O
WP_046824479.1	outer membrane beta-barrel protein	155	17.1	969000	a	Outer Membrane	
WP_052448969.1	DUF4981 domain-containing protein	1129	128.3	869488		Extracellular	
WP_046826224.1	sirohydrochlorin cobaltochelatase	311	35.2	820347	a, b	Cytoplasmic	
WP_052449099.1	DUF3857 domain-containing protein	648	72.8	727815		Periplasmic	
WP_004585095.1	MULTISPECIES: GLPGLI family protein	238	27.0	691407		Cytoplasmic	
WP_178387126.1	InlB B-repeat-containing protein, partial	386	23.2	675220		Periplasmic	
WP_014225615.1	patatin-like phospholipase family protein	767	87.7	657152		Outer Membrane	
WP_046825606.1	porin	381	42.6	642137	a	Outer Membrane	
WP_087879733.1	Ig-like domain-containing protein	356	36.8	592833		Extracellular	
WP_046826227.1	GDSL-type esterase/lipase family protein	692	78.5	562303		Cytoplasmic	
WP_046825543.1	hypothetical protein	507	57.6	510352		Outer Membrane	
WP_087879745.1	xanthan lyase	1001	112.1	425337		Outer Membrane	
WP_046824688.1	TraB/GumN family protein	319	36.6	349438	a	Cytoplasmic	O
WP_014224694.1	gliding motility protein GldN	370	42.6	315555	a	Periplasmic	
WP_046825182.1	glycosyl hydrolase family 28 protein	493	54.9	310960	a	Cytoplasmic	
WP_041590639.1	galactose mutarotase	376	41.2	295625	a, b	Extracellular	O
WP_161794960.1	LamG domain-containing protein	263	28.7	244461		Periplasmic	O
WP_080948644.1	Ig-like domain-containing protein	634	65.9	214638		Outer Membrane	
WP_052448942.1	gliding motility-associated C-terminal domain-containing protein	440	49.6	184677		Extracellular	
WP_041591331.1	glycerophosphodiester phosphodiesterase	260	29.6	161748	a	Cytoplasmic	
WP_080948640.1	hypothetical protein	446	51.2	157509		Cytoplasmic	
WP_201774570.1	FAD-dependent oxidoreductase	528	59.0	149364		Cytoplasmic	
WP_014226380.1	YtxH domain-containing protein	111	12.2	135322		Periplasmic	
WP_046825839.1	hypothetical protein	467	53.9	127972	a, b	Cytoplasmic	O
WP_046824878.1	alpha-L-rhamnosidase	911	102.9	86377		Extracellular	O
WP_046824591.1	bifunctional metallophosphatase/5'-nucleotidase	478	53.8	62178		Cytoplasmic	
WP_046824784.1	SUMF1/EgtB/PvdO family nonheme iron enzyme	479	54.9	53363		Extracellular	O
WP_014223652.1	preprotein translocase subunit YajC	112	12.1	51502		Inner Membrane	
WP_046824463.1	LysM peptidoglycan-binding domain-containing protein	596	68.4	47889		Outer Membrane	
WP_046825315.1	membrane protein	214	23.9	41528	a	Outer Membrane	
WP_080948611.1	alpha/beta fold hydrolase	455	49.8	39991		Cytoplasmic	
WP_080948582.1	fibronectin type III domain-containing protein	606	66.5	37536		Periplasmic	
WP_046824940.1	erythromycin esterase family protein	610	70.5	28957		Cytoplasmic	
WP_046825018.1	cell surface protein SprA	2482	282.0	25632		Outer Membrane	
WP_014225032.1	alpha/beta hydrolase-fold protein	565	66.6	25597	a	Periplasmic	

Accession	Definition	Amino acid	M.W. (kDa)	iBAQ	Previously reported proteins of Tf OMVs	Predicted Subsellular Location[c]	Lipoprotein[d]
WP_046825480.1	nitroreductase	228	25.1	24553		Periplasmic	O
WP_052449031.1	lamin tail domain-containing protein	473	52.2	15418		Extracellular	
WP_014225269.1	elongation factor Tu	395	43.3	10343		Cytoplasmic	
WP_046824756.1	zinc-dependent metalloprotease	876	99.3	7514		Cytoplasmic	
WP_052449025.1	TANFOR domain-containing protein	3078	343.6	4576		Periplasmic	

a The *T. forsythia* OMVs protein previously reported by Veith et al. 2015.
b The *T. forsythia* OMVs protein previously reported by Friedrich et al. 2015.
c The subcellular location of each protein was predicted by CELLO v.2.5 (Molecular Bioinformatics Center of National Chiao Tung University).
d The lipid attachment site of each protein was predicted by ExPASy - PROSITE database.

1.4 *T. forsythia* cultured in EV-free conditioned medium of macrophages released EVs.

To verify whether the EVs in TF-F5 were directly released from live *T. forsythia*, EVs derived from macrophages treated with heat-killed *T. forsythia* were isolated and characterized (Figure 9). NTA showed that nanoparticles were not enriched in F5 (Figure 9a). TEM image also showed that vesicular structures were detected in F2 but not in F5 (Figure 9b). These results suggested that only live *T. forsythia* release EVs.

Bacteria regulate the release of EVs to adapt to their surroundings [93]. Encounters with macrophages can be a stressful condition for *T. forsythia* since macrophages are sentinels against microbial infection and nutrients available in the CM are not sufficient for the growth of *T. forsythia*. To identify whether the CM of THP-1 macrophages promotes the release of EVs from *T. forsythia*, live *T. forsythia* were incubated in EV-free CM of macrophages, and EVs were isolated (Figure 10a). The EVs in the CM of non-infected and *T. forsythia*-infected macrophages were eliminated by 100 kDa MWCO ultrafiltration. The EV-free CM from non-infected macrophages and *T. forsythia*-infected macrophages were designated NI-100K and TF-100K, respectively. NTA confirmed that NI-100K and TF-100K were free of nanoparticles (data not shown). Interestingly, *T. forsythia* released EVs in both NI-100K and TF-100K but not in RPMI 1640 medium without cell contact (Figure 10b). *T. forsythia* cultured in TF-100K released EVs more than that cultured in NI-100K (Figure 10b). TEM imaging and immunoblotting showed that F5 was enriched with vesicles and *T. forsythia* proteins (Figure 10c and 10d). These results suggest that 1) the CM of THP-1 macrophages was stressful condition for *T. forsythia*, 2) EVs in TF-F5 were directly released from *T. forsythia* and not from macrophages, and 3) unknown soluble molecules under 100 kDa in the CM of macrophages promoted *T. forsythia* to release EVs.

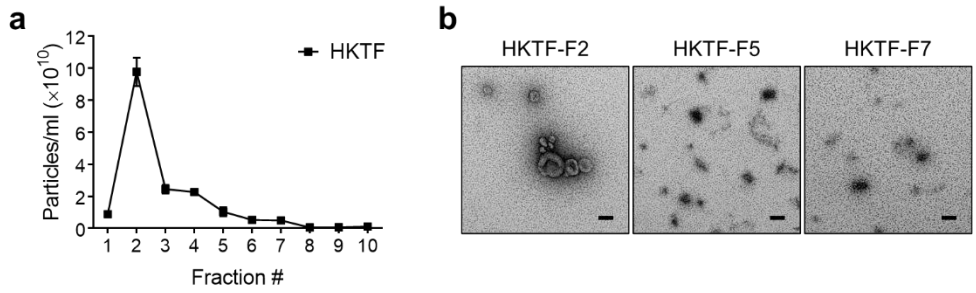

Figure 9. Characterization of EVs derived from THP-1 macrophages treated with heat-killed *T. forsythia*. (a) Nanoparticle concentration of each density gradient fraction was analyzed by NTA. (b) The indicated fractions were negatively stained and imaged by TEM. Scale bar: 100 nm. The experiments were performed at least two times independently. HKTF, heat-killed *T. forsythia* treatment.

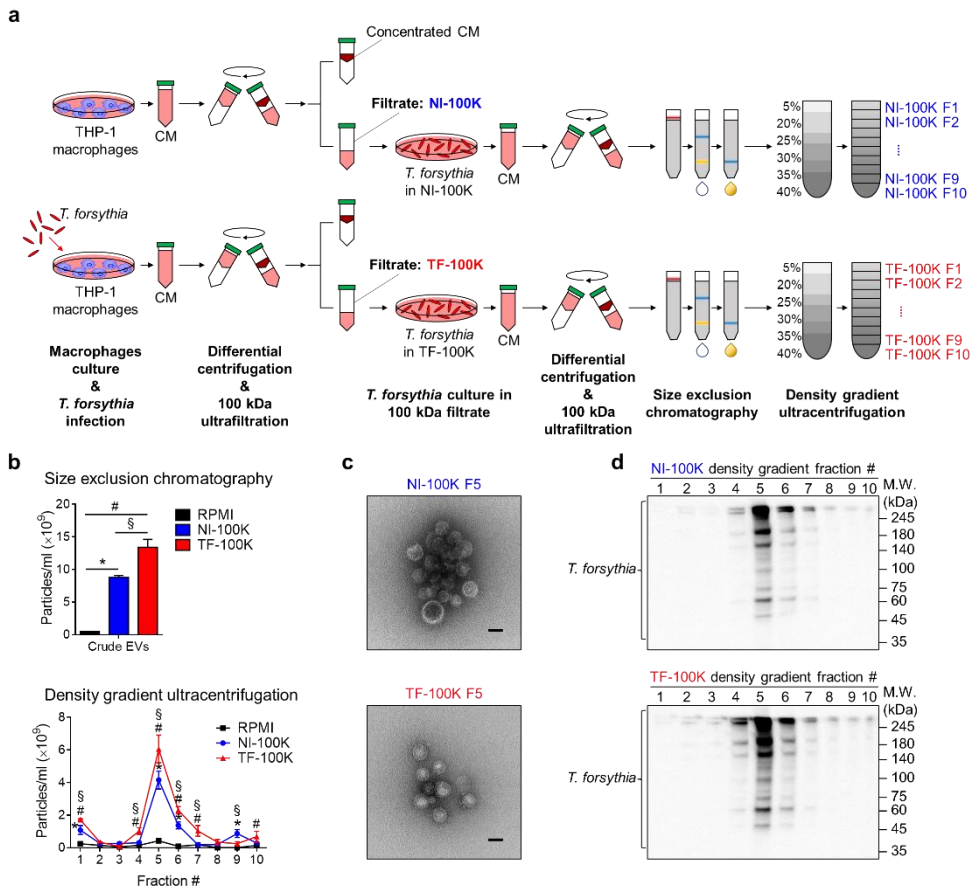

Figure 10. Identification of EVs released from live *T. forsythia* cultured in EV-free CM of macrophages. (a) Schematic diagram of *T. forsythia* incubation in EV-free macrophage CM. (b) The nanoparticle concentration of crude EVs and density gradient fractions was analyzed by NTA. (c) The indicated fractions were negatively stained and imaged by TEM. Scale bar: 50 nm. (d) Immunoblotting of density gradient fractions using *T. forsythia*-specific antibody. The experiments were performed at least three times independently. Data are presented as the mean ± *SD* of triplicate assays and were analyzed by one-way and two-way ANOVA, respectively. * $p < 0.05$ compared between NI-100K and RPMI, # $p < 0.05$ compared between TF-100K and RPMI, and § $p < 0.05$ compared between NI-100K and TF-100K.

1.5 Macrophage-derived EVs and *T. forsythia*-derived EVs induced pro-inflammatory responses.

Bacterial and host EVs can transfer their biological molecules to the host recipient cells [94, 95]. Therefore, it is investigated that the inflammatory responses of EVs in TF-F2 and TF-F5 by measuring the expression of pro-inflammatory cytokines using THP-1 macrophages.

When THP-1 macrophages were treated with TF-F2, TNF-α expression was significantly higher than in cells treated with NI-F2 (Figure 11). There was no significant difference in the expression level of IL-1β and IL-8 between NI-F2- and TF-F2-treated macrophages. IL-6 was not detected in cells treated with TF-F2 or NI-F2. The levels of cytokines in TF-F2 without cell treatment were also measured since TF-F2 itself had significant amounts of TNF-α, IL-β, and IL-8 (Table 1 and Figure 7a). Cytokines were not detected in cell-free NI-F2 and TF-F2 by ELISA (Figure 11).

To investigate the immunostimulatory effects of *T. forsythia* virulence factors in TF-F5, TF-F5 were treated to CHO/CD14/TLR2 and CHO/CD14/TLR4 reporter cells. TF-F5 activated TLR2 but did not activate TLR4 (Figure 12a and 12b). To determine whether TF-F5 could stimulate host cells through TLR2, TF-F5 was treated to WT and TLR2$^{-/-}$ THP-1 macrophages, and the expression level of pro-inflammatory cytokines was measured by ELISA. TF-F5 significantly induced TNF-α, IL-1β, IL-6, and IL-8 in WT THP-1 macrophages but not in TLR2$^{-/-}$ macrophages (Figure 13). These results indicate that TF-F5 could stimulate host cells to release pro-inflammatory cytokines through the TLR2 signaling pathway.

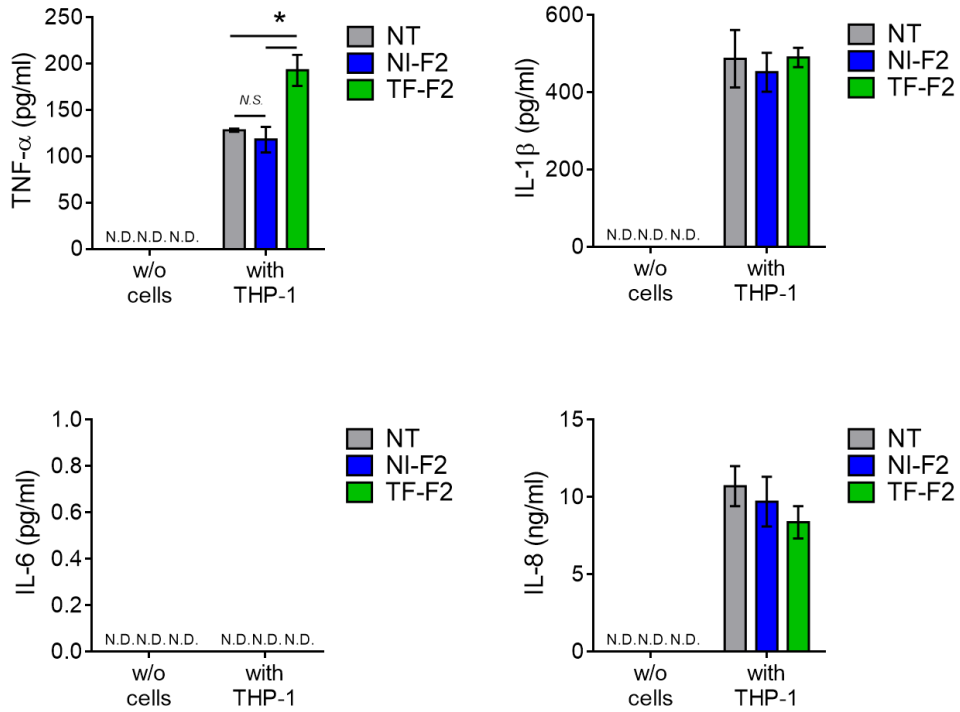

Figure 11. Pro-inflammatory cytokines induced by macrophage-derived EVs. THP-1 macrophages were treated with EVs of NI-F2 and TF-F2 (1×10^9 particles/ml) for 4 hours. The expression level of TNF-α, IL-1β, IL-6, and IL-8 in the culture supernatants was measured by ELISA. The cell-free medium treated with NI-F2 and TF-F2 (1×10^9 particles/ml) were also measured. The experiments were performed at least three times independently. Data are presented as the mean ± *SD* of triplicate assays and were analyzed by two-way ANOVA. NT, non-treatment. N.D., not detected. N.S., not significant. * $p < 0.05$.

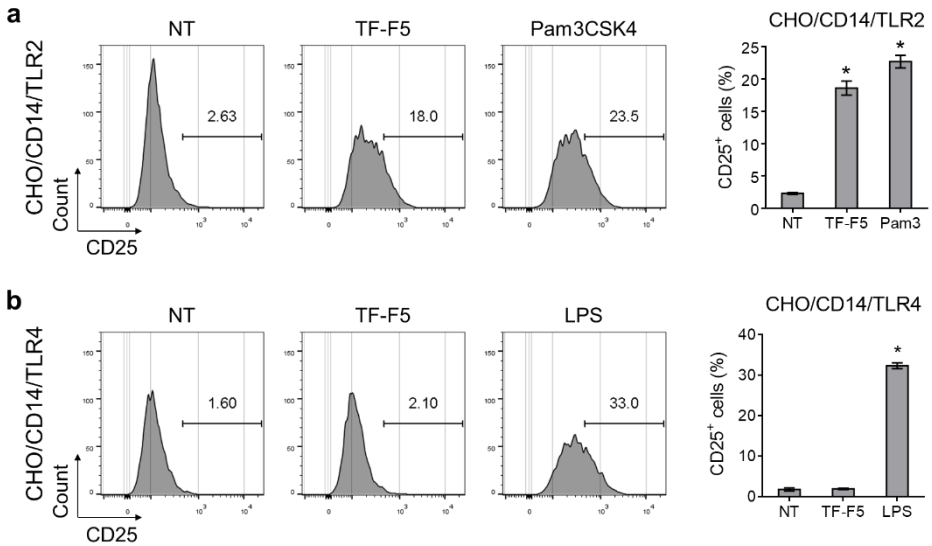

Figure 12. Analysis of TLR signaling pathway activation by *T. forsythia*-derived EVs. CHO/CD14/TLR2 (a) and CHO/CD14/TLR4 (b) reporter cells were stimulated with TF-F5 (1×10^9 particles/ml) for 20 hours. The level of CD25 on the cell surface induced by TLRs activation was measured by flow cytometry. The experiments were performed three times independently, and representative data are shown in the histograms (left panel) and by the ratio of $CD25^+$ cells (right panel). Data are presented as the mean ± *SD* of triplicate assays and were analyzed by one-way ANOVA. NT, non-treatment; Pam3, Pam3CSK4; LPS, ultrapure LPS. * $p < 0.05$.

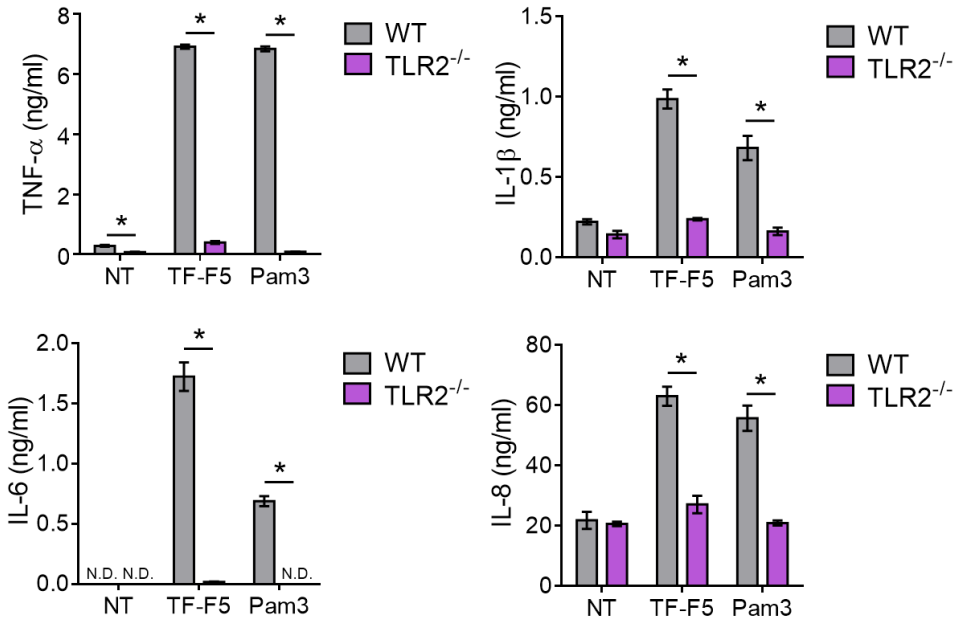

Figure 13. TLR2 mediated pro-inflammatory cytokine secretion by *T. forsythia*-derived EVs. THP-1 macrophages were treated with TF-F5 (1×10^9 particles/ml) and Pam3CSK4 (10 ng/ml) for 24 hours. The expression level of TNF-α, IL-1β, IL-6, and IL-8 in the culture supernatants were measured by ELISA. The experiments were performed at least three times independently. Data are presented as the mean ± *SD* of triplicate assays and were analyzed by two-way ANOVA. NT, non-treatment. N.D., not detected; Pam3, Pam3CSK4. * $p < 0.05$.

2. Identification of the role in BMDCs maturation and helper T cell differentiation by periodontal pathogen OMVs

2.1 Periodontal pathogen OMVs were isolated and characterized.

OMVs of *P. gingivalis*, *T. denticola*, and *T. forsythia* were isolated from bacterial culture supernatants by ultracentrifugation combined with DGUC (Figure 14a). The OMVs showed a round and cup-shaped morphology in the negatively stained TEM images, and their sizes ranged from 50 nm to 400 nm (Figure 14b). Approximately 750 μg protein (1.1×10^{12} particles) of *P. gingivalis* OMVs, 210 μg protein (8.0×10^{11} particles) of *T. denticola* OMVs, and 1200 μg protein (1.7×10^{12} particles) of *T. forsythia* OMVs were harvested from 400 ml of each bacterial culture supernatants. The number of particles in 10 μg OMV protein of *P. gingivalis* OMVs and *T. forsythia* OMVs is similar, but *T. denticola* OMVs is about three times higher than others (Figure 15).

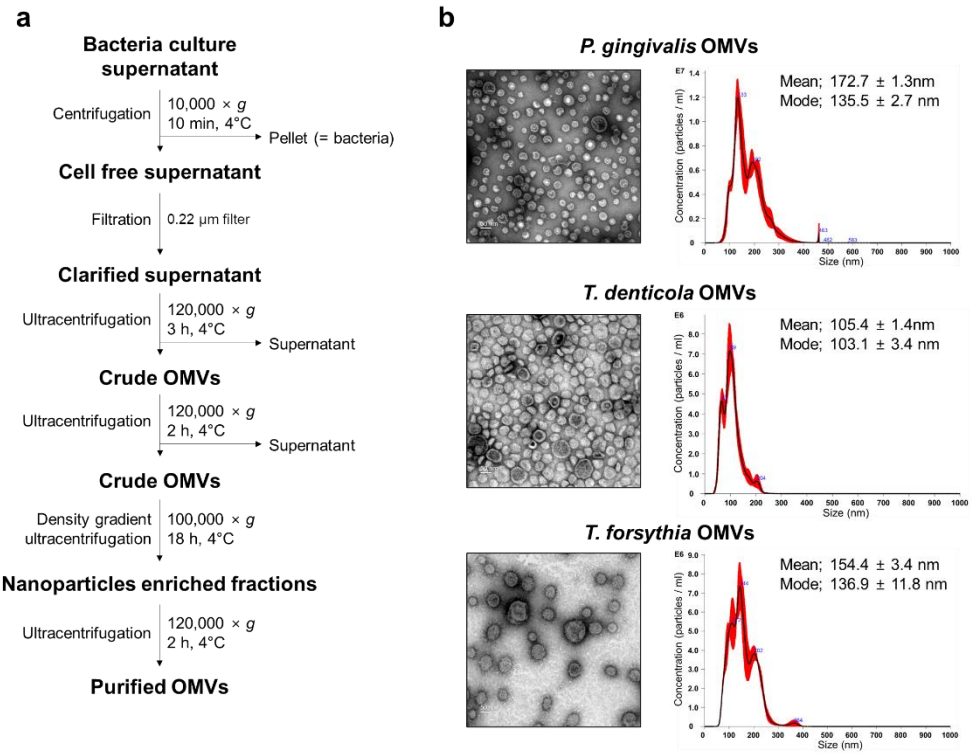

Figure 14. Isolation and characterization of periodontal pathogen OMVs. (a) Schematic diagram of OMV isolation procedures. (b) The OMVs were negatively stained with uranyl acetate and observed via TEM at 120 kV (left panel) with a magnification of 40,000×. Scale bars represent 50 nm. The size and concentration of the indicated OMVs were measured by NTA (right panel).

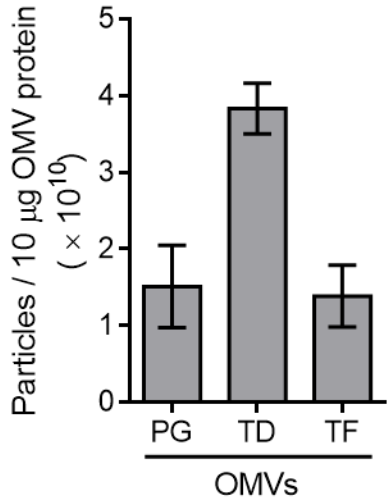

Figure 15. The amount of OMVs in 10 μg OMV protein. The particles and protein concentration of each OMV were analyzed by NTA and BCA assays, respectively. The number of OMVs in 10 μg OMV protein was analyzed. PG, *P. gingivalis* OMVs; TD, *T. denticola* OMVs; TF, *T. forsythia* OMVs.

2.2 Periodontal pathogen OMVs induced maturation of BMDCs.

Activation of APCs by microbial components is essential for initiating naïve $CD4^+$ T cell differentiation [96]. Activated DCs are mature and express high levels of major histocompatibility complex (MHC) class II and costimulatory molecules, including CD80, CD86, and CD40, on the cell surface to signal to naïve $CD4^+$ T cells [96]. To analyze the maturation of BMDCs, they were stimulated with OMVs of periodontal pathogens for 24 hours, and the expression levels of MHC class II and costimulatory molecules on the cell surface were analyzed via flow cytometry. All OMVs significantly induced the expression of MHC class II, CD80, CD86, and CD40 (Figure 16). These results suggest that OMVs of periodontal pathogens induced the maturation of BMDCs.

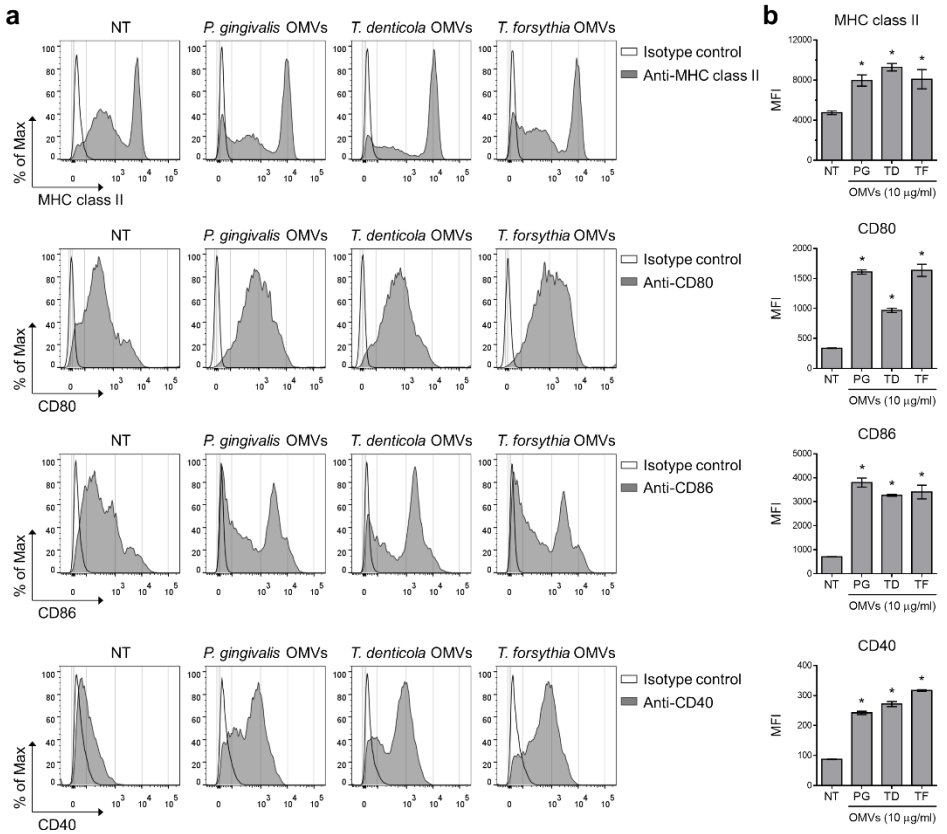

Figure 16. Maturation of BMDCs induced by periodontal pathogen OMVs. BMDCs were stimulated with 10 μg/ml of the indicated OMVs for 24 hours. The expression of MHC class II (I-A/I-E), CD80, CD86, and CD40 on BMDCs was analyzed via flow cytometry. The experiments were performed three times independently, and representative data are shown in the histograms (a) and by the mean fluorescence intensity (MFI) (b). The empty solid lines represent the isotype control. Data are presented as the mean ± *SD* of triplicate assays and were analyzed by one-way ANOVA. * $p < 0.05$ compared to the control (NT). NT, non-treatment; PG, *P. gingivalis*; TD, *T. denticola*; TF, *T. forsythia*.

2.3 OMV-primed BMDCs secreted pro-inflammatory cytokines

Since the polarization of naïve $CD4^+$ T cells is regulated by cytokine milieu [96], the levels of cytokines released from BMDCs upon stimulation with OMVs of periodontal pathogens were quantified using ELISA. IL-12p70 was measured for Th1 cell polarization, and IL-4 for Th2 cell polarization. IL-1β, IL-6, and IL-23 were measured for Th17 cell polarization. *P. gingivalis* OMVs and *T. forsythia* OMVs significantly induced the secretion of IL-12p70, IL-1β, IL-6, and IL-23 from BMDCs (Figure 17a). *T. denticola* OMVs induced small amount of IL-6 but did not induce IL-12p70, IL-1β, or IL-23 secretion. No OMVs induced IL-4 secretion. As *T. denticola* OMVs stimulated BMDCs as efficiently as other OMVs, as judged by the expression of costimulatory molecules (Figure 16), it was speculated that *T. denticola* OMVs might have the ability to degrade cytokines secreted from BMDCs. As expected, *T. denticola* OMVs significantly induced *Il12a*, *Il1b*, *Il6*, and *Il23a*, similar to or less than *P. gingivalis* OMVs and *T. forsythia* OMVs (Figure 17b). To examine the proteolytic activity of the OMVs of periodontal pathogens, recombinant murine pro-inflammatory cytokines were incubated with the OMVs, and the remaining cytokines were measured via ELISA. *T. denticola* OMVs degraded IL-1β, IL-6, and IL-23 but not IL-12p70 in a dose-dependent manner (Figure 17c). To determine whether *T. denticola* OMVs were able to degrade cytokines secreted from BMDM stimulated with Pam3CSK4, a synthetic lipopeptide known to mimic bacterial lipoproteins, the culture supernatants of BMDCs were harvested and then incubated with *T. denticola* OMVs. *T. denticola* OMVs significantly degraded IL-1β, IL-6, and IL-23 in BMDM culture supernatants (Figure 18a). Heat- or PMSF-treated *T. denticola* OMVs lost their proteolytic activity against IL-1β, IL-6, and IL-23 (Figure 18a). In addition, heat-treated *T. denticola* OMVs induced more IL-1β, IL-6, and IL-23 than ice-treated *T. denticola* OMVs from BMDCs (Figure 18b). These results suggest that *T. denticola* OMVs induced

the production of IL-1β, IL-6, and IL-23, which were subsequently degraded. *P. gingivalis* OMVs also degraded IL-1β and IL-23 but to a lesser extent than *T. denticola* OMVs. *T. forsythia* OMVs degraded IL-1β. Therefore, the OMVs of periodontal pathogens are likely to induce Th1 or Th17 polarization and that *T. denticola* OMVs possess strong proteolytic activity against pro-inflammatory cytokines compared to other OMVs.

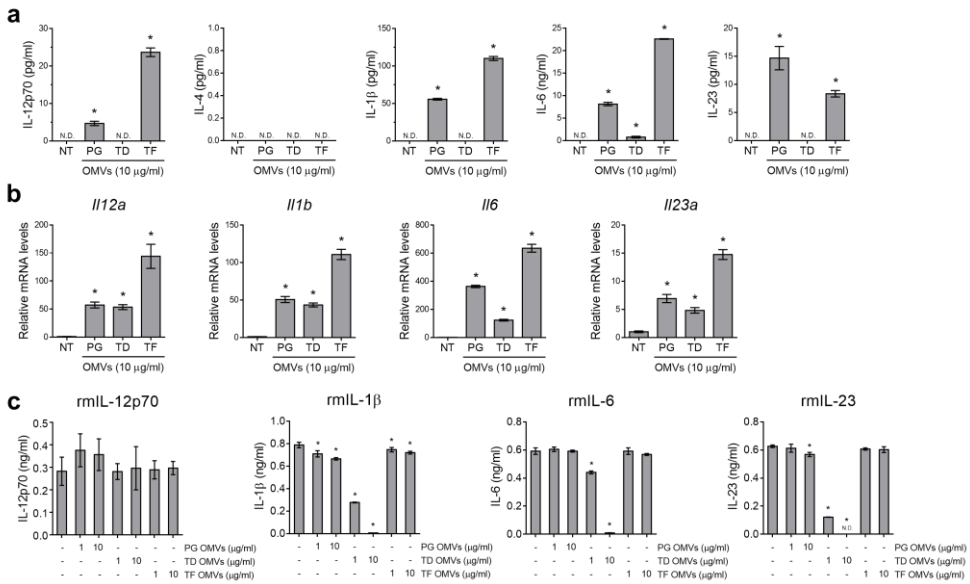

Figure 17. Effects of periodontal pathogen OMVs on pro-inflammatory cytokine secretion in BMDCs and cytokine degradation. (a) BMDCs were stimulated with 10 μg/ml of the indicated OMVs for 24 hours. The expression levels of IL-12p70, IL-4, IL-1β, IL-6, and IL-23 in the culture supernatants were measured with ELISA. (b) BMDCs were stimulated with 10 μg/ml of the indicated OMVs for 3 hours. The relative mRNA levels of the indicated genes were analyzed via qRT-PCR. (c) One nanogram per ml of recombinant murine IL-12p70, IL-1β, IL-6, and IL-23 were coincubated with the indicated OMVs at 37°C for 24 hours in RPMI 1640 complete medium. The level of the cytokines remaining in the medium was analyzed using ELISA. The experiments were performed three times independently. Data are presented as the mean ± *SD* of triplicate assays and were analyzed by one-way ANOVA. * $p < 0.05$ compared to the control (NT). NT, non-treatment; N.D., not detected. PG, *P. gingivalis*; TD, *T. denticola*; TF, *T. forsythia*.

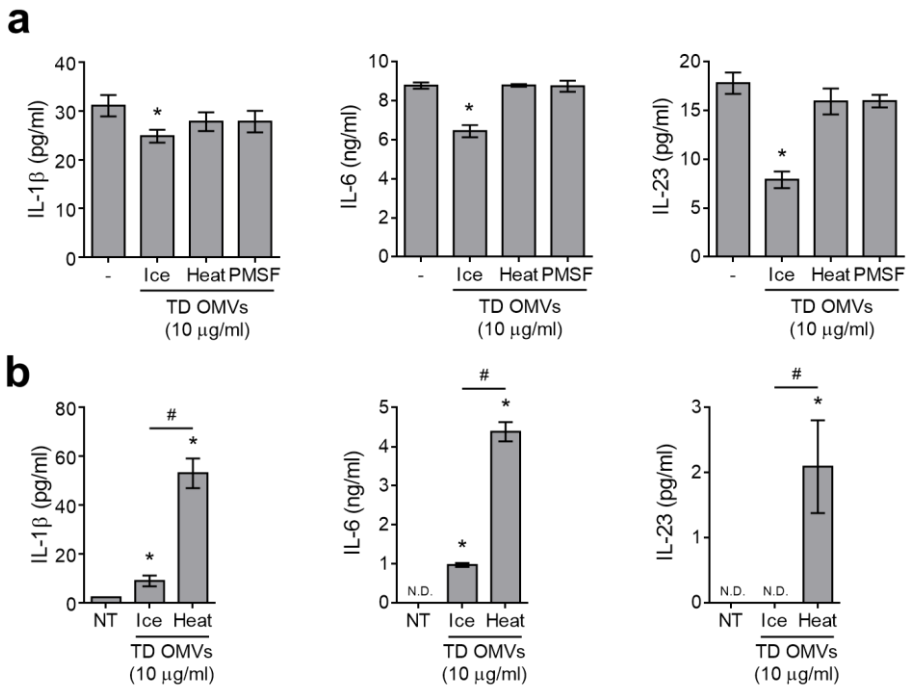

Figure 18. Proteolytic activity of *T. denticola* OMVs against pro-inflammatory cytokines secreted from BMDCs. (a) BMDCs were treated with Pam3CSK4 (100 ng/ml) for 24 hours. The culture supernatants of BMDCs were harvested and then incubated with heat- or PMSF-treated *T. denticola* OMVs for 1 hour. The level of the cytokines that remained in the culture supernatants was analyzed using ELISA. (b) BMDCs were treated with ice-incubated and heat-treated *T. denticola* OMVs for 24 hours. The level of the cytokines in the culture supernatants was analyzed using ELISA. Data are presented as means ± *SD* of triplicate assays and were analyzed by one-way ANOVA. * $p < 0.05$ compared to the control (NT) and # $p < 0.05$ compared to the indicated groups. NT, non-treatment; TD, *T. denticola*.

2.4 Naïve $CD4^+$ T cells were differentiated by OMV-primed BMDCs

Naïve $CD4^+$ T cells were cocultured with OMV-primed BMDCs to analyze the effect of OMVs on T cell polarization. To exclude the possibility that OMVs of periodontal pathogens can degrade cytokines from OMV-primed BMDCs, OMV-primed BMDCs were vigorously washed at 5 hours post treatment and then were cocultured with naïve $CD4^+$ T cells. BMDCs stimulated with OMVs of *P. gingivalis* and *T. denticola* induced IL-$17A^+$ cells, while *T. forsythia* OMV-primed BMDCs mainly induced IFN-γ^+ cells along with some IL-$17A^+$ cells (Figure 19a and 19b). IL-4^+ cells were not detected in any coculture. In addition, the expression of transcription factors t-bet and RORγt, which are essential for Th1 and Th17 differentiation, were also analyzed (Figure 20). As expected, BMDCs primed with OMVs of *P. gingivalis* and *T. denticola* induced RORγt^+ cells, whereas *T. forsythia* OMV-primed BMDCs induced t-bet^+ cells.

It was also analyzed that whether BMDCs infected with live periodontal pathogens showed similar mode of $CD4^+$ T cells differentiation to OMVs. Similar to the OMVs, live *P. gingivalis*- and live *T. denticola*-infected BMDCs induced IL-$17A^+$ cells, while live *T. forsythia*-infected BMDCs induced IFN-γ^+ cells (Figure 21).

These results indicate that OMVs and live whole cell of *P. gingivalis* and *T. denticola* induced Th17 polarization, whereas OMVs and live whole cell of *T. forsythia* favored Th1 polarization rather than Th17.

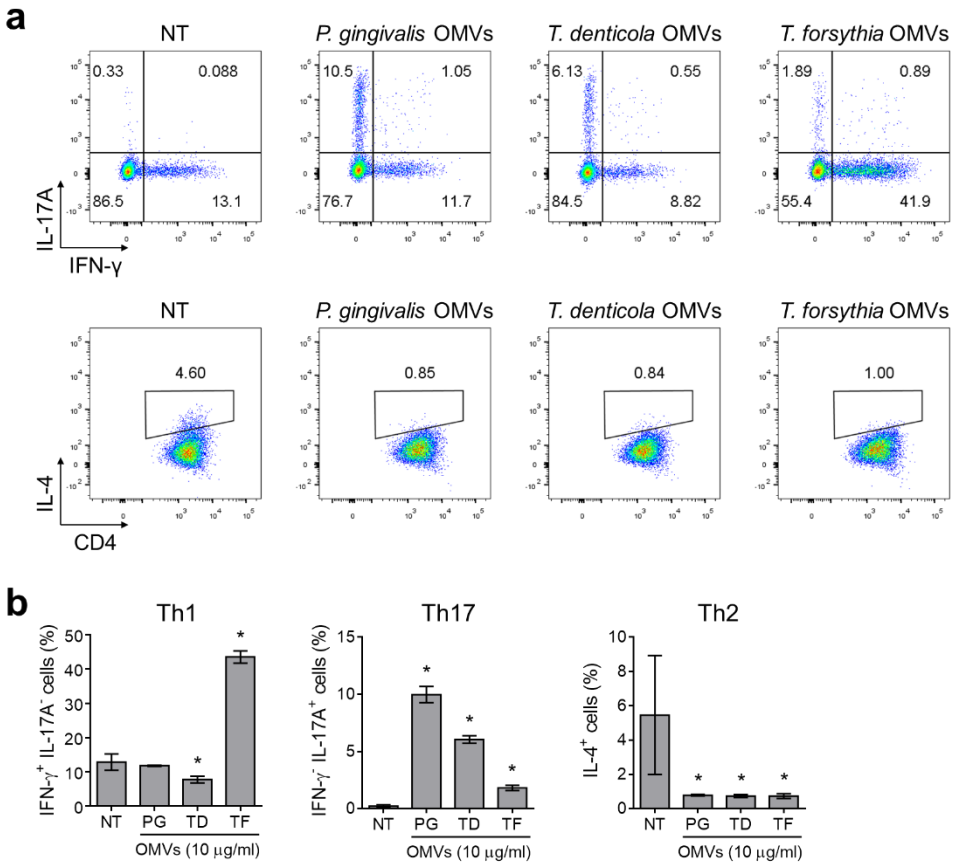

Figure 19. Differentiation of CD4$^+$ T cells by OMV-primed BMDCs. BMDCs were stimulated with 10 μg/ml of the indicated OMVs for 5 hours. After three times of washing with PBS, the BMDCs were cocultured with naïve CD4$^+$ T cells for 4 days in the presence of soluble anti-CD3ε antibody and analyzed via flow cytometry. The experiments were performed four times independently, and representative data are shown as dot plots (a) and the proportions of intracellular IFN-γ, IL-17A, and IL-4 in CD4$^+$ T cells (b). Data are presented as the mean ± *SD* of triplicate assays and were analyzed by one-way ANOVA. * $p < 0.05$ compared to the control (NT). N.S., not significant; NT, non-treatment; PG, *P. gingivalis*; TD, *T. denticola*; TF, *T. forsythia*.

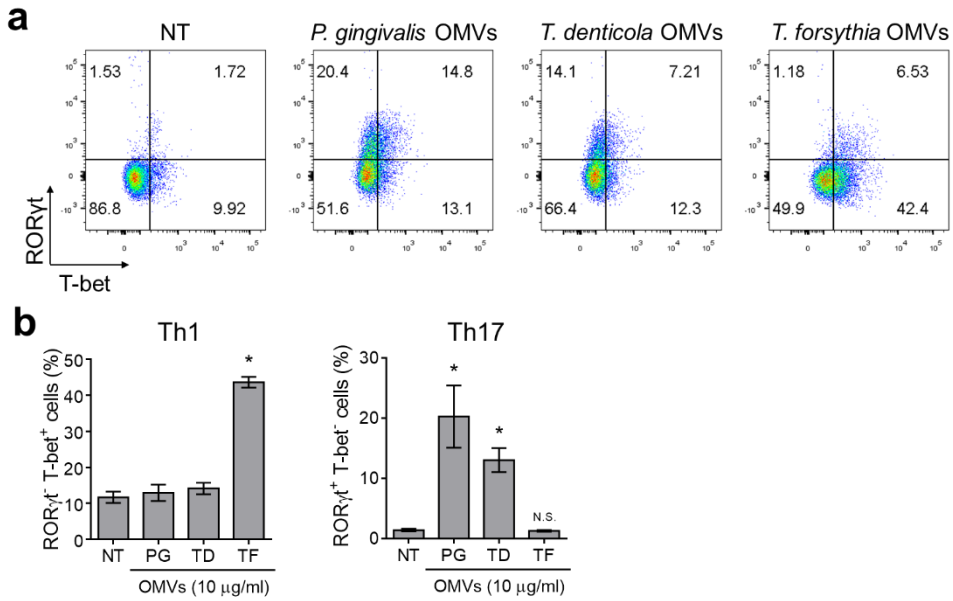

Figure 20. Analysis of transcription factors of CD4$^+$ T cells differentiated by OMV-primed BMDCs. BMDCs were stimulated with 10 μg/ml of the indicated OMVs for 5 hours. After three times of washing with PBS, the BMDCs were cocultured with naïve CD4$^+$ T cells for 4 days in the presence of soluble anti-CD3ε antibody and analyzed via flow cytometry. The experimental data are shown as dot plots (a) and the proportions of intranuclear t-bet and RORγt in CD4$^+$ T cells (b). Data are presented as the mean ± *SD* of triplicate assays and were analyzed by one-way ANOVA. * $p < 0.05$ compared to the control (NT). N.S., not significant; NT, non-treatment; PG, *P. gingivalis*; TD, *T. denticola*; TF, *T. forsythia*.

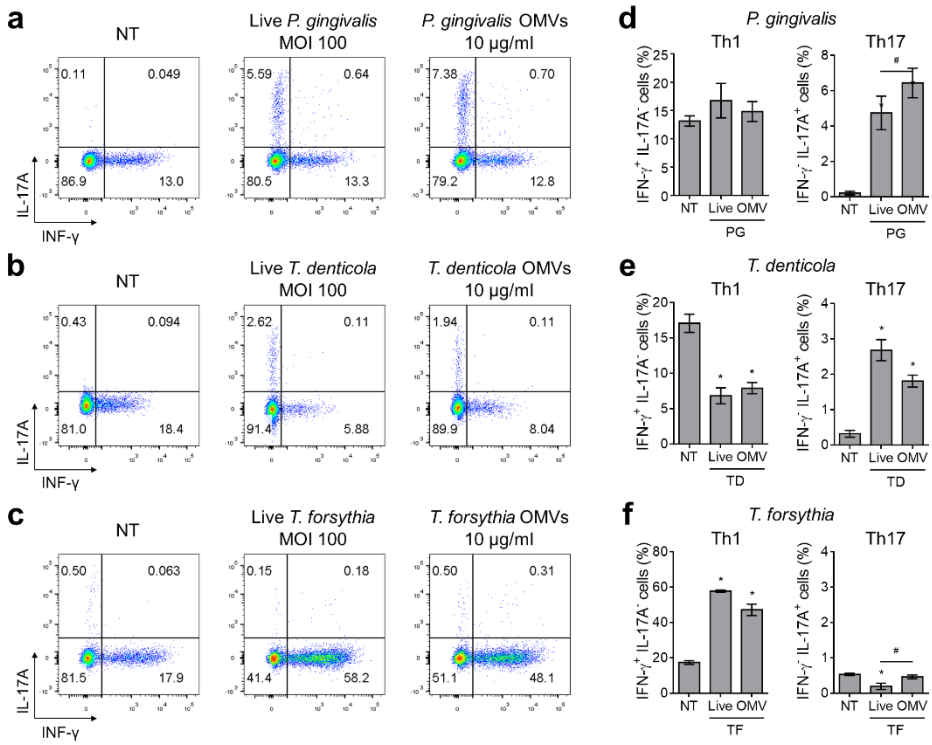

Figure 21. Differentiation of CD4$^+$ T cells by live oral pathogen- or OMV-primed BMDCs. BMDCs were treated with indicated live oral pathogens (MOI 100) or OMVs (10 μg/ml) for 5 hours. After three times of washing with PBS, the BMDCs were cocultured with naïve CD4$^+$ T cells for 4 days in the presence of soluble anti-CD3ε antibody and analyzed via flow cytometry. The representative data are shown as dot plots (a to c) and the proportions of intracellular IFN-γ and IL-17A in CD4$^+$ T cells (d to f). Data are presented as the mean ± *SD* of triplicate assays and were analyzed by one-way ANOVA with Tukey's post-hoc test. * $p < 0.05$ compared to the control (NT), # $p < 0.05$ compared to the indicated groups. N.S., not significant; NT, non-treatment; PG, *P. gingivalis*; TD, *T. denticola*; TF, *T. forsythia*.

2.5 IL-6 and IL-12 play a key role in the differentiation of naïve $CD4^+$ T cells by OMV-primed BMDCs into Th17 and Th1 cells, respectively.

To evaluate which cytokine contributes to the differentiation of Th1 or Th17 cells induced by OMV-primed BMDCs, neutralizing antibodies against IL-12 and IL-6 were treated to OMV-primed BMDCs during coculture and then analyzed $CD4^+$ T cell differentiation. Neutralization of IL-6 significantly increased IFN-γ^+ cells but reduced IL-$17A^+$ cells in the coculture of each periodontal pathogen derived OMV-primed BMDC with naïve $CD4^+$ T cells (Figure 22a–c). Neutralization of IL-12p40 decreased IFN-γ^+ cells but increased IL-$17A^+$ cells in the coculture of *T. forsythia* OMV-primed BMDCs with naïve $CD4^+$ T cells (Figure 23c). However, IFN-γ^+ and IL-$17A^+$ cells were not affected in the coculture of *P. gingivalis* OMV- and *T. denticola* OMV-primed BMDCs with naïve $CD4^+$ T cells (Figure 23a and 23b). These results suggest that IL-6 is a major cytokine in Th17 differentiation by OMVs of *P. gingivalis* and *T. denticola*, whereas IL-12 is responsible for Th1 differentiation by *T. forsythia* OMVs.

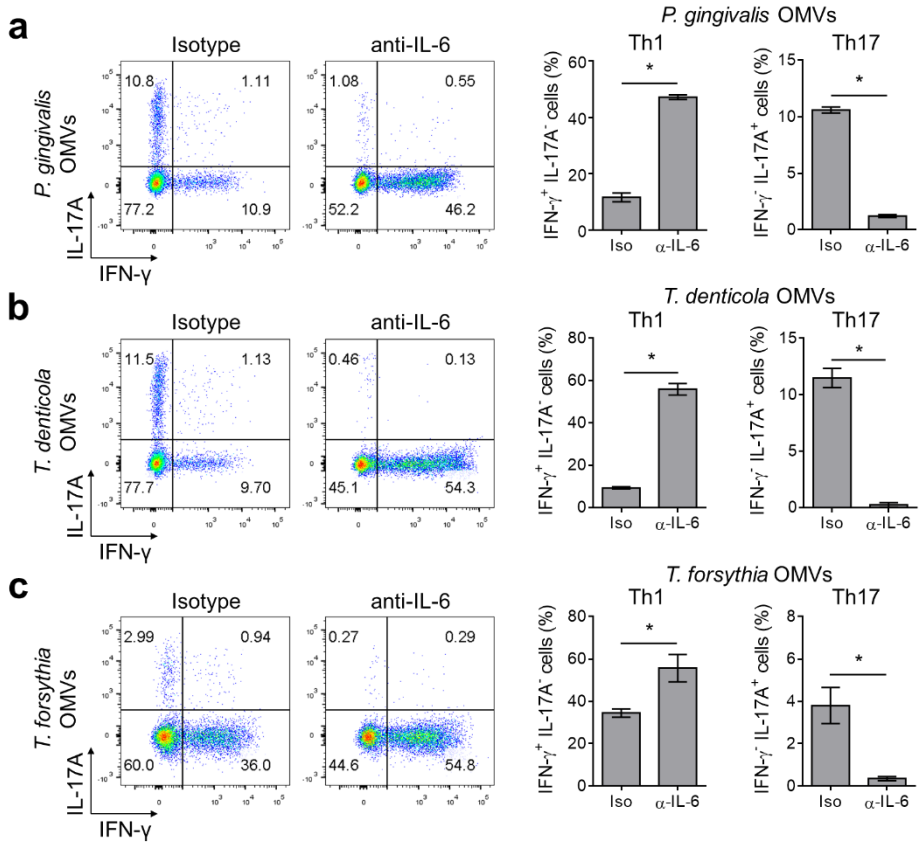

Figure 22. Analysis of the role of IL-6 for Th17 differentiation by OMV-primed BMDCs. BMDCs were stimulated with 10 μg/ml *P. gingivalis* OMVs (a), *T. denticola* OMVs (b), and *T. forsythia* OMVs (c) for 5 hours. After three times of washing with PBS, the BMDCs were cocultured with naïve $CD4^+$ T cells for 4 days in the presence of soluble anti-CD3ε antibody and 10 μg/ml anti-IL-6 antibody and then analyzed via flow cytometry. Representative data are shown as dot plots (left panel) and the proportion of cells (right panel) expressing intracellular IFN-γ and IL-17A among $CD4^+$ T cells. The experiments were performed three times independently. Data are presented as the mean ± *SD* of triplicate assays and were analyzed by Student's *t*-test. * $p < 0.05$ compared to the control (isotype). PG, *P. gingivalis*; TD, *T. denticola*; TF, *T. forsythia*.

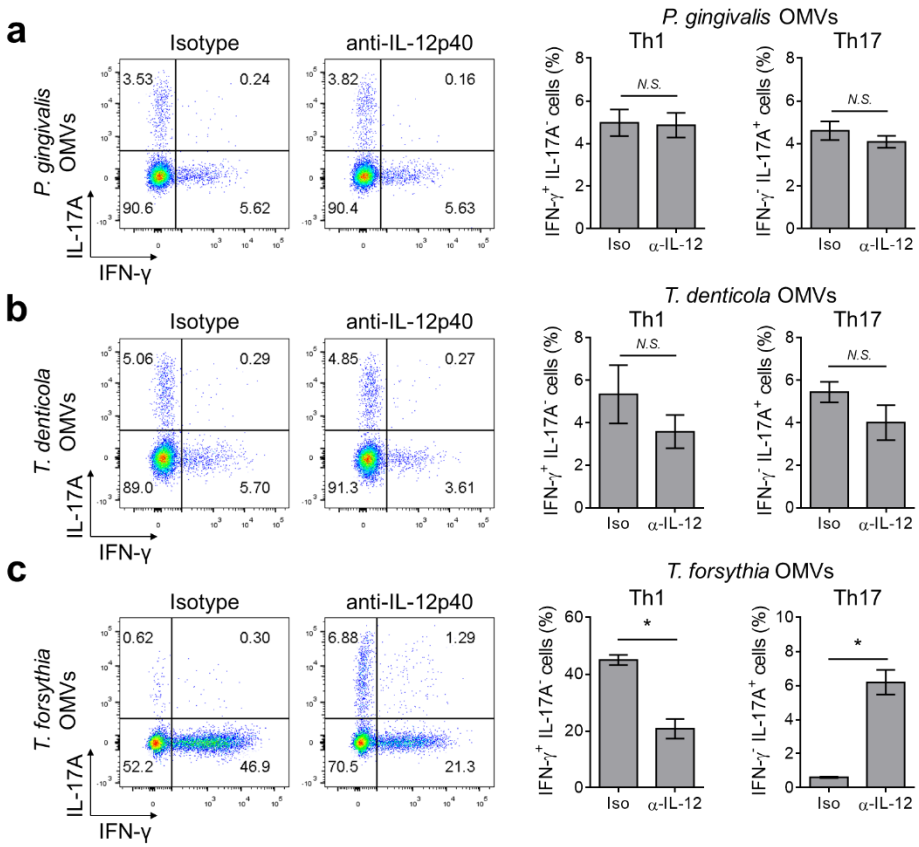

Figure 23. Analysis of the role of IL-12 for Th1 differentiation by OMV-primed BMDCs. BMDCs were stimulated with 10 μg/ml *P. gingivalis* OMVs (a), *T. denticola* OMVs (b), and *T. forsythia* OMVs (c) for 5 hours. After three times of washing with PBS, the BMDCs were cocultured with naïve $CD4^+$ T cells for 4 days in the presence of soluble anti-CD3ε antibody and 10 μg/ml anti-IL-12p40 antibody and then analyzed via flow cytometry. Representative data are shown as dot plots (left panel) and the proportion of cells (right panel) expressing intracellular IFN-γ and IL-17A among $CD4^+$ T cells. The experiments were performed three times independently. Data are presented as the mean ± *SD* of triplicate assays and were analyzed by Student's *t*-test. * $p < 0.05$ compared to the control (isotype). N.S., not significant. PG, *P. gingivalis*; TD, *T. denticola*; TF, *T. forsythia*.

IV. Discussion

1. Identification of proteome and immune responses of EVs derived from macrophages infected with *T. forsythia*

Periodontal pathogens release virulence factors that induce inflammatory responses. In this study, the proteome profile of EVs released from *T. forsythia*-infected macrophages was analyzed to identify the virulence factors contained in EVs that are responsible for the induction of inflammatory responses. During infection, *T. forsythia* as well as macrophages released EVs. Macrophage-derived EVs carried pro-inflammatory cytokines and inflammatory mediators, while *T. forsythia*-derived EVs carried bacterial virulence factors that activated the TLR2 signaling pathway and increased pro-inflammatory responses in host cells. This is the first report on the interaction of periodontal pathogens with innate immune cells, revealing that periodontal pathogens directly release EVs that induce inflammatory responses and immune cells to also release EVs, which can further upregulate the immune responses.

According to the GOBP results, TF-F2 is enriched with proteins associated with neutrophil/granulocyte activation, secretion by exocytosis, and leukocyte-mediated immunity compared with NI-F2. Additionally, TF-F2 induced TNF-α secretion from macrophages. TF-F2 contains various proteins that play a role in the activation of immune cells and pathogenesis of periodontitis. Among the proteins increased in TF-F2, the expression level of TNF-α, IL-8, and IL-1β was remarkably high. These are pro-inflammatory cytokines that are highly detected in the saliva or gingival crevicular fluids of patients with chronic periodontitis [97, 98]. TNF-α and IL-1β are associated with several inflammatory events including the induction of adhesion molecules and other mediators, that facilitate and amplify the inflammatory response, stimulate MMPs, and cause bone resorption [99]. IL-8 is a chemoattractant cytokine that recruits neutrophils, which are the major

immigrant cells in periodontitis and are responsible for the destruction of periodontal tissues [100]. Levels of inflammatory mediators, including CPNE1, SPP1, PLSCR1, P2RX4, MMP9, SARS, VARS, STXBP2, HVCN1, CD82, RFTN1, LCP1, and ATP2B1, are also increased in EVs from *T. forsythia*-infected macrophages. CPNE1 is related with the TNF-α receptor signaling pathway [101], and is highly expressed in the osteosarcoma [102]. SPP1 enhances the production of IL-12 from DCs and IFN-γ from T cells [103]. PLSCR1 enhances IFN response, which potentiates antiviral activity [104]. P2RX4 promotes activation of Th17 cells and modulates ROS production and inflammasome activation in gingival epithelial cells [105, 106]. MMP9 plays a major role in bone resorption and is one of the major biomarkers of periodontitis [107]. SARS and VARS are aminoacyl tRNA synthases (ARSs) that are associated with not only protein translation but also various physiological and pathological processes [108]. ARSs play a role in the pathogenesis of inflammatory diseases. According to the salivary metabolite analysis, valine is upregulated in patients with periodontitis, and aminoacyl-tRNA biosynthesis is a significantly upregulated pathway by based on pathway enrichment analysis [109]. STXBP2 is necessary for cytotoxic function of natural killer (NK) cells [110]. HVCN1 maintains high level of ROS production in the phagosomes of neutrophils to effectively eliminate bacteria [111]. CD82 is involved in T cell activation through the formation of immune synapses [112]. RFTN1 mediates LPS-induced internalization of TLR4 in DCs and macrophages [113]. LCP1 plays a crucial role in surface expression of co-stimulatory receptors, including CD2 and CD28, on T cells [114]. ATP2B1 is crucial for the regulation of bone homeostasis by modulating $Ca2^{+}$ signaling in osteoclasts [115]. Therefore, it is possible that when macrophages are infected with *T. forsythia*, they release EVs with various pro-inflammatory cytokines and inflammatory mediators that upregulate inflammatory responses associated with periodontal disease caused by various immune cells, including, macrophages, DCs, T cells, NK

cells, and neutrophils. Neutrophils, macrophages, and T cells play a pivotal role in the pathogenesis of periodontitis [50, 60, 68]. Neutrophils are particularly abundant in the gingival crevice and periodontal pocket, and their numbers increase during inflammation [61]. Individuals with leukocyte adhesion deficiency, a genetic defect that impairs neutrophil migration, have a low number of neutrophils in periodontal tissue, resulting in aggressive periodontitis [60, 64]. Therefore, macrophage-derived EVs, which are enriched with proteins that activate neutrophils/granulocytes, enhance neutrophil function against periodontal pathogen infection.

Environmental factors, such as temperature changes, oxidative stress, iron deficiency, and malnutrition, act as stressors to bacteria; in response, they release EVs [116]. Releasing EVs is one of the survival strategies of bacteria in terms of nutrient utilization [117, 118]. For oral bacteria, the microenvironment of the host periodontal tissue makes it difficult to survive. Numerous *T. forsythia* proteins play a role in nutrient uptake and utilization in *T. forsythia*-derived EVs and include TonB-dependent receptors, RagB/SusD family nutrient uptake outer membrane proteins, and HmuY family protein (WP_046825712.1). RagB/SusD homologous proteins combine with their counterpart TonB-dependent receptors to capture specific nutrients in the environment and transport them into cells [119]. The HmuY family protein, also known as Tfo, is a heme-binding protein that is upregulated under low-iron/heme conditions in both *T. forsythia* whole cells and OMVs [120]. Heme is required for the optimal growth of *T. forsythia* and other periodontal pathogens [121]. To enhance nutrient utilization under nutrient-deficient conditions, such as in host tissues, *T. forsythia* releases EVs to capture nutrients in the microenvironment. Uptake of EVs by *T. forsythia* or nearby periodontal pathogens could utilize EV-captured nutrients for their survival. Therefore, releasing EVs might be a useful strategy for *T. forsythia* to survive in periodontal tissues by enhancing nutrient utilization.

Bacterial EVs are enriched with various virulence factors, which can initiate inflammatory responses. In the present study, *T. forsythia*-derived EVs (TF-F5) induced pro-inflammatory responses and activated the TLR2 signaling pathway. Diverse MAMPs of *T. forsythia*-derived EVs might be responsible for the pro-inflammatory responses through the TLR2 signaling pathway. Through in-depth quantitative proteomic analysis, several TLR2 agonists were identified in *T. forsythia*-derived EVs, including 95 bacterial lipoproteins and leucine-rich-repeat family virulence factor BspA (WP_052449061.1). Bacterial lipoproteins are produced by all bacteria and are known as major TLR2 ligands [122]. BspA, one of the virulence factors of *T. forsythia*, activates TLR2 and induces the release of pro-inflammatory cytokines from macrophages [28]. Additionally, Exo-alpha-sialidase (WP_046826229.1), beta-glucosidase BglX (WP_080948511.1), family 20 glycosyl hydrolase (HexA; WP_046825029.1), Chaperonin GroEL (WP_046825748.1), and two S9 family peptidases (WP_046825437.1 and WP_046824629.1), which are non-TLR2 agonist virulence factors related to the pathogenesis of periodontal disease, were also identified in *T. forsythia*-derived EVs. Glycosyl hydrolases, including, exo-alpha-sialidase, BglX, and family 20 glycosyl hydrolase, might play a role in disrupting of periodontal tissue and supporting the growth of nearby oral bacteria since it hydrolyzes oligosaccharides and proteoglycans in periodontal tissue, gingival crevicular fluid, or saliva [18]. Chaperonin GroEL (WP_046825748.1) induces the pro-inflammatory response and synergizes with IL-17 for inflammatory bone resorption [123]. S9 family peptidases, also known as dipeptidyl peptidase IV (DppIV), are serine proteases that degrade collagens of the periodontium in periodontitis [124]. Our results are consistent with a study on EVs derived from macrophages infected with *Mycobacterium tuberculosis*, the causative agent of tuberculosis [125]. EVs released from *M. tuberculosis* can induce inflammatory responses because they contain MAMPs, such as lipoproteins and lipoglycans, of *M. tuberculosis*. In the present study, bacterial lipoproteins

as well as non-TLR2 agonist virulence factors were found in the pathogen-derived EVs. Therefore, when periodontal pathogens encounter innate immune cells, they will release EVs that contain virulence factors, which can induce both local and systemic inflammatory responses without cell-to-cell interactions.

To survive within host tissue, *T. forsythia* may release EVs, which is detrimental to the host. *T. forsythia*-derived EVs contain MAMPs that can induce innate immune responses through TLR2 stimulation. Periodontal pathogen OMVs can also induce innate immune responses [126, 127]; however, the mode of the adaptive immune response against periodontal pathogen OMVs has not been studied yet. Therefore, the maturation of BMDCs induced by periodontal pathogen OMVs and the type of helper T cells induced by periodontal pathogen OMV-primed BMDCs were analyzed in Part 2.

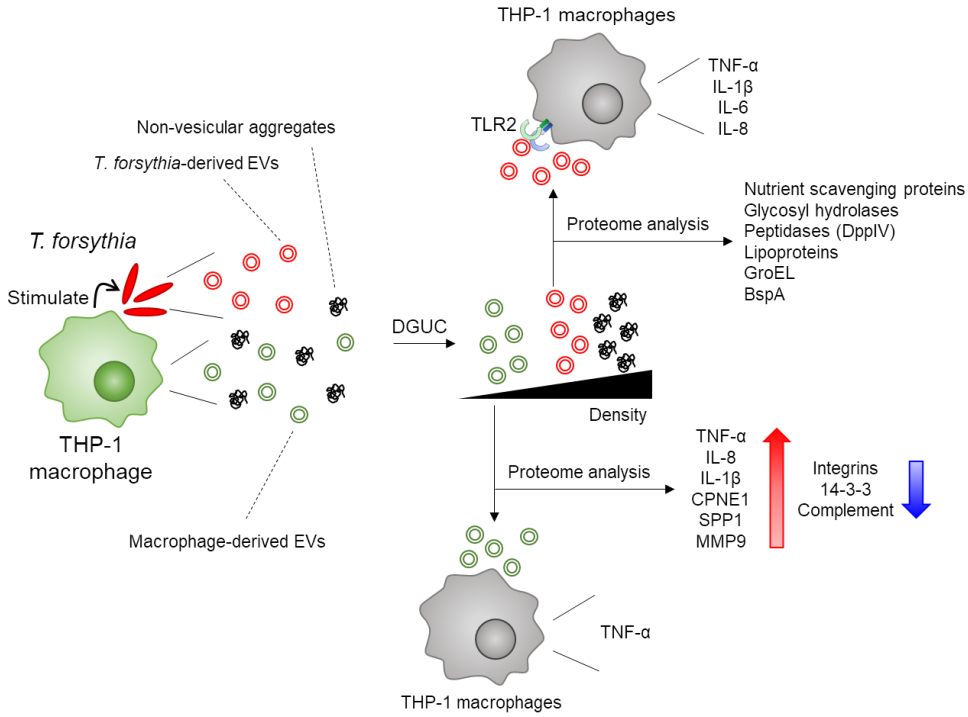

Figure 24. Graphical summary of the proteome and inflammatory responses of EVs derived from THP-1 macrophages infected with *T. forsythia*. EVs derived from THP-1 macrophages infected with *T. forsythia* were purified by DGUC. Proteome of macrophage-derived EVs and *T. forsythia*-derived EVs was analyzed by label-free in-depth quantitative proteomics. Macrophage-derived EVs induced TNF-α in THP-1 macrophages. *T. forsythia*-derived EVs induced TNF-α, IL-1β, IL-6, and IL-8 in THP-1 macrophages via TLR2 activation.

2. Identification of the role in BMDCs maturation and helper T cell differentiation by periodontal pathogen OMVs

The responses of T lymphocytes to dysbiotic oral bacteria play an essential role in the immunopathogenesis of periodontal disease [128]. As OMVs harbor various immunostimulatory molecules [70], the present study determined the role of the OMVs of periodontal pathogens in helper T cell polarization through DC maturation. The OMVs of periodontal pathogens activated DCs to secrete effector cytokines of Th1 and Th17 cells but not Th2 cells. *P. gingivalis* OMV- and *T. denticola* OMV-primed BMDCs induced the differentiation of naïve $CD4^+$ T cells into Th17 cells. In contrast, *T. forsythia* OMV-primed BMDCs favored the polarization of Th1 cells rather than Th17 cells.

The maturation of DCs is essential for linking innate immunity to adaptive immunity [96]. There is some evidence that DC maturation by the OMVs of periodontal pathogens might occur through TLR signaling pathways. First, the “red complex” bacteria induce immune responses mainly through TLR2 and TLR4 [24, 48, 129]. Second, the OMVs of periodontal pathogens harbor various MAMPs, such as LPS/LOS, lipoproteins, peptidoglycan, DNA, and RNA, which are the ligands of TLRs [126]. Several studies have reported that other bacterial OMVs can induce DC maturation through TLR signaling pathways [130-132]. Furthermore, since OMVs are potent immune stimulators and deliver bacteria-specific antigens without the bacteria being present, OMVs are receiving attention as an ideal vaccine against infectious diseases [133]. Therefore, further studies are needed to identify the molecular mechanisms of TLR signaling that are responsible for DC maturation induced by MAMPs in the periodontal pathogen OMVs.

For normalization of OMV treatment, one must choose either a biomolecule or a number of OMVs. According to Cecil et al. (2016), the amounts of protein, LPS, lipoprotein, peptidoglycan, DNA, and RNA were too different in the same number of OMVs of *P. gingivalis*, *T. denticola*, and *T. forsythia*

[126]. In the report, the degree of TLR2 and TLR4 activation by the same amount of OMV proteins was similar to each other, but the degree of TLR2 and TLR4 activation by the same number of OMVs was very different, especially in the case of *T. denticola* OMVs. Although the particle number in 10 μg proteins of *P. gingivalis* OMVs and *T. forsythia* OMVs was similar, their ability to induce Th1 or Th17 differentiation was different. The particle number in 10 μg proteins of *T. denticola* OMVs was higher than that in 10 μg proteins of *P. gingivalis* OMVs and *T. forsythia* OMVs, but showed similar BMDC-activating abilities to *P. gingivalis* OMVs and *T. forsythia* OMVs. Therefore, protein quantification of OMVs is a reliable criterion for assessing host response to OMVs and that different T cell polarization by each OMVs might be due to their different qualitative rather than quantitative nature.

The present study demonstrated that *P. gingivalis* OMVs induced DC-mediated Th17 polarization. In addition, the ability of *P. gingivalis* OMVs to induce Th17 polarization is similar to that of *P. gingivalis* whole cells. *P. gingivalis* induces Th17 responses *in vivo* and *in vitro* by activating DCs and monocytes [134-137]. *P. gingivalis* LPS has been found to upregulate Th17 cell differentiation from activated human naïve $CD4^+$ T cells in the presence of Th17-driven cytokines [138]. Th17 cells induced by *P. gingivalis* affect the pathogenesis of periodontitis and systemic diseases, such as rheumatoid arthritis [139]. *P. gingivalis* oral infection induces alveolar bone resorption and aggravates the severity of arthritis, which may be associated with increased systemic Th17 responses [140, 141]. Since *P. gingivalis* OMVs can spread to host tissues through the bloodstream [77], *P. gingivalis* OMVs may induce Th17 differentiation, leading to periodontitis and other systemic diseases. Since only the *P. gingivalis* ATCC 33277 strain was used in this study, it is necessary to analyze various *P. gingivalis* strains, including W50 and gingipain mutant strains, for DC maturation and T cell differentiation.

Unlike *P. gingivalis*, the role of *T. denticola* in $CD4^+$ T cell responses has not been well studied yet. The present study demonstrated for the first time

that *T. denticola* whole cells and *T. denticola* OMVs induced DC-mediated Th17 polarization but not Th1. IL-6 released from both *P. gingivalis* OMV- and *T. denticola* OMV-primed BMDCs was found to play a pivotal role in Th17 polarization. Among various cytokines from mature DCs, IL-6 is an essential cytokine for the commitment of Th17 cells [142, 143]. IL-6 activates the STAT3 signaling pathway through gp130 on naïve $CD4^+$ T cells [142], and STAT3 is a crucial transcription factor for Th17 cell differentiation [143]. In addition, IL-6 inhibits the differentiation of Th1 cells by inhibiting SOCS1 function [144].

In contrast to *P. gingivalis* OMV- and *T. denticola* OMV-primed BMDCs, *T. forsythia* OMV-primed BMDCs preferentially induced the differentiation of Th1 cells rather than Th17 cells. IL-12 was found to play a pivotal role in Th1 differentiation by *T. forsythia* OMV-primed BMDCs. IL-12 is known as an inducer of naïve $CD4^+$ T cell differentiation into Th1 cells [145]. *T. forsythia* OMVs significantly induced IL-12p70 expression in BMDCs compared to OMVs of *P. gingivalis* and *T. denticola*. Indeed, the neutralization of IL-12 reduced Th1 cells but increased Th17 cells in the coculture of *T. forsythia* OMV-primed BMDCs with naïve $CD4^+$ T cells. Furthermore, the S-layer glycan of *T. forsythia* was previously reported to restrain Th17 cell responses in a mouse model and human peripheral blood mononuclear cell study [31, 146]. The S-layer glycan is a typical structure of *T. forsythia* and protects the bacterium from recognition by DCs [31]. Further studies are needed to identify the detailed molecular mechanisms underlying the ability of OMVs from different bacterial species to differentially regulate T cell polarization.

Among the three periodontal pathogen OMVs, *T. denticola* OMVs showed the highest proteolytic activity against pro-inflammatory cytokines. Dentilisin is a chymotrypsin-like protease located in the outer membrane of *T. denticola* [147]. Veith et al. showed that dentilisin is one of the abundant proteins in *T. denticola* OMVs, and its topology on *T. denticola* OMVs faces

the extracellular space [148]. It has been shown that dentilisin can degrade several host proteins, including pro-inflammatory cytokines, such as TNF-α, IL-1β, IL-6, and IL-8 [149]. Ginginpains are well-characterized proteolytic enzymes and virulence factors of *P. gingivalis* [150]. There are three types of gingipains. RgpA and RgpB are arginine-specific cysteine proteases, and Kgp is a lysine-specific cysteine protease [151]. Gingipains are abundant on *P. gingivalis* OMVs [152] and contribute to evasion of the host immune surveillance system by degrading cytokines such as IL-1β, IL-6, and IFN-γ [39]. In this study, *P. gingivalis* OMVs degraded recombinant murine IL-1β and IL-23 but not IL-6 and IL-12p70. Therefore, OMV secretion is a useful tool of *T. denticola* and *P. gingivalis* for evading host immune systems.

Periodontal pathogen OMVs induced helper T cell differentiation via BMDCs similar to live bacteria. Periodontal pathogen OMVs might play a key role in induction of DC maturation and Th1/Th17 cell differentiation which are associated with pathogenesis of periodontitis and other systemic diseases since OMVs are easily spread to the various tissues [75]. Therefore, further *in vivo* studies are needed to clarify the role of periodontal pathogen OMVs in pathogenesis of periodontitis and periodontitis-associated systemic diseases.

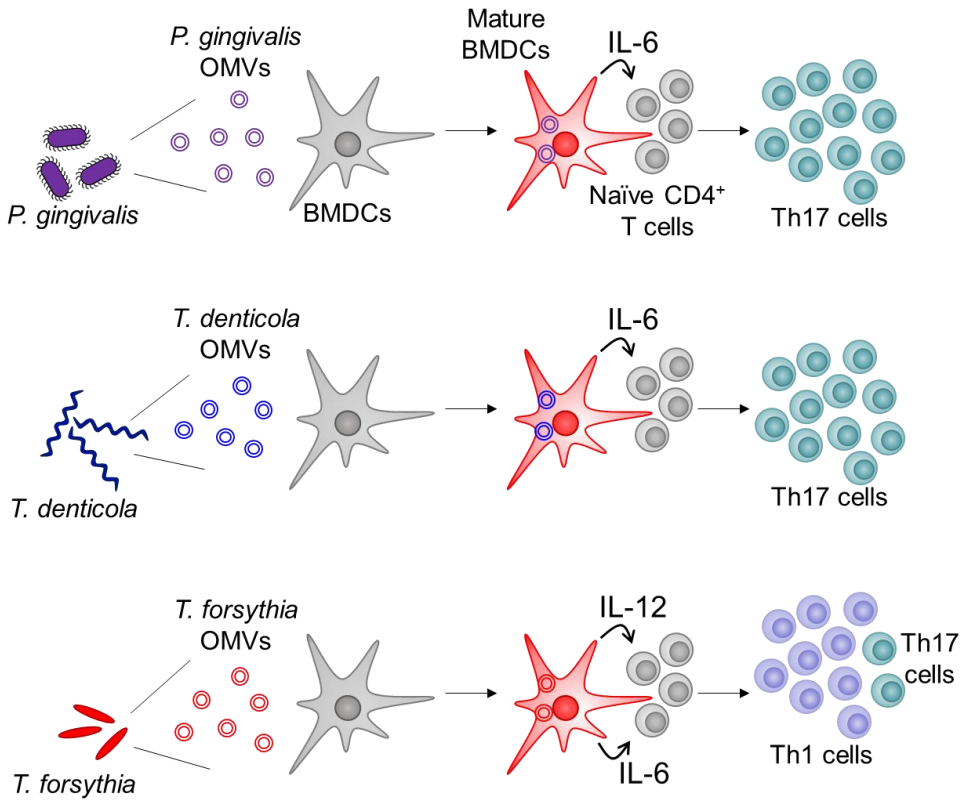

Figure 25. Graphical summary of naïve CD4⁺ T cell differentiation by periodontal pathogen OMV-primed BMDCs. OMVs of periodontal pathogens, *P. gingivalis*, *T. denticola*, and *T. forsythia*, induced the expression of MHC class II and CD80, CD86, and CD40 on BMDCs. *P. gingivalis* OMV- and *T. denticola* OMV-primed BMDCs induced differentiation of naïve CD4+ T cells into Th17 cells by release through IL-6. However, *T. forsythia* OMV-primed BMDCs preferentially induced Th1 cell differentiation via IL-12.

V. Conclusion

EVs derived from macrophages infected with *T. forsythia* carried pro-inflammatory cytokines and inflammatory mediators that play a role in the inflammatory responses in periodontitis. *T. forsythia*-derived EVs contained various virulence factors and induced pro-inflammatory responses through TLR2 activation. OMVs of *P. gingivalis* and *T. denticola* induced differentiation of Th17 cells, while *T. forsythia* OMVs favored Th1 cell polarization rather than Th17 cells. These results demonstrate that in pathogen-infected cells, EVs derived from host cells and a pathogen can have a synergistic effect on the inflammatory response. OMVs derived from the "red complex" bacteria induced BMDCs maturation and differentiation of naïve $CD4^+$ T cells into Th1 or Th17 cells.

This study revealed that EVs derived from both host cells and periodontal pathogens induced innate and adaptive immune responses that may contribute to the pathogenesis of periodontitis. Taken together, EVs may be a useful tool for understanding the pathogenic mechanisms of periodontal pathogens.

Further *in vivo* animal model studies are needed to clarify the roles of periodontal pathogen OMVs in the pathogenesis of periodontal diseases. Additionally, clinical studies using EVs isolated from the blood or saliva of patients with periodontitis may help for identifying biological markers of periodontitis.

VI. References

1. Cavicchioli R, Ripple WJ, Timmis KN, et al. Scientists' warning to humanity: microorganisms and climate change. Nat Rev Microbiol. 2019;17:569-586. DOI: 10.1038/s41579-019-0222-5
2. Berg G, Rybakova D, Fischer D, et al. Microbiome definition re-visited: old concepts and new challenges. Microbiome. 2020;8:103. DOI: 10.1186/s40168-020-00875-0
3. Pasolli E, Asnicar F, Manara S, et al. Extensive unexplored human microbiome diversity revealed by over 150,000 genomes from metagenomes spanning age, geography, and lifestyle. Cell. 2019;176:649-662 e620. DOI: 10.1016/j.cell.2019.01.001
4. Shreiner AB, Kao JY, Young VB. The gut microbiome in health and in disease. Curr Opin Gastroenterol. 2015;31:69-75. DOI: 10.1097/MOG.0000000000000139
5. Clapp M, Aurora N, Herrera L, Bhatia M, Wilen E, Wakefield S. Gut microbiota's effect on mental health: The gut-brain axis. Clin Pract. 2017;7:987. DOI: 10.4081/cp.2017.987
6. Shoubridge AP, Choo JM, Martin AM, et al. The gut microbiome and mental health: advances in research and emerging priorities. Mol Psychiatry. 2022;27:1908-1919. DOI: 10.1038/s41380-022-01479-w
7. Peng X, Cheng L, You Y, et al. Oral microbiota in human systematic diseases. Int J Oral Sci. 2022;14:14. DOI: 10.1038/s41368-022-00163-7
8. Belkaid Y, Hand TW. Role of the microbiota in immunity and inflammation. Cell. 2014;157:121-141. DOI: 10.1016/j.cell.2014.03.011
9. Macpherson AJ, Hunziker L, McCoy K, Lamarre A. IgA responses in the intestinal mucosa against pathogenic and non-pathogenic microorganisms. Microbes Infect. 2001;3:1021-1035. DOI: 10.1016/s1286-4579(01)01460-5

10. Hooks KB, O'Malley MA. Dysbiosis and its discontents. mBio. 2017;8. DOI: 10.1128/mBio.01492-17
11. Kilian M, Chapple IL, Hannig M, et al. The oral microbiome - an update for oral healthcare professionals. Br Dent J. 2016;221:657-666. DOI: 10.1038/sj.bdj.2016.865
12. Kinane DF, Stathopoulou PG, Papapanou PN. Periodontal diseases. Nat Rev Dis Primers. 2017;3:17038. DOI: 10.1038/nrdp.2017.38
13. Nazir MA. Prevalence of periodontal disease, its association with systemic diseases and prevention. Int J Health Sci (Qassim). 2017;11:72-80
14. Silva N, Abusleme L, Bravo D, et al. Host response mechanisms in periodontal diseases. J Appl Oral Sci. 2015;23:329-355. DOI: 10.1590/1678-775720140259
15. Socransky SS, Haffajee AD, Cugini MA, Smith C, Kent RL, Jr. Microbial complexes in subgingival plaque. J Clin Periodontol. 1998;25:134-144. DOI: 10.1111/j.1600-051x.1998.tb02419.x
16. Xu W, Zhou W, Wang H, Liang S. Roles of *Porphyromonas gingivalis* and its virulence factors in periodontitis. Adv Protein Chem Struct Biol. 2020;120:45-84. DOI: 10.1016/bs.apcsb.2019.12.001
17. Sela MN. Role of *Treponema denticola* in periodontal diseases. Crit Rev Oral Biol Med. 2001;12:399-413. DOI: 10.1177/10454411010120050301
18. Sharma A. Virulence mechanisms of *Tannerella forsythia*. Periodontol 2000. 2010;54:106-116. DOI: 10.1111/j.1600-0757.2009.00332.x
19. Hajishengallis G, Chavakis T. Local and systemic mechanisms linking periodontal disease and inflammatory comorbidities. Nat Rev Immunol. 2021;21:426-440. DOI: 10.1038/s41577-020-00488-6
20. Bui FQ, Almeida-da-Silva CLC, Huynh B, et al. Association between periodontal pathogens and systemic disease. Biomed J. 2019;42:27-35. DOI: 10.1016/j.bj.2018.12.001

21. Tanner A, Listgarten M, Ebersole J, Strzempko M. *Bacteroides forsythus* sp. nov., a slow-growing, fusiform Bacteroides sp. from the human oral cavity. International journal of systematic and evolutionary microbiology. 1986;36:213-221. DOI: 10.1099/00207713-36-2-213
22. Tanner AC, Izard J. *Tannerella forsythia*, a periodontal pathogen entering the genomic era. Periodontol 2000. 2006;42:88-113. DOI: 10.1111/j.1600-0757.2006.00184.x
23. Sharma A, Inagaki S, Honma K, Sfintescu C, Baker PJ, Evans RT. *Tannerella forsythia*-induced alveolar bone loss in mice involves leucine-rich-repeat BspA protein. J Dent Res. 2005;84:462-467. DOI: 10.1177/154405910508400512
24. Myneni SR, Settem RP, Connell TD, Keegan AD, Gaffen SL, Sharma A. TLR2 signaling and Th2 responses drive *Tannerella forsythia*-induced periodontal bone loss. J Immunol. 2011;187:501-509. DOI: 10.4049/jimmunol.1100683
25. Pavlic V, Peric D, Kalezic IS, et al. Identification of periopathogens in atheromatous plaques obtained from carotid and coronary arteries. Biomed Res Int. 2021;2021:9986375. DOI: 10.1155/2021/9986375
26. Hottmann I, Mayer VMT, Tomek MB, et al. N-acetylmuramic acid (MurNAc) auxotrophy of the oral pathogen *Tannerella forsythia*: characterization of a MurNAc kinase and analysis of its role in cell wall metabolism. Front Microbiol. 2018;9:19. DOI: 10.3389/fmicb.2018.00019
27. Chukkapalli SS, Rivera-Kweh MF, Velsko IM, et al. Chronic oral infection with major periodontal bacteria *Tannerella forsythia* modulates systemic atherosclerosis risk factors and inflammatory markers. Pathog Dis. 2015;73. DOI: 10.1093/femspd/ftv009
28. Myneni SR, Settem RP, Sojar HT, et al. Identification of a unique TLR2-interacting peptide motif in a microbial leucine-rich repeat protein. Biochem Biophys Res Commun. 2012;423:577-582. DOI:

10.1016/j.bbrc.2012.06.008

29. Onishi S, Honma K, Liang S, et al. Toll-like receptor 2-mediated interleukin-8 expression in gingival epithelial cells by the *Tannerella forsythia* leucine-rich repeat protein BspA. Infect Immun. 2008;76:198-205. DOI: 10.1128/IAI.01139-07
30. Hasebe A, Yoshimura A, Into T, et al. Biological activities of *Bacteroides forsythus* lipoproteins and their possible pathological roles in periodontal disease. Infect Immun. 2004;72:1318-1325. DOI: 10.1128/IAI.72.3.1318-1325.2004
31. Settem RP, Honma K, Nakajima T, et al. A bacterial glycan core linked to surface (S)-layer proteins modulates host immunity through Th17 suppression. Mucosal Immunol. 2013;6:415-426. DOI: 10.1038/mi.2012.85
32. Yang HW, Huang YF, Chou MY. Occurrence of *Porphyromonas gingivalis* and *Tannerella forsythensis* in periodontally diseased and healthy subjects. J Periodontol. 2004;75:1077-1083. DOI: 10.1902/jop.2004.75.8.1077
33. Kawada M, Yoshida A, Suzuki N, et al. Prevalence of *Porphyromonas gingivalis* in relation to periodontal status assessed by real-time PCR. Oral Microbiol Immunol. 2004;19:289-292. DOI: 10.1111/j.1399-302X.2004.00154.x
34. Hajishengallis G, Liang S, Payne MA, et al. Low-abundance biofilm species orchestrates inflammatory periodontal disease through the commensal microbiota and complement. Cell Host Microbe. 2011;10:497-506. DOI: 10.1016/j.chom.2011.10.006
35. Hajishengallis G, Darveau RP, Curtis MA. The keystone-pathogen hypothesis. Nat Rev Microbiol. 2012;10:717-725. DOI: 10.1038/nrmicro2873
36. Smalley JW, Olczak T. Heme acquisition mechanisms of *Porphyromonas gingivalis* - strategies used in a polymicrobial

community in a heme-limited host environment. Mol Oral Microbiol. 2017;32:1-23. DOI: 10.1111/omi.12149

37. Bostanci N, Belibasakis GN. *Porphyromonas gingivalis*: an invasive and evasive opportunistic oral pathogen. FEMS Microbiol Lett. 2012;333:1-9. DOI: 10.1111/j.1574-6968.2012.02579.x
38. Yilmaz O, Watanabe K, Lamont RJ. Involvement of integrins in fimbriae-mediated binding and invasion by *Porphyromonas gingivalis*. Cell Microbiol. 2002;4:305-314. DOI: 10.1046/j.1462-5822.2002.00192.x
39. Hajishengallis G. Immune evasion strategies of *Porphyromonas gingivalis*. J Oral Biosci. 2011;53:233-240. DOI: 10.2330/joralbiosci.53.233
40. Zhang J, Xie M, Huang X, et al. The effects of *Porphyromonas gingivalis* on atherosclerosis-related cells. Front Immunol. 2021;12:766560. DOI: 10.3389/fimmu.2021.766560
41. Ishihara K. Virulence factors of *Treponema denticola*. Periodontol 2000. 2010;54:117-135. DOI: 10.1111/j.1600-0757.2009.00345.x
42. Charon NW, Cockburn A, Li C, et al. The unique paradigm of spirochete motility and chemotaxis. Annu Rev Microbiol. 2012;66:349-370. DOI: 10.1146/annurev-micro-092611-150145
43. Dashper SG, Seers CA, Tan KH, Reynolds EC. Virulence factors of the oral spirochete *Treponema denticola*. J Dent Res. 2011;90:691-703. DOI: 10.1177/0022034510385242
44. Kasuga Y, Ishihara K, Okuda K. Significance of detection of *Porphyromonas gingivalis*, *Bacteroides forsythus* and *Treponema denticola* in periodontal pockets. Bull Tokyo Dent Coll. 2000;41:109-117. DOI: 10.2209/tdcpublication.41.109
45. Lee SF, Andrian E, Rowland E, Marquez IC. Immune response and alveolar bone resorption in a mouse model of *Treponema denticola* infection. Infect Immun. 2009;77:694-698. DOI: 10.1128/IAI.01004-08

46. Edwards AM, Jenkinson HF, Woodward MJ, Dymock D. Binding properties and adhesion-mediating regions of the major sheath protein of *Treponema denticola* ATCC 35405. Infect Immun. 2005;73:2891-2898. DOI: 10.1128/IAI.73.5.2891-2898.2005

47. Ganther S, Radaic A, Malone E, et al. *Treponema denticola* dentilisin triggered TLR2/MyD88 activation upregulates a tissue destructive program involving MMPs via Sp1 in human oral cells. PLoS Pathog. 2021;17:e1009311. DOI: 10.1371/journal.ppat.1009311

48. Nussbaum G, Ben-Adi S, Genzler T, Sela M, Rosen G. Involvement of Toll-like receptors 2 and 4 in the innate immune response to *Treponema denticola* and its outer sheath components. Infect Immun. 2009;77:3939-3947. DOI: 10.1128/IAI.00488-09

49. Dutzan N, Abusleme L, Bridgeman H, et al. On-going mechanical damage from mastication drives homeostatic Th17 cell responses at the oral barrier. Immunity. 2017;46:133-147. DOI: 10.1016/j.immuni.2016.12.010

50. Dutzan N, Kajikawa T, Abusleme L, et al. A dysbiotic microbiome triggers Th17 cells to mediate oral mucosal immunopathology in mice and humans. Sci Transl Med. 2018;10. DOI: 10.1126/scitranslmed.aat0797

51. Schenkein HA, Koertge TE, Brooks CN, Sabatini R, Purkall DE, Tew JG. IL-17 in sera from patients with aggressive periodontitis. J Dent Res. 2010;89:943-947. DOI: 10.1177/0022034510369297

52. Rodríguez-Montaño R, Ruiz-Gutiérrez AdC, Martínez-Rodríguez VMdC, et al. Levels of IL-23/IL-17 axis in plasma and gingival tissue of periodontitis patients according to the new classification. Applied Sciences. 2022;12:8051

53. Kitamoto S, Nagao-Kitamoto H, Jiao Y, et al. The intermucosal connection between the mouth and gut in commensal pathobiont-driven colitis. Cell. 2020;182:447-462 e414. DOI: 10.1016/j.cell.2020.05.048

54. Cabeza-Cabrerizo M, Cardoso A, Minutti CM, Pereira da Costa M, Reis e Sousa C. Dendritic cells revisited. Annu Rev Immunol. 2021;39:131-166. DOI: 10.1146/annurev-immunol-061020-053707
55. Zhou L, Chong MM, Littman DR. Plasticity of $CD4^+$ T cell lineage differentiation. Immunity. 2009;30:646-655. DOI: 10.1016/j.immuni.2009.05.001
56. Figueredo CM, Lira-Junior R, Love RM. T and B Cells in Periodontal Disease: New Functions in A Complex Scenario. Int J Mol Sci. 2019;20. DOI: 10.3390/ijms20163949
57. Mahanonda R, Champaiboon C, Subbalekha K, et al. Human Memory B Cells in Healthy Gingiva, Gingivitis, and Periodontitis. J Immunol. 2016;197:715-725. DOI: 10.4049/jimmunol.1600540
58. Han YK, Jin Y, Miao YB, Shi T, Lin XP. Improved RANKL production by memory B cells: A way for B cells promote alveolar bone destruction during periodontitis. Int Immunopharmacol. 2018;64:232-237. DOI: 10.1016/j.intimp.2018.08.033
59. Kawai T, Matsuyama T, Hosokawa Y, et al. B and T lymphocytes are the primary sources of RANKL in the bone resorptive lesion of periodontal disease. Am J Pathol. 2006;169:987-998. DOI: 10.2353/ajpath.2006.060180
60. Scott DA, Krauss J. Neutrophils in periodontal inflammation. Front Oral Biol. 2012;15:56-83. DOI: 10.1159/000329672
61. Moutsopoulos NM, Konkel JE. Tissue-Specific Immunity at the Oral Mucosal Barrier. Trends Immunol. 2018;39:276-287. DOI: 10.1016/j.it.2017.08.005
62. Schiott CR, Loe H. The origin and variation in number of leukocytes in the human saliva. J Periodontal Res. 1970;5:36-41. DOI: 10.1111/j.1600-0765.1970.tb01835.x
63. Ryder MI. Comparison of neutrophil functions in aggressive and chronic periodontitis. Periodontol 2000. 2010;53:124-137. DOI:

10.1111/j.1600-0757.2009.00327.x

64. Moutsopoulos NM, Konkel J, Sarmadi M, et al. Defective neutrophil recruitment in leukocyte adhesion deficiency type I disease causes local IL-17-driven inflammatory bone loss. Sci Transl Med. 2014;6:229ra240. DOI: 10.1126/scitranslmed.3007696
65. Hirayama D, Iida T, Nakase H. The phagocytic function of macrophage-enforcing innate immunity and tissue homeostasis. Int J Mol Sci. 2017;19. DOI: 10.3390/ijms19010092
66. Lappin DF, Kjeldsen M, Sander L, Kinane DF. Inducible nitric oxide synthase expression in periodontitis. J Periodontal Res. 2000;35:369-373. DOI: 10.1034/j.1600-0765.2000.035006369.x
67. Lam RS, O'Brien-Simpson NM, Lenzo JC, et al. Macrophage depletion abates *Porphyromonas gingivalis*-induced alveolar bone resorption in mice. J Immunol. 2014;193:2349-2362. DOI: 10.4049/jimmunol.1400853
68. Clark D, Halpern B, Miclau T, Nakamura M, Kapila Y, Marcucio R. The contribution of macrophages in old mice to periodontal disease. J Dent Res. 2021;100:1397-1404. DOI: 10.1177/00220345211009463
69. Thery C, Witwer KW, Aikawa E, et al. Minimal information for studies of extracellular vesicles 2018 (MISEV2018): a position statement of the International Society for Extracellular Vesicles and update of the MISEV2014 guidelines. J Extracell Vesicles. 2018;7:1535750. DOI: 10.1080/20013078.2018.1535750
70. Thery C, Ostrowski M, Segura E. Membrane vesicles as conveyors of immune responses. Nat Rev Immunol. 2009;9:581-593. DOI: 10.1038/nri2567
71. Kuipers ME, Hokke CH, Smits HH, Nolte-'t Hoen ENM. Pathogen-derived extracellular vesicle-associated molecules that affect the host immune system: an overview. Front Microbiol. 2018;9:2182. DOI: 10.3389/fmicb.2018.02182

72. Pitt JM, Charrier M, Viaud S, et al. Dendritic cell-derived exosomes as immunotherapies in the fight against cancer. J Immunol. 2014;193:1006-1011. DOI: 10.4049/jimmunol.1400703
73. Arteaga-Blanco LA, Bou-Habib DC. The role of extracellular vesicles from human macrophages on host-pathogen interaction. Int J Mol Sci. 2021;22. DOI: 10.3390/ijms221910262
74. Toyofuku M, Nomura N, Eberl L. Types and origins of bacterial membrane vesicles. Nat Rev Microbiol. 2019;17:13-24. DOI: 10.1038/s41579-018-0112-2
75. Bittel M, Reichert P, Sarfati I, et al. Visualizing transfer of microbial biomolecules by outer membrane vesicles in microbe-host-communication *in vivo*. J Extracell Vesicles. 2021;10:e12159. DOI: 10.1002/jev2.12159
76. Villard A, Boursier J, Andriantsitohaina R. Microbiota-derived extracellular vesicles and metabolic syndrome. Acta Physiol (Oxf). 2021;231:e13600. DOI: 10.1111/apha.13600
77. Zhang Z, Liu D, Liu S, Zhang S, Pan Y. The role of *Porphyromonas gingivalis* outer membrane vesicles in periodontal disease and related systemic diseases. Front Cell Infect Microbiol. 2020;10:585917. DOI: 10.3389/fcimb.2020.585917
78. Nara PL, Sindelar D, Penn MS, Potempa J, Griffin WST. *Porphyromonas gingivalis* outer membrane vesicles as the major driver of and explanation for neuropathogenesis, the cholinergic hypothesis, iron dyshomeostasis, and salivary lactoferrin in Alzheimer's disease. J Alzheimers Dis. 2021;82:1417-1450. DOI: 10.3233/JAD-210448
79. Kim HY, Song MK, Gho YS, Kim HH, Choi BK. Extracellular vesicles derived from the periodontal pathogen *Filifactor alocis* induce systemic bone loss through Toll-like receptor 2. J Extracell Vesicles. 2021;10:e12157. DOI: 10.1002/jev2.12157
80. Jun HK, Lee SH, Lee HR, Choi BK. Integrin alpha5beta1 activates the

NLRP3 inflammasome by direct interaction with a bacterial surface protein. Immunity. 2012;36:755-768. DOI: 10.1016/j.immuni.2012.05.002

81. Suh J, Han D, Ku JH, Kim HH, Kwak C, Jeong CW. Next-generation proteomics-based discovery, verification, and validation of urine biomarkers for bladder cancer diagnosis. Cancer Res Treat. 2022;54:882-893. DOI: 10.4143/crt.2021.642
82. Cox J, Mann M. MaxQuant enables high peptide identification rates, individualized p.p.b.-range mass accuracies and proteome-wide protein quantification. Nat Biotechnol. 2008;26:1367-1372. DOI: 10.1038/nbt.1511
83. Cox J, Neuhauser N, Michalski A, Scheltema RA, Olsen JV, Mann M. Andromeda: a peptide search engine integrated into the MaxQuant environment. J Proteome Res. 2011;10:1794-1805. DOI: 10.1021/pr101065j
84. Tyanova S, Temu T, Sinitcyn P, et al. The Perseus computational platform for comprehensive analysis of (prote)omics data. Nat Methods. 2016;13:731-740. DOI: 10.1038/nmeth.3901
85. Ge SX, Jung D, Yao R. ShinyGO: a graphical gene-set enrichment tool for animals and plants. Bioinformatics. 2020;36:2628-2629. DOI: 10.1093/bioinformatics/btz931
86. Szklarczyk D, Morris JH, Cook H, et al. The STRING database in 2017: quality-controlled protein-protein association networks, made broadly accessible. Nucleic Acids Res. 2017;45:D362-D368. DOI: 10.1093/nar/gkw937
87. Yu CS, Cheng CW, Su WC, et al. CELLO2GO: a web server for protein subCELlular LOcalization prediction with functional gene ontology annotation. PLoS One. 2014;9:e99368. DOI: 10.1371/journal.pone.0099368
88. Lim H, Kim YU, Sun H, et al. Proatherogenic conditions promote

autoimmune T helper 17 cell responses in vivo. Immunity. 2014;40:153-165. DOI: 10.1016/j.immuni.2013.11.021

89. Jeppesen DK, Fenix AM, Franklin JL, et al. Reassessment of exosome composition. Cell. 2019;177:428-445 e418. DOI: 10.1016/j.cell.2019.02.029
90. Friedrich V, Gruber C, Nimeth I, et al. Outer membrane vesicles of *Tannerella forsythia*: biogenesis, composition, and virulence. Mol Oral Microbiol. 2015;30:451-473. DOI: 10.1111/omi.12104
91. Veith PD, Chen YY, Chen D, et al. *Tannerella forsythia* outer membrane vesicles are enriched with substrates of the type IX secretion system and TonB-dependent receptors. J Proteome Res. 2015;14:5355-5366. DOI: 10.1021/acs.jproteome.5b00878
92. Yoo JY, Kim HC, Zhu W, et al. Identification of *Tannerella forsythia* antigens specifically expressed in patients with periodontal disease. FEMS Microbiol Lett. 2007;275:344-352. DOI: 10.1111/j.1574-6968.2007.00906.x
93. Schwechheimer C, Kuehn MJ. Outer-membrane vesicles from gram-negative bacteria: biogenesis and functions. Nat Rev Microbiol. 2015;13:605-619. DOI: 10.1038/nrmicro3525
94. Shao S, Fang H, Li Q, Wang G. Extracellular vesicles in inflammatory skin disorders: from pathophysiology to treatment. Theranostics. 2020;10:9937-9955. DOI: 10.7150/thno.45488
95. Nahui Palomino RA, Vanpouille C, Costantini PE, Margolis L. Microbiota-host communications: bacterial extracellular vesicles as a common language. PLoS Pathog. 2021;17:e1009508. DOI: 10.1371/journal.ppat.1009508
96. Huang G, Wang Y, Chi H. Regulation of Th17 cell differentiation by innate immune signals. Cell Mol Immunol. 2012;9:287-295. DOI: 10.1038/cmi.2012.10
97. Noh MK, Jung M, Kim SH, et al. Assessment of IL-6, IL-8 and TNF-

alpha levels in the gingival tissue of patients with periodontitis. Exp Ther Med. 2013;6:847-851. DOI: 10.3892/etm.2013.1222

98. Gomes FI, Aragao MG, Barbosa FC, Bezerra MM, de Paulo Teixeira Pinto V, Chaves HV. Inflammatory cytokines interleukin-1beta and tumour necrosis factor-alpha - novel biomarkers for the detection of periodontal diseases: a literature review. J Oral Maxillofac Res. 2016;7:e2. DOI: 10.5037/jomr.2016.7202
99. Graves DT, Cochran D. The contribution of interleukin-1 and tumor necrosis factor to periodontal tissue destruction. J Periodontol. 2003;74:391-401. DOI: 10.1902/jop.2003.74.3.391
100. Bickel M. The role of interleukin-8 in inflammation and mechanisms of regulation. J Periodontol. 1993;64:456-460
101. Tang H, Pang P, Qin Z, et al. The CPNE family and their role in cancers. Front Genet. 2021;12:689097. DOI: 10.3389/fgene.2021.689097
102. Jiang Z, Jiang J, Zhao B, et al. CPNE1 silencing inhibits the proliferation, invasion and migration of human osteosarcoma cells. Oncol Rep. 2018;39:643-650. DOI: 10.3892/or.2017.6128
103. Renkl AC, Wussler J, Ahrens T, et al. Osteopontin functionally activates dendritic cells and induces their differentiation toward a Th1-polarizing phenotype. Blood. 2005;106:946-955. DOI: 10.1182/blood-2004-08-3228
104. Dong B, Zhou Q, Zhao J, et al. Phospholipid scramblase 1 potentiates the antiviral activity of interferon. J Virol. 2004;78:8983-8993. DOI: 10.1128/JVI.78.17.8983-8993.2004
105. Hung SC, Choi CH, Said-Sadier N, et al. P2X4 assembles with P2X7 and pannexin-1 in gingival epithelial cells and modulates ATP-induced reactive oxygen species production and inflammasome activation. PLoS One. 2013;8:e70210. DOI: 10.1371/journal.pone.0070210
106. Hamoudi C, Zhao C, Abderrazak A, et al. The purinergic receptor P2X4 promotes Th17 activation and the development of arthritis. J Immunol.

2022;208:1115-1127. DOI: 10.4049/jimmunol.2100550

107. Luchian I, Goriuc A, Sandu D, Covasa M. The role of matrix metalloproteinases (MMP-8, MMP-9, MMP-13) in periodontal and peri-implant pathological processes. Int J Mol Sci. 2022;23. DOI: 10.3390/ijms23031806
108. Nie A, Sun B, Fu Z, Yu D. Roles of aminoacyl-tRNA synthetases in immune regulation and immune diseases. Cell Death Dis. 2019;10:901. DOI: 10.1038/s41419-019-2145-5
109. Baima G, Iaderosa G, Citterio F, et al. Salivary metabolomics for the diagnosis of periodontal diseases: a systematic review with methodological quality assessment. Metabolomics. 2021;17:1. DOI: 10.1007/s11306-020-01754-3
110. Saltzman RW, Monaco-Shawver L, Zhang K, Sullivan KE, Filipovich AH, Orange JS. Novel mutation in STXBP2 prevents IL-2-induced natural killer cell cytotoxicity. J Allergy Clin Immunol. 2012;129:1666-1668. DOI: 10.1016/j.jaci.2011.12.1003
111. Okochi Y, Okamura Y. Regulation of neutrophil functions by Hv1/VSOP voltage-gated proton channels. Int J Mol Sci. 2021;22. DOI: 10.3390/ijms22052620
112. Delaguillaumie A, Lagaudriere-Gesbert C, Popoff MR, Conjeaud H. Rho GTPases link cytoskeletal rearrangements and activation processes induced via the tetraspanin CD82 in T lymphocytes. J Cell Sci. 2002;115:433-443. DOI: 10.1242/jcs.115.2.433
113. Tatematsu M, Yoshida R, Morioka Y, et al. Raftlin controls lipopolysaccharide-induced TLR4 internalization and TICAM-1 signaling in a cell type-specific manner. J Immunol. 2016;196:3865-3876. DOI: 10.4049/jimmunol.1501734
114. Wabnitz GH, Kocher T, Lohneis P, et al. Costimulation induced phosphorylation of L-plastin facilitates surface transport of the T cell activation molecules CD69 and CD25. Eur J Immunol. 2007;37:649-

662. DOI: 10.1002/eji.200636320

115. Kim HJ, Prasad V, Hyung SW, et al. Plasma membrane calcium ATPase regulates bone mass by fine-tuning osteoclast differentiation and survival. J Cell Biol. 2012;199:1145-1158. DOI: 10.1083/jcb.201204067
116. Klimentova J, Stulik J. Methods of isolation and purification of outer membrane vesicles from gram-negative bacteria. Microbiol Res. 2015;170:1-9. DOI: 10.1016/j.micres.2014.09.006
117. Liu Y, Defourny KAY, Smid EJ, Abee T. Gram-positive bacterial extracellular vesicles and their impact on health and disease. Front Microbiol. 2018;9:1502. DOI: 10.3389/fmicb.2018.01502
118. Caruana JC, Walper SA. Bacterial membrane vesicles as mediators of microbe - microbe and microbe - host community interactions. Front Microbiol. 2020;11:432. DOI: 10.3389/fmicb.2020.00432
119. Bolam DN, van den Berg B. TonB-dependent transport by the gut microbiota: novel aspects of an old problem. Curr Opin Struct Biol. 2018;51:35-43. DOI: 10.1016/j.sbi.2018.03.001
120. Bielecki M, Antonyuk S, Strange RW, et al. *Tannerella forsythia* Tfo belongs to *Porphyromonas gingivalis* HmuY-like family of proteins but differs in heme-binding properties. Biosci Rep. 2018;38. DOI: 10.1042/BSR20181325
121. Yoo H-J, Lee S-H. Heme effects of hemin on growth of peridontopathogens. Journal of Dental Rehabilitation and Applied Science. 2021;37:31-38
122. Oliveira-Nascimento L, Massari P, Wetzler LM. The role of TLR2 in infection and immunity. Front Immunol. 2012;3:79. DOI: 10.3389/fimmu.2012.00079
123. Jung YJ, Choi YJ, An SJ, Lee HR, Jun HK, Choi BK. *Tannerella forsythia* GroEL induces inflammatory bone resorption and synergizes with interleukin-17. Mol Oral Microbiol. 2017;32:301-313. DOI:

10.1111/omi.12172

124. Yost S, Duran-Pinedo AE. The contribution of *Tannerella forsythia* dipeptidyl aminopeptidase IV in the breakdown of collagen. Mol Oral Microbiol. 2018;33:407-419. DOI: 10.1111/omi.12244
125. Athman JJ, Wang Y, McDonald DJ, Boom WH, Harding CV, Wearsch PA. Bacterial membrane vesicles mediate the release of *Mycobacterium tuberculosis* lipoglycans and lipoproteins from infected macrophages. J Immunol. 2015;195:1044-1053. DOI: 10.4049/jimmunol.1402894
126. Cecil JD, O'Brien-Simpson NM, Lenzo JC, et al. Differential responses of pattern recognition receptors to outer membrane vesicles of three periodontal pathogens. PLoS One. 2016;11:e0151967. DOI: 10.1371/journal.pone.0151967
127. Cecil JD, O'Brien-Simpson NM, Lenzo JC, et al. Outer Membrane Vesicles Prime and Activate Macrophage Inflammasomes and Cytokine Secretion In Vitro and In Vivo. Front Immunol. 2017;8:1017. DOI: 10.3389/fimmu.2017.01017
128. Zenobia C, Herpoldt KL, Freire M. Is the oral microbiome a source to enhance mucosal immunity against infectious diseases? NPJ Vaccines. 2021;6:80. DOI: 10.1038/s41541-021-00341-4
129. Lin M, Hu Y, Wang Y, Kawai T, Wang Z, Han X. Different engagement of TLR2 and TLR4 in *Porphyromonas gingivalis* vs. ligature-induced periodontal bone loss. Braz Oral Res. 2017;31:e63. DOI: 10.1590/1807-3107BOR-2017.vol31.0063
130. Alaniz RC, Deatherage BL, Lara JC, Cookson BT. Membrane vesicles are immunogenic facsimiles of *Salmonella typhimurium* that potently activate dendritic cells, prime B and T cell responses, and stimulate protective immunity *in vivo*. J Immunol. 2007;179:7692-7701. DOI: 10.4049/jimmunol.179.11.7692
131. Durand V, Mackenzie J, de Leon J, et al. Role of lipopolysaccharide in the induction of type I interferon-dependent cross-priming and IL-10

production in mice by meningococcal outer membrane vesicles. Vaccine. 2009;27:1912-1922. DOI: 10.1016/j.vaccine.2009.01.109

132. Schetters STT, Jong WSP, Horrevorts SK, et al. Outer membrane vesicles engineered to express membrane-bound antigen program dendritic cells for cross-presentation to $CD8^+$ T cells. Acta Biomater. 2019;91:248-257. DOI: 10.1016/j.actbio.2019.04.033
133. Zhu Z, Antenucci F, Villumsen KR, Bojesen AM. Bacterial outer membrane vesicles as a versatile tool in vaccine research and the fight against antimicrobial resistance. mBio. 2021;12:e0170721. DOI: 10.1128/mBio.01707-21
134. Moutsopoulos NM, Kling HM, Angelov N, et al. *Porphyromonas gingivalis* promotes Th17 inducing pathways in chronic periodontitis. J Autoimmun. 2012;39:294-303. DOI: 10.1016/j.jaut.2012.03.003
135. Cheng WC, van Asten SD, Burns LA, et al. Periodontitis-associated pathogens *P. gingiva*lis and *A. actinomycetemcomitans* activate human $CD14^+$ monocytes leading to enhanced Th17/IL-17 responses. Eur J Immunol. 2016;46:2211-2221. DOI: 10.1002/eji.201545871
136. Bittner-Eddy PD, Fischer LA, Kaplan DH, Thieu K, Costalonga M. Mucosal langerhans cells promote differentiation of Th17 cells in a murine model of periodontitis but are not required for *Porphyromonas gingivalis*-driven alveolar bone destruction. J Immunol. 2016;197:1435-1446. DOI: 10.4049/jimmunol.1502693
137. Bittner-Eddy PD, Fischer LA, Costalonga M. Transient expression of IL-17A in Foxp3 fate-tracked cells in *Porphyromonas gingivalis*-mediated oral dysbiosis. Front Immunol. 2020;11:677. DOI: 10.3389/fimmu.2020.00677
138. Zhang L, Gao L, Xu C, et al. *Porphyromonas gingivali*s lipopolysaccharide promotes T- helper 17 cell differentiation from human $CD4^+$ naive T cells via Toll-like receptor-2 in vitro. Arch Oral Biol. 2019;107:104483. DOI: 10.1016/j.archoralbio.2019.104483

139. Perricone C, Ceccarelli F, Saccucci M, et al. *Porphyromonas gingivalis* and rheumatoid arthritis. Curr Opin Rheumatol. 2019;31:517-524. DOI: 10.1097/BOR.0000000000000638
140. Marchesan JT, Gerow EA, Schaff R, et al. *Porphyromonas gingivalis* oral infection exacerbates the development and severity of collagen-induced arthritis. Arthritis Res Ther. 2013;15:R186. DOI: 10.1186/ar4376
141. Zhou N, Zou F, Cheng X, et al. *Porphyromonas gingivalis* induces periodontitis, causes immune imbalance, and promotes rheumatoid arthritis. J Leukoc Biol. 2021;110:461-473. DOI: 10.1002/JLB.3MA0121-045R
142. Nishihara M, Ogura H, Ueda N, et al. IL-6-gp130-STAT3 in T cells directs the development of IL-17^+ Th with a minimum effect on that of Treg in the steady state. Int Immunol. 2007;19:695-702. DOI: 10.1093/intimm/dxm045
143. Tripathi SK, Chen Z, Larjo A, et al. Genome-wide analysis of STAT3-mediated transcription during early human Th17 cell differentiation. Cell Rep. 2017;19:1888-1901. DOI: 10.1016/j.celrep.2017.05.013
144. Diehl S, Anguita J, Hoffmeyer A, et al. Inhibition of Th1 differentiation by IL-6 is mediated by SOCS1. Immunity. 2000;13:805-815. DOI: 10.1016/s1074-7613(00)00078-9
145. Trinchieri G. Interleukin-12 and the regulation of innate resistance and adaptive immunity. Nat Rev Immunol. 2003;3:133-146. DOI: 10.1038/nri1001
146. Tomek MB, Maresch D, Windwarder M, et al. A general protein *O*-glycosylation gene cluster encodes the species-specific glycan of the oral pathogen *Tannerella forsythia*: *O*-glycan biosynthesis and immunological implications. Front Microbiol. 2018;9:2008. DOI: 10.3389/fmicb.2018.02008
147. Godovikova V, Goetting-Minesky MP, Fenno JC. Composition and

localization of *Treponema denticola* outer membrane complexes. Infect Immun. 2011;79:4868-4875. DOI: 10.1128/IAI.05701-11

148. Veith PD, Glew MD, Gorasia DG, Chen D, O'Brien-Simpson NM, Reynolds EC. Localization of outer membrane proteins in *Treponema denticola* by quantitative proteome analyses of outer membrane vesicles and cellular fractions. J Proteome Res. 2019;18:1567-1581. DOI: 10.1021/acs.jproteome.8b00860
149. Miyamoto M, Ishihara K, Okuda K. The *Treponema denticola* surface protease dentilisin degrades interleukin-1 beta (IL-1 beta), IL-6, and tumor necrosis factor alpha. Infect Immun. 2006;74:2462-2467. DOI: 10.1128/IAI.74.4.2462-2467.2006
150. Jia L, Han N, Du J, Guo L, Luo Z, Liu Y. Pathogenesis of important virulence factors of *Porphyromonas gingivalis* via Toll-like receptors. Front Cell Infect Microbiol. 2019;9:262. DOI: 10.3389/fcimb.2019.00262
151. NM OB-S, Veith PD, Dashper SG, Reynolds EC. *Porphyromonas gingivalis* gingipains: the molecular teeth of a microbial vampire. Curr Protein Pept Sci. 2003;4:409-426. DOI: 10.2174/1389203033487009
152. Veith PD, Chen YY, Gorasia DG, et al. *Porphyromonas gingivalis* outer membrane vesicles exclusively contain outer membrane and periplasmic proteins and carry a cargo enriched with virulence factors. J Proteome Res. 2014;13:2420-2432. DOI: 10.1021/pr401227e

List of Publications

This thesis was written including the following original paper.

Lim, Y., Kim, H. Y., An, S. J., & Choi, B. K. (2022). Activation of bone marrow-derived dendritic cells and CD4+ T cell differentiation by outer membrane vesicles of periodontal pathogens. *Journal of Oral Microbiology*, *14*(1), 2123550. DOI: 10.1080/20002297.2022.2123550

국 문 초 록

대식세포와 치주병원균 유래 세포 밖 소포체의 면역 활성에 관한 연구

임 영 갑

서울대학교 대학원

치의과학과 면역 및 분자미생물학 전공

목적

세포 밖 소포체는 살아있는 세포에서 방출되는 나노 크기의 소포이며 다양한 생물학적 분자를 운반한다. 세포 밖 소포체는 세포간의 상호작용에 의한 생리적, 병리학적 역할 때문에 학계와 산업계에서 주목받고 있다. 하지만, 현재까지 치주 병원균에 감염된 숙주 세포 유래 세포 밖 소포체와 치주 병원균 유래 외막 소포체에 의한 도움 T 세포 분화에 대한 정보는 매우 제한적이다.

따라서 본 연구에서는 치주 병원균에 감염된 숙주 세포 유래 세포 밖 소포체의 단백질체와 염증 반응을 분석하고, 치주 병원균 유래 외막 소포체에 의해 유도되는 도움 T 세포 분화 양상을 확인하고자 한다.

방법

*Tannerella forsythia*에 감염된 THP-1 대식세포 유래 세포 밖 소포체는 크기 배제 크로마토그래피(size exclusion chromatography)와 밀도 구배 초원심분리(density gradient ultracentrifugation, DGUC)를 통해 분리 및 정제하였다. 나노 입

자 추적 분석(nanoparticle tracking analysis, NTA)을 통해 세포 밖 소포체의 크기와 농도를 측정하였다. 세포 밖 소포체의 형태는 투과 전자 현미경(transmission electron microscopy, TEM)으로 확인하였다. 세포 밖 소포체의 전반적인 단백질 패턴을 분석하기 위해, 폴리아크릴아미드 겔 전기영동(sodium dodecyl sulfate polyacrylamide gel electrophoresis, SDS-PAGE)을 수행 후, 겔을 단백질 겔 염색 용액으로 염색하여 극자외선 투과 조명기(ultraviolet transilluminator)로 크기에 따른 단백질의 분포를 확인하였다. 진핵생물의 세포 밖 소포체와 비-소포성 응집체의 표지 및 *T. forsythia* 단백질은 숙주단백질과 세균단백질에 특이적인 항체를 이용한 면역블롯팅법으로 분석하였다. 세포 밖 소포체의 총 단백질체는 심층 정량적 단백질체 분석법으로 분석하였다. 세포 밖 소포체의 THP-1 대식세포에 대한 면역자극 효과를 평가하기 위해, 세포 밖 소포체를 대식세포에 처리한 다음 배양 상층액의 염증성 사이토카인을 효소 결합 면역흡착 분석법(enzyme-linked immunosorbent assay, ELISA)으로 측정하였다.

Porphyromonas gingivalis, *Treponema denticola*, *T. forsythia* 세 가지 치주 병원균의 외막 소포체는 초원심분리 및 밀도구배 초원심분리를 통해 분리 및 정제 하였다. 외막 소포체의 크기와 농도는 NTA로 측정했고, 외막 소포체의 형태는 TEM을 통해 확인하였다. 외막 소포체에 의한 수지상 세포의 면역 활성 및 도움 T 세포의 분화를 확인하기 위해, 마우스 골수 유래 수지상 세포를 8주령 C57BL/6N 골수 세포로부터 분화시키고, 항원과 아직 만나지 않은 미분화 $CD4^+$ T 세포를 8주령 C57BL/6N 마우스의 비장에서 분리하였다. 골수 유래 수지상 세포를 치주 병원균 유래 외막 소포체로 처리하고 세포 표면의 2형 주 조직 적합성 복합체(MHC class II), CD80, CD86, 및 CD40 분자의 발현 수준을 유세

포 분석기로 측정하였다. 골수 유래 수지상세포의 배양 상층액에서 염증성 사이토카인인 IL-12p70, IL-1β, IL-6, IL-23의 발현 정도를 ELISA로 측정하였다. 정량적 실시간 중합효소 연쇄 반응(qRT-PCR)을 수행하여 골수 유래 수지상세포에서 *Il12a, Il1b, Il6, Il23a*의 발현을 메신저 리보핵산(mRNA) 수준에서 확인하였다. 염증성 사이토카인에 대한 치주 병원균 유래 외막 소포체의 단백질 분해 활성을 분석하기 위해 재조합 설치류 IL-12p70, IL-1β, IL-6, IL-23을 치주 병원균 유래 외막 소포체로 처리하고 남은 사이토카인의 양을 ELISA로 측정하였다. 도움 T 세포의 분화를 확인하기 위해, 미분화 $CD4^+$ T 세포를 외막 소포체로 자극된 골수 유래 수지상세포와 4일 동안 공동 배양하였다. $CD4^+$ T 세포의 Th1 또는 Th17 세포로의 분화는 $CD4^+$ T 세포내의 INF-γ 및 IL-17A의 발현 정도를 유세포 분석기로 측정하여 분석하였다. 골수 유래 수지상세포에서 분비되는 IL-6 및 IL-12가 Th1 또는 Th17 세포의 분화에 미치는 영향을 평가하기 위해, 미분화 $CD4^+$ T 세포를 IL-6 및 IL-12에 대한 중화 항체와 함께 외막 소포체로 자극된 골수 유래 수지상세포와 4일 동안 공동 배양 후 $CD4^+$ T 세포내의 INF-γ 및 IL-17A의 발현 정도를 유세포 분석기로 분석하였다.

결과

*T. forsythia*에 감염된 THP-1 대식세포 유래 세포 밖 소포체는 그 밀도에 따라 대식세포 유래 세포 밖 소포체와 *T. forsythia* 유래 세포 밖 소포체로 분리되었다. 대식세포 유래 세포 밖 소포체는 저밀도 분획에, *T. forsythia* 유래 세포 밖 소포체는 중간 밀도 분획에 위치했다. 두 개의 서로 다른 세포 밖 소포체의 크기와 형태는 비슷했지만 단백질 패턴은 완전히 달랐다. 진핵생물의 세포

밖 소포체 표지인 CD9, CD63, 및 Alix는 대식세포 유래 세포 밖 소포체에서만 검출되었고, *T. forsythia* 단백질은 *T. forsythia* 유래 EV에서 매우 높은 정도로 검출되었다. 감염되지 않은 대식세포의 세포 밖 소포체와 비교하면 TNF-α, CXCL8, IL-1β, CPNE1, SPP1, PLSCR1, P2RX4, MMP9, SARS, VARS, STXBP2, HVCN1, CD82, RFTN1, LCP1 및 ATP2B1은 *T. forsythia*에 감염된 대식세포 유래 세포 밖 소포체에서 증가함을 단백질체 분석을 통해 확인했다. 대식세포 유래 세포 밖 소포체는 THP-1 대식세포로부터 TNF-α의 발현을 유도했다. 단백질체 분석을 통해 *T. forsythia* 유래 세포 밖 소포체에서는 영양분 흡수 단백질, 단백질 분해효소, 탄수화물 가수분해효소, 박테리아 지질단백질, GroEL 및 BspA를 포함한 *T. forsythia*의 병인 요소가 확인되었다. *T. forsythia* 유래 세포 밖 소포체는 TLR2 신호 전달 경로를 통해 THP-1 대식세포에서 TNF-α, IL-1β, IL-6 및 IL-8을 유도하였다. 흥미롭게도, THP-1 대식세포에서 분비되는 생리활성물질은 *T. forsythia*에서 세포 밖 소포체의 방출을 촉진하였다.

레드 콤플렉스(red complex)라고도 불리는 3가지 치주 병원균인 *P. gingivalis*, *T. denticola* 및 *T. forsythia*의 외막 소포체가 처리된 골수 유래 수지상세포에서 2형 주 조직 적합성 복합체, CD80, CD86 및 CD40 분자의 발현이 증가하였다. *P. gingivalis* 및 *T. forsythia*의 외막 소포체는 골수 유래 수지상세포에서 염증성 사이토카인인 IL-1β, IL-6, IL-23 및 IL-12p70의 발현을 유도하였다. 그러나, *T. denticola* 외막 소포체에 의해 자극된 수지상세포의 경우, 세포 배양 상층액에서 염증성 사이토카인이 거의 검출되지 않았다. 이는 *T. denticola* 외막 소포체의 높은 단백질 분해 특성에 의해 분해된 것이었다. 미분화 $CD4^+$ T 세포와 외막 소포체로 자극된 골수 유래 수지상세포와의 공배양에서, *P. gingivalis*와

*T. denticola*의 외막 소포체는 Th17 세포의 분화를 유도한 반면, *T. forsythia* 외막 소포체는 Th1 세포 분화를 주로 유도했다. 외막 소포체에 의해 자극된 골수 유래 수지상세포에서 분비된 IL-6 및 IL-12는 각각 Th17 및 Th1 분화에 중추적인 역할을 했다.

결론

*T. forsythia*에 감염된 대식세포 유래 세포 밖 소포체는 치주염의 진행과정에서 염증 반응을 유도 할 수 있는 염증성 사이토카인과 염증 매개체 단백질들을 가지고 있었다. *T. forsythia* 유래 세포 밖 소포체는 다양한 병독성 인자를 포함했고, TLR2 활성화를 통해 대식세포에서 염증성 사이토카인의 발현을 유도하였다. *P. gingivalis*와 *T. denticola* 외막 소포체는 Th17 세포로의 분화를 유도한 반면, *T. forsythia* 외막 소포체는 Th1 세포로의 분화를 유도하였다. 이러한 결과는 세포가 병원균에 감염되었을 때, 숙주 세포 유래 세포 밖 소포체와 병원균 유래한 세포 밖 소포체가 염증 반응에 동반 상승 효과를 낼 수 있음을 보여줌으로써 치주 병원균에 감염된 세포에서 유래한 세포 밖 소포체의 특성에 대한 통찰력을 제공한다. 'Red complex' 치주 병원균에서 유래한 외막 소포체는 골수 유래 수지상세포의 성숙과 미분화 $CD4^+$ T 세포의 Th1 또는 Th17 세포로의 분화를 유도하였다. 따라서 세포 밖 소포체는 치주 병원균의 병원성 메커니즘을 이해하는 데 유용한 도구가 될 수 있다.

주요어: 단백질체 분석, 대식세포, 세포 밖 소포체, 수지상세포, 치주염, T 세포

학번: 2018-32257